Western University
Scholarship@Western

Digitized Theses | Digitized Special Collections

1994

An In Vivo Proton And Phosphorus Mr Spectroscopy Study Of Schizophrenia

Jeff A. Stanley

Follow this and additional works at: https://ir.lib.uwo.ca/digitizedtheses

Recommended Citation
Stanley, Jeff A., "An In Vivo Proton And Phosphorus Mr Spectroscopy Study Of Schizophrenia" (1994). *Digitized Theses*. 2467.
https://ir.lib.uwo.ca/digitizedtheses/2467

This Dissertation is brought to you for free and open access by the Digitized Special Collections at Scholarship@Western. It has been accepted for inclusion in Digitized Theses by an authorized administrator of Scholarship@Western. For more information, please contact tadam@uwo.ca, wlswadmin@uwo.ca.

AN IN VIVO 1H AND 31P MR SPECTROSCOPY STUDY OF SCHIZOPHRENIA

by

Jeff A. Stanley

Department of Medical Biophysics

Submitted in partial fulfilment
of the requirements for the degree of
Doctor of Philosophy

Faculty of Graduate Studies
The University of Western Ontario
London, Ontario
September 1994

© Jeff A. Stanley 1994

National Library of Canada
Acquisitions and Bibliographic Services Branch
395 Wellington Street
Ottawa, Ontario
K1A 0N4

Bibliothèque nationale du Canada
Direction des acquisitions et des services bibliographiques
395, rue Wellington
Ottawa (Ontario)
K1A 0N4

Your file Votre référence

Our file Notre référence

The author has granted an irrevocable non-exclusive licence allowing the National Library of Canada to reproduce, loan, distribute or sell copies of his/her thesis by any means and in any form or format, making this thesis available to interested persons.

L'auteur a accordé une licence irrévocable et non exclusive permettant à la Bibliothèque nationale du Canada de reproduire, prêter, distribuer ou vendre des copies de sa thèse de quelque manière et sous quelque forme que ce soit pour mettre des exemplaires de cette thèse à la disposition des personnes intéressées.

The author retains ownership of the copyright in his/her thesis. Neither the thesis nor substantial extracts from it may be printed or otherwise reproduced without his/her permission.

L'auteur conserve la propriété du droit d'auteur qui protège sa thèse. Ni la thèse ni des extraits substantiels de celle-ci ne doivent être imprimés ou autrement reproduits sans son autorisation.

ISBN 0-315-93240-6

Canada

ABSTRACT

Schizophrenia is a brain disease that affects about one in every 100 Canadians. Approximately 40% of patients affected with schizophrenia have a lifelong debilitating illness. Numerous studies have been conducted yet, the pathophysiology of this disease is still unclear. Magnetic resonance spectroscopy (MRS) is a noninvasive technique that provides a biochemical analysis of living tissue from a defined region in the brain, which is not possible with any other technique. Consequently, MRS opens a new window into the research of schizophrenia.

Quantifying the metabolite levels observed in *in vivo* ^{1}H MR spectra acquired with a short echo time sequence is problematic due to complex overlapping resonances. A technique was developed to quantify these metabolites with the input of *a priori* knowledge of the individual metabolites into a spectral lineshape fitting routine. The accuracy and precision of modelling these metabolites were investigated with simulated spectra of varying signal-to-noise ratios and relative metabolite levels. The efficacy of this technique was then tested on repeated *in vivo* measures. The coefficients of variation were less than 10% for N-acetylaspartate, phosphocreatine plus creatine and choline, and approximately 20% for glutamate.

In vivo ^{1}H and phosphorus (^{31}P) MR spectra from the left dorsolateral prefrontal region of first episode drug-naive (DN), newly-diagnosed medicated

(NDM) and chronic medicated (CM) schizophrenia patients were acquired and compared to controls of similar gender, education, parental education and handedness. The ^{1}H results suggest the resting glutamate level and neuronal cell viability are not altered in the DN or CM patients. In the NDM patients, the altered glutamate and glutamine levels would suggest that the neuroleptic medication increases the presynaptic glutamate release. The increased glutamine level of the CM patients (which correlated with the length of illness) may suggest that glia volume increases as the illness progresses.

In the ^{31}P study, alterations in the membrane phospholipid metabolism were observed in the DN patients compared to controls. No differences in the high-energy phosphate metabolite levels were observed in the patients, except for decreased inorganic orthophosphate levels in the NDM patients. The intracellular free magnesium concentration was higher in all three patient groups compared to controls.

ACKNOWLEDGEMENTS

I would like to take this opportunity to acknowledge those people who have been a great source of encouragement, knowledge and guidance over the past four and a half years.

To Dr. Dick Drost for allowing me the opportunity to work at the Lawson Research Institute and for introducing me to the world of in vivo spectroscopy, and to Dr. Peter Williamson for giving me the opportunity to work on a very challenging and rewarding Ph.D. project on schizophrenia.

To Dr. Terry Thompson for the many in depth discussions on NMR, and to Drs. Tom Carr, Jane Rylett, Steve Sims and Frank Prato all of whom have generously contributed their time and expertise.

To Rob Bartha for all of the E-mail messages, faxes and invaluable help over the last two months. Good luck in the future!

To my parents who have never questioned the fact that one day I would finally finish school, although they've often wondered when!

Finally to Christine for all your patience when times were very busy at work, and for the help and support that you have given me on this journey.

TABLE of CONTENTS

LIST of TABLES

LIST of FIGURES

LIST of APPENDICES

ABBREVIATIONS

Acq - acquisition period

Asp - aspartate

ATP - adenosine triphosphate

C - cerebellum

^{13}C - carbon nuclei

CHESS - chemical shift selective

Cho - choline

Cho_t - choline-containing compounds

CM - chronic medicated

CSF - cerebrospinal fluid

CSI - chemical shift imaging

df - degrees of freedom

DN - drug-naive

EAA - excitatory amino acid

EEG - electroencephalogram

F - female

f_{CSF} - fraction of cerebrospinal fluid volume

f_{grey} - fraction of grey matter volume

f_{white} - fraction of white matter volume

FID - free induction decay

FL - frontal lobe

FROGS - fast rotating gradient spectroscopy

FWHM - full width at half maximum

GABA - γ-aminobutyric acid

Glc - glucose

Gln - glutamine

Glu - glutamate

GPCho - glycerophosphorylcholine

GPE - glycerophosphorylethanolamine

^1H - hydrogen nuclei (proton)

h(t) - Lorentzian-to-Gaussian transformation

HCl - hydrochloric acid

H_2O - water

IP_3 - inositol-(1,4,5)-triphosphate

ISIS - image-selected *in vivo* spectroscopy

J - spin-spin coupling constant

L_1 - amygdala

L_2 - parahippocampal gyrus

L_3 - hypothalamus

L_4 - hippocampus and dentate

LN - globus pallidus

LN_1 - lateral segment of the globus pallidus

LN_2 - medial segment of the globus pallidus

LOI - length of illness

LPSVD - linear prediction and singular value decomposition

M - male

max - maximum

Mg^{2+} - magnesium cation

$[Mg^{2+}]_{intra}$ - intracellular free magnesium concentration

min - minimum

$MnCl_2$ - manganese chloride

MRI - magnetic resonance imaging

MRS - magnetic resonance spectroscopy

myo-Ins - *myo*-inositol

^{15}N - nitrogen nuclei

NAA - N-acetylaspartate

NAAG - N-acetylaspartylglutamate

NaOH - sodium hydroxide

NDM - newly diagnosed medicated

NMDA - N-methyl-D-aspartate

NMR - nuclear magnetic resonance

N_{rms} - root mean square of the noise

OL - occipital lobe

^{31}P - phosphorus nuclei

PCho - phosphorylcholine

PCP - phencyclidine

PCr - phosphocreatine

PCr+Cr - phosphocreatine plus creatine

PDE - phosphodiester

PE - phosphorylethanolamine

PET - positron emission tomography

Pi - inorganic orthophosphate

PL - parietal lobe

PLA_1 - phospholipase A_1

PLA_2 - phospholipase A_2

PLC - phospholipase C

PME - phosphomonoester

ppm - parts per million

PS - phosphorylserine

PtdCho - phosphatidylcholine

PtdE - phosphatidylethanolamine

QUALITY - quantification improvement by converting lineshapes to the Lorentzian type

RF - radio frequency

RML - relative metabolite level

rms - root mean square

RNA - ribonucleic acid

S_1 - caudate nucleus

S_2 - putamen

SANS - scale for the assessment of negative symptoms

SAPS - scale for the assessment of positive symptoms

SCID - structured clinical interview for DSM-III-R

scyllo-Ins - *scyllo*-inositol

SD - standard deviation

S/N - signal-to-noise ratio

STEAM - stimulated echo acquisition mode

T_1 - spin-lattice relaxation time constant

T_2 - spin-spin relaxation decay constant

T_2^* - spin-spin relaxation decay constant which includes the static magnetic field inhomogeneity term

Tau - taurine

TE - echo time

TL - temporal lobe

TM - time between the 2nd and 3rd pulse

TR - pulse repetition time

TSP - sodium 3-trimethylsilylpropionic acid

VOI - volume of interest

The author of this thesis has granted The University of Western Ontario a non-exclusive license to reproduce and distribute copies of this thesis to users of Western Libraries. Copyright remains with the author.

Electronic theses and dissertations available in The University of Western Ontario's institutional repository (Scholarship@Western) are solely for the purpose of private study and research. They may not be copied or reproduced, except as permitted by copyright laws, without written authority of the copyright owner. Any commercial use or publication is strictly prohibited.

The original copyright license attesting to these terms and signed by the author of this thesis may be found in the original print version of the thesis, held by Western Libraries.

The thesis approval page signed by the examining committee may also be found in the original print version of the thesis held in Western Libraries.

Please contact Western Libraries for further information:
E-mail: libadmin@uwo.ca
Telephone: (519) 661-2111 Ext. 84796
Web site: http://www.lib.uwo.ca/

CHAPTER I

Magnetic Resonance Spectroscopy

In 1938, Rabi and colleagues first demonstrated the principles of nuclear magnetic resonance (NMR) (Rabi et al. 1938). Nearly 60 years later, NMR spectroscopy (or magnetic resonance spectroscopy (MRS)) is on the "cutting edge" of biomedical research (Frahm 1992). MRS is a non-invasive, non-destructive investigational tool that provides a biochemical analysis of living tissue from within a defined volume of interest (VOI). Numerous *in vivo* MRS studies in the last decade have enhanced the understanding of normal and pathological metabolism in organs including the brain, muscle, heart and liver (Bottomley 1989; Kauppinen et al. 1993). The defined VOI where the MR signal is obtained may be as small as several cm^3 (Ernst et al. 1989) and can be placed in a specified region of the brain such as, the dorsolateral prefrontal region, the basal ganglia, or the hippocampus. With improved design and performance of whole body MR units, MRS experiments on most modern clinical MRI units, with a static magnetic field strength of 1.5 Tesla or greater, are possible. For these reasons, the use of MRS introduces a new avenue for the research of neuropsychiatric disorders including schizophrenia.

The following introduces basic MR theory, relevant terminologies, a description of two localization techniques, the information obtainable from MR spectra, and a discussion on the hardware and software employed. Chapter II

follows with an introduction to schizophrenia, a discussion on previous MRS studies of schizophrenia. The objectives and hypotheses of this thesis are then presented.

I.1 The Basic Concepts of MR.

I.1.1 The Resonant Frequency.

In a MR experiment, the basic components required are a large static magnetic field, an oscillating radio frequency (RF) field, a probe (or coil) to transmit the RF field and to also receive the MR signal, and a sample to be investigated. The sample, however, must contain atoms which possess an angular momentum and a dipole magnetic moment. Fortunately, the human body is relatively rich in these nuclei including hydrogen (or protons, ^{1}H), phosphorus (^{31}P), carbon (^{13}C) and nitrogen (^{15}N) nuclei. By exposing the human body to a large static magnetic field, B_0 (which is the case during clinical magnetic resonance imaging (MRI)), these nuclei (or spins) will experience a torque due to the interaction of the magnetic field with the magnetic moments possessing an angular momentum. Consequently, this torque will cause the spins to precess about the static magnetic field at an angular frequency. This precessional angular frequency, ω_0 (also known as the Larmor frequency with units of rad/sec), is dependent on a constant, γ (gyromagnetic ratio, which is unique for each nucleus), and the strength of the local magnetic field experienced at the nucleus. This relationship can be written as:

$$\omega_0 = 2\pi \cdot \nu_0 = \gamma \cdot B_0 \qquad [I.1]$$

where ν_0 is referred to as the resonant frequency of that nucleus. With a B_0 of 1.5 Tesla, the ^1H nuclei will have a resonant frequency of $\approx$ 63MHz while the ^{31}P nuclei will resonate at $\approx$ 27MHz.

I.1.2 Chemical Shift

The resonance condition, Eq. [I.1], is based only on the interaction between a magnetic moment and the static magnetic field, B_0. There is an additional interaction between B_0 and the cloud of electrons about each of the nuclei, that can modify the local magnetic field at the nucleus. By exposing these nuclei to B_0, orbital currents are induced in the electron clouds and these currents generate their own small, secondary magnetic field at the sites of the nucleus. The secondary magnetic field is proportional to B_0 and it opposes B_0 (i.e., "shields" the nucleus from the applied B_0). The resonant frequency thus becomes

$$\nu = \frac{\gamma}{2\pi} \cdot (B_0 - B_0\sigma) = \frac{\gamma}{2\pi} \cdot B_0 \cdot (1 - \sigma) \qquad [I.2]$$

where $B_0\sigma$ term is the secondary magnetic field and σ is the shielding constant. Eq. [I.2] implies that nuclei with different shielding constants (i.e., different chemical environments) will have slightly different resonant frequencies. This is the basis of spectroscopy where different metabolites can be identified from the body by their unique resonant frequencies. These resonant frequencies are expressed as a chemical shift, δ, relative to a reference standard. For example, the chemical shift of nucleus X is defined as

$$\delta = \frac{\nu_x - \nu_{ref}}{\nu_{ref}} \cdot 10^6 \qquad [I.3]$$

where ν_x is the resonant frequency of nucleus X, ν_{ref} is the resonant frequency of the reference standard, and the 10^6 factor gives the units of parts per million (ppm). The reference standard used for in vivo ^1H and ^{31}P MRS are the resonance of the CH_3 group from the N-acetylaspartate (NAA) molecule at 2.024ppm (where the resonance of sodium 3-trimethylsilylpropionic acid is 0.000ppm) and the phosphocreatine (PCr) resonance at 0.00ppm, respectively.

I.1.3 Scalar Spin-Spin Coupling.

There is an additional through-bond interaction which is mediated by electrons that occurs between neighbouring nuclei from the same molecule. This interaction is referred to as scalar spin-spin coupling and the strength of the interaction is characterized by a scalar spin-spin coupling constant, J, which is independent of B_0. The result of this interaction splits the individual resonant lines into multiplet structures. For example, the adenosine triphosphate (ATP) molecule gives rise to three different resonances due to the three phosphate groups (α, β and γ), as illustrated in Figure I.1. With this additional scalar coupling interaction, the α- and γ-ATP resonances are each split into two peaks that are separated by their constants, $J_{\alpha\beta}$ and $J_{\gamma\beta}$, respectively (Figure I.1). The β-ATP resonance is split into four peaks (i.e., the multiplet structure is refered to as a doublet of doublet and in this case the two middle peaks are superimposed) with separations of $J_{\alpha\beta}$ and $J_{\gamma\beta}$ as indicated in Figure I.1. A

Adenosine triphosphate (ATP)

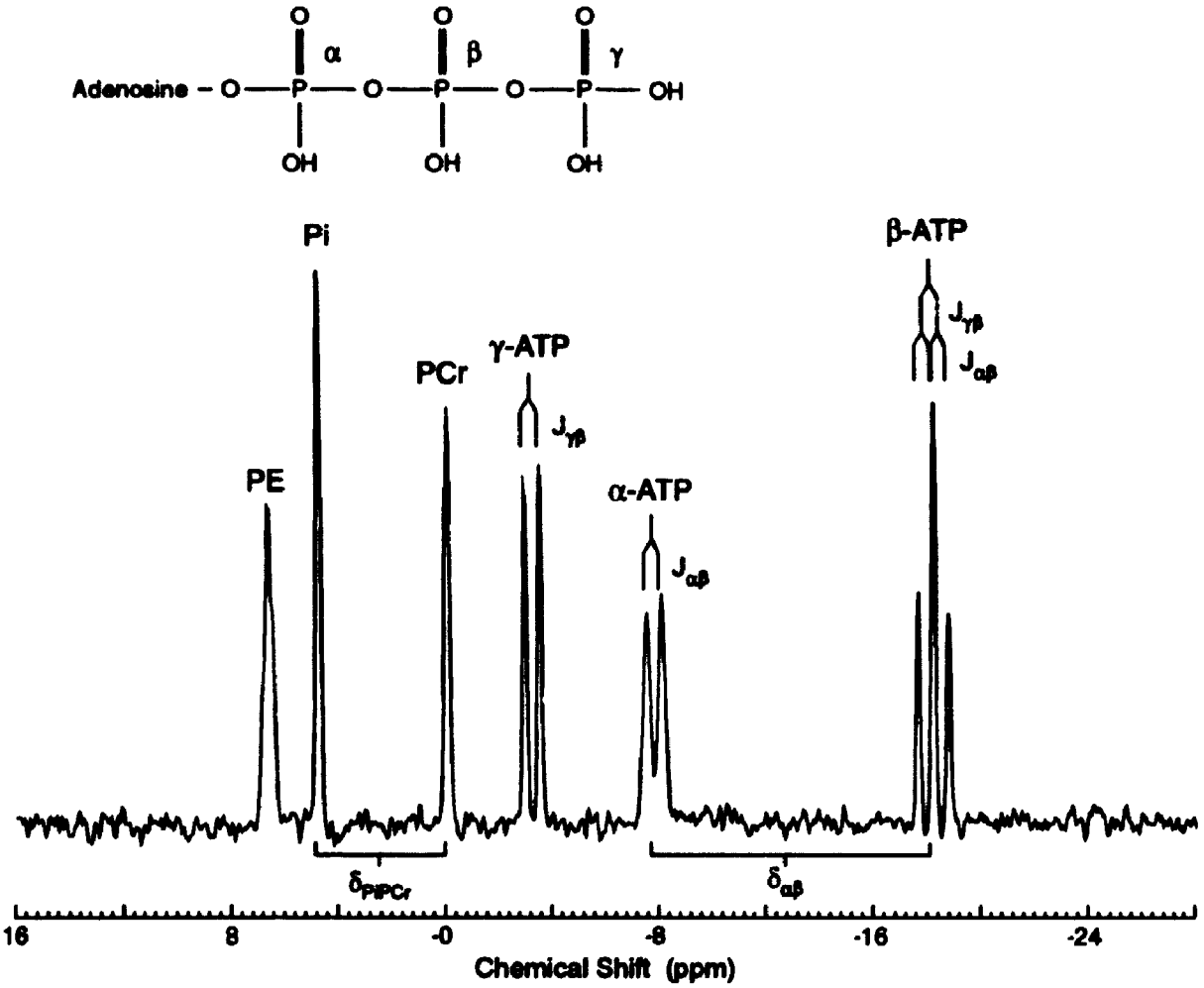

Figure I.1 *In vitro* ^{31}P MR spectrum of ATP, PCr, Pi and PE. (top) Consists of the molecular structure of adenosine triphosphate (ATP). (bottom) Includes an *in vitro* ^{31}P MR spectrum of ATP, PCr, Pi and PE in aqueous solution. The assignment of the resonances are as indicated. The γ- and α-ATP resonances are doublets with separation of $J_{\gamma\beta}$ and $J_{\alpha\beta}$, respectively. The β-ATP resonance is a doublet of doublet where the two middle peaks are superimposed and the two outer peaks are separated by $2xJ_{\alpha\beta}$. The chemical shift differences between Pi and PCr, and between α- and β-ATP are indicated with δ_{PiPCr} and $\delta_{\alpha\beta}$, respectively.

further discussion of scalar spin-spin coupling is given in Appendix A.

I.1.4 The Magnetization.

According to quantum mechanics, nuclei that are exposed to a static magnetic field will have two possible energy states. These two energy states can be interpreted as spins precessing about B_0 with their precessional axis in the direction of the B_0 field (i.e., spins that are up, the lower energy state) or in the direction opposing the B_0 field (i.e., spins that are down, the higher energy state). The energy separation, ΔE, between the two spin states is given by

$$\Delta E = h \cdot \nu_0 = \frac{h \cdot \gamma}{2\pi} \cdot B_0 \qquad [I.4]$$

where h is Planck's constant. At thermal equilibrium, these spins assume a Boltzmann distribution where more spins tend to be up (the preferred state). Consequently, the ensemble of spins in the body give rise to a net magnetization, M_0 (i.e., the sum of the magnetic moments), where the amplitude is proportional to the population difference between the two states. In the absence of a magnetic field, this net magnetization would be zero because the spins are then randomly oriented.

I.1.5 The Applied RF Field.

To observe a MR signal, the net magnetization from the body must first be perturbed (or rotated) from its equilibrium position. This is accomplished by transmitting a RF pulse (burst of energy) or a series of RF pulses to the coil where the RF is at or near the resonant frequency of the nuclei being observed.

This coil which surrounds the body (or part of it) is located in the B_0 field and oriented such that the direction of the applied RF field is perpendicular to B_0. It is convenient to view the magnetization in a frame rotating about B_0 with a frequency at or near the resonant frequency. Therefore, in the rotating frame the magnetization vector will appear stationary if the frequency of the rotating frame coincides with the Larmor frequency. The axes of this rotating frame are x', y' and z' where the z'-axis coincides with the z-axis in the laboratory frame. The laboratory frame with x, y and z axes represents the frame of the B_0 field. Figure I.2a includes an illustration of the laboratory and rotating frames.

The strength and duration of the applied RF pulse dictates the angle of rotation that the net magnetization is tipped from its equilibrium position along B_0. A 90^0 RF pulse, implies that the net magnetization has rotated onto the x',y'-plane and a 180^0 RF pulse, the net magnetization has rotated into the negative z-direction, as indicated in Figure I.2. In medical imaging of the human head, the strength of a 90^0 RF pulse with a duration of $\approx$ 2.5ms is $\approx$ 100Watts. The duration of the RF pulse also dictates the excitation bandwidth of resonant frequencies. For example, a 1ms RF pulse with a square envelope has an excitation bandwidth of ±1kHz and a 1μs RF pulse has an excitation bandwidth of ±1MHz, as illustrated in Figure I.3a and b.

I.1.6 T_1 and T_2 Relaxation.

During the excitation with a RF pulse, the spins in the body absorb energy. Consequently, transitions occur as spins in the lower energy state

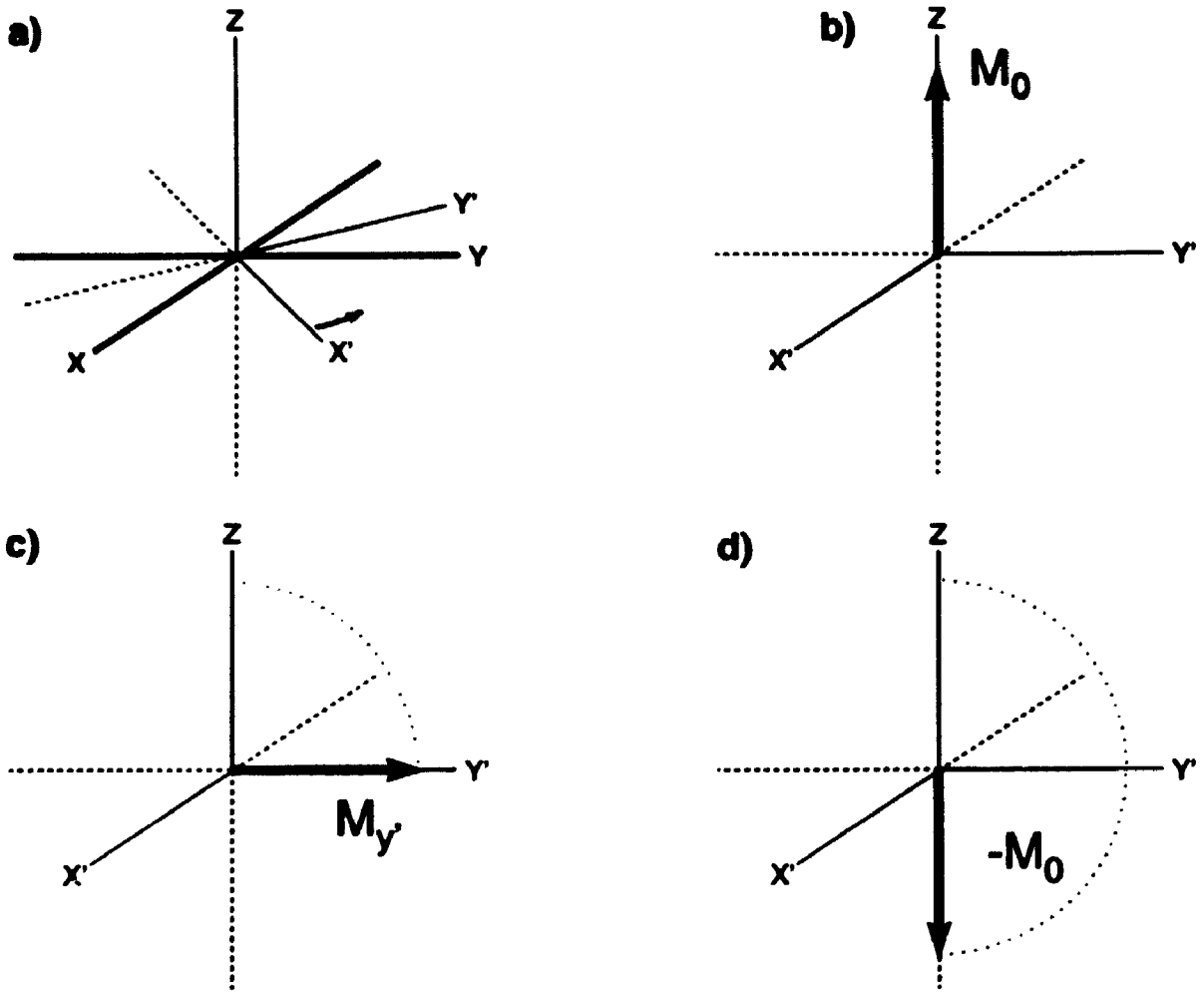

Figure I.2 Rotation of the magnetization with 90^0 and 180^0 RF pulses. a) The laboratory frame has the x-, y- and z-axes while the rotating frame has the x'-, y'- and z-axes. b) Illustrates the magnetization along the z-axis at equilibrium in the rotating frame. c) The magnetization has rotated through 90^0 in the rotating frame such that it lies along the y'-axis. d) The magnetization has rotated through 180^0 in the rotating frame such that it lies along the -z-axis.

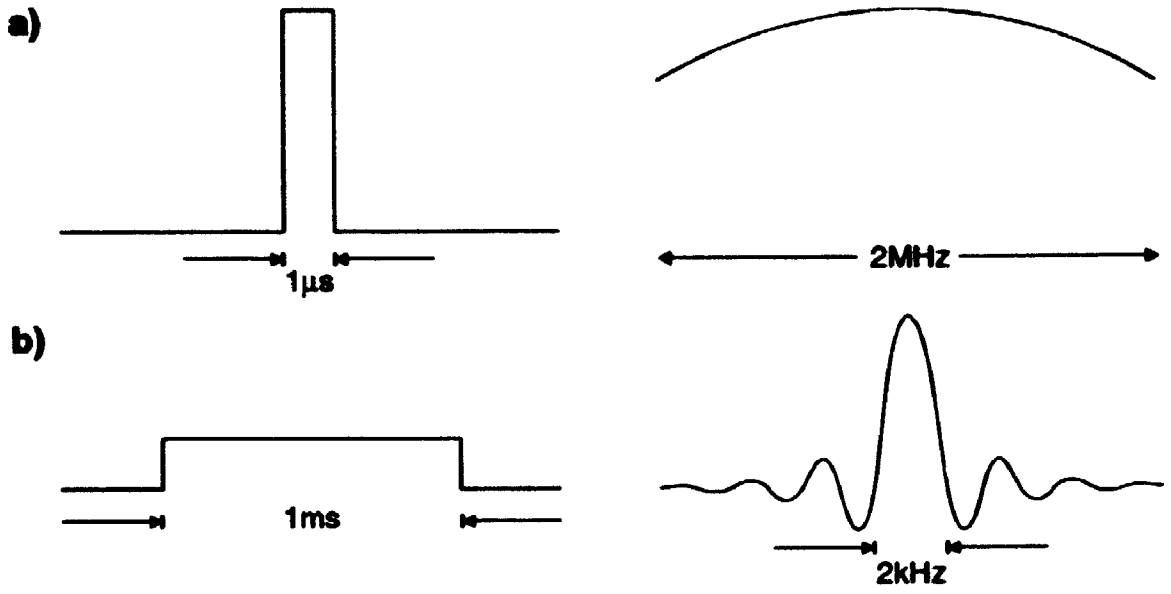

Figure I.3 The dependency of the RF pulse width on the excitation bandwidth of the resonant frequencies. On the left are two rectangular shaped RF pulses of different widths, a) and b), and on the right are their Fourier transform which represents their excitation bandwidth.

populate to the higher energy state which causes the net magnetization to rotate away from the B_0. For example, after a 90^0 RF pulse, the net magnetization is perpendicular to the direction of B_0. Therefore, the population difference is zero as the number of spins up is now equal to the number of spins down. Immediately following the excitation, the magnetization re-establishes or "relaxes" back to thermal equilibrium (i.e., the net magnetization along B_0). Two processes occur during relaxation: *i)* the components of the magnetization in the x',y'-plane, $M_{x'}$ and $M_{y'}$, decay or dephase to zero with a characteristic time T_2, and *ii)* the component of the magnetization along the z-axis, M_z, regrows with a time constant of T_1. T_2 is referred to as the spin-spin relaxation time constant and T_1 is the spin-lattice relaxation time constant where $T_2 \leq T_1$. The time evolution of the relaxation for the magnetization components M_z, $M_{x'}$ and $M_{y'}$ have the following behaviour:

$$M_z(t) = M_0 \cdot (1 - \exp(-\frac{t}{T_1})) + M_z(0) \cdot \exp(-\frac{t}{T_1}) \qquad [I.5]$$

$$M_{x'}(t) = M_{x'}(0) \cdot \exp(-\frac{t}{T_2}) \qquad [I.6]$$

$$M_{y'}(t) = M_{y'}(0) \cdot \exp(-\frac{t}{T_2}) \qquad [I.7]$$

where

$$M_{x'y'} = M_{x'} + iM_{y'} \qquad [I.8]$$

represents the complex signal and $M_{x'}(0)$, $M_{y'}(0)$ and $M_z(0)$ are the initial magnetizations following the RF pulse. Appendix A includes a further discussion on T_1 and T_2.

Due to inhomogeneity of the static magnetic field, enhanced dephasing of the magnetization in the x',y'-plane occurs. The inhomogeneity causes nuclei in different portions of the sample to experience different B_0's and hence different resonant frequencies. Therefore, the observed decay rate of the magnetization in the x',y'-plane due to T_2 relaxation and B_0 inhomogeneity becomes

$$\frac{1}{T_2^*} = \frac{1}{T_2} + \frac{\gamma \cdot \Delta B_0}{2} \qquad [I.9]$$

where ΔB_0 is the variation in the magnetic field across the sample.

I.1.7 The MR Signal.

As mentioned earlier, a coil is also used to receive the MR signal. During relaxation, the rotating magnetization in the x,-y-plane induces a voltage in the coil. This time domain signal which is called a free induction decay (FID) due to its decay characteristic (i.e., T_2^*), is collected. The acquisition process includes amplifying the signal, removing or demodulating the resonant frequency component from the signal and digitizing the signal. To observe the different resonant frequencies, a Fourier transformation is applied. In the frequency domain, the signal (i.e., spectral peak) is measured by its area, which is proportional to the number of nuclei associated with that metabolite. It must

be noted that other factors including T_1 and T_2^* combined with the collection timing parameters, can influence the area of the spectral peak.

The signal-to-noise ratio (S/N) of the MR signal can be improved by averaging several acquisitions. In doing so, the RF pulse train is first applied, followed by acquiring the MR signal for a duration of $\approx 5xT_2^*$. A time delay period is then given to allow the magnetization to re-establish equilibrium (i.e., $5xT_1$), and then the acquisition is repeated starting with the RF pulse train. The pulse repetition time is referred to as the TR time. If the TR is less than $5xT_1$, then the observed MR signal, which is not fully relaxed, will have a magnitude less than the fully relaxed MR signal (at equilibrium). This effect is referred to as partial saturation.

I.2 Acquiring Localized MR Spectra.

The objective of localized *in vivo* MRS is to acquire a MR signal from a specified volume in a region of interest. The simplest method to achieve this requires a single shot acquisition sequence with a surface coil positioned over the region of interest. Another method is based on varying the magnitude of B_0 linearly in a particular direction with a magnetic field gradient, G. This changes the resonant frequency by the following relationship

$$\nu_z = \frac{\gamma}{2\pi} \cdot (B_0 + G_z \cdot z) \qquad [I.10]$$

where G_z is a gradient varying in the z-direction. Hence, the resonant frequency becomes a function of position along the z-direction. Therefore, by

applying a RF pulse during a gradient, G_z, the rotation of the magnetization will only affect the spins at points encompassing a cross-section of thickness Δz in the sample/tissue that are at or near resonance. This thickness Δz, which is defined as the slice thickness, is dependent on the strength of the gradient and the bandwidth of the RF pulse. Figure I.4a illustrates the effect of exciting only the spins within a slice traversing through a sample. Furthermore, to produce a rectangular envelope of frequencies for the excitation slice, the time domain RF pulse is modulated with a truncated, filtered sinc-shaped envelope. These RF pulses with a gradient, are referred to as slice-selective RF pulses.

Variations on these two methods for localizing were utilized in this thesis. To acquire the localized ^{1}H and ^{31}P MRS data, the stimulated echo acquisition mode (STEAM) and fast rotating gradient spectroscopy (FROGS) pulse sequences were used, respectectively.

I.2.1 The STEAM Pulse Sequence.

The localized ^{1}H MR spectra were acquired with a STEAM sequence (Frahm et al. 1989a; Frahm et al. 1990). The concept was first introduced by Hahn in 1950. The sequence consists of applying three 90^0 RF pulses to generate a stimulated echo as indicated in Figure I.5 (top). The abbreviated form of this sequence is

$$90^0 \text{ --TE/2 --}90^0 \text{ --TM --}90^0 \text{ --TE/2 --Acq} \qquad [I.11]$$

where TE is the echo time, TM is the mixing period, and Acq is the acquisition period. The stimulated echo refers to the magnetization that regrows to a

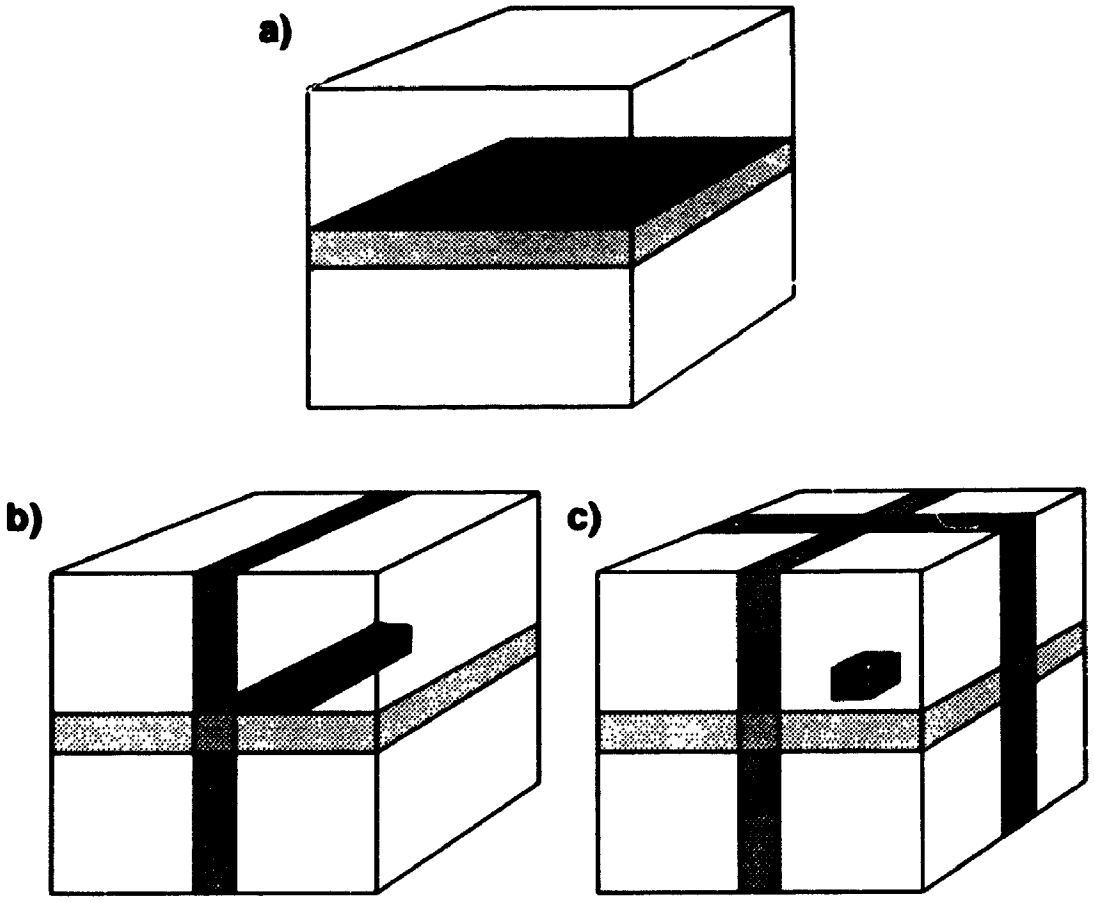

Figure I.4 Slice-selecting a VOI. a) A slice traversing through the sample of finite thickness has been defined by applying a slice-selective RF pulse. b) As a result of applying two orthogonal slice-selective pulses, the intercept generates a defined volume shaped like a long column (shaded in black). c) The intercept of three orthogonal slice-selective pulses that are traversing through the sample generates a cube shaped volume (shaded in black).

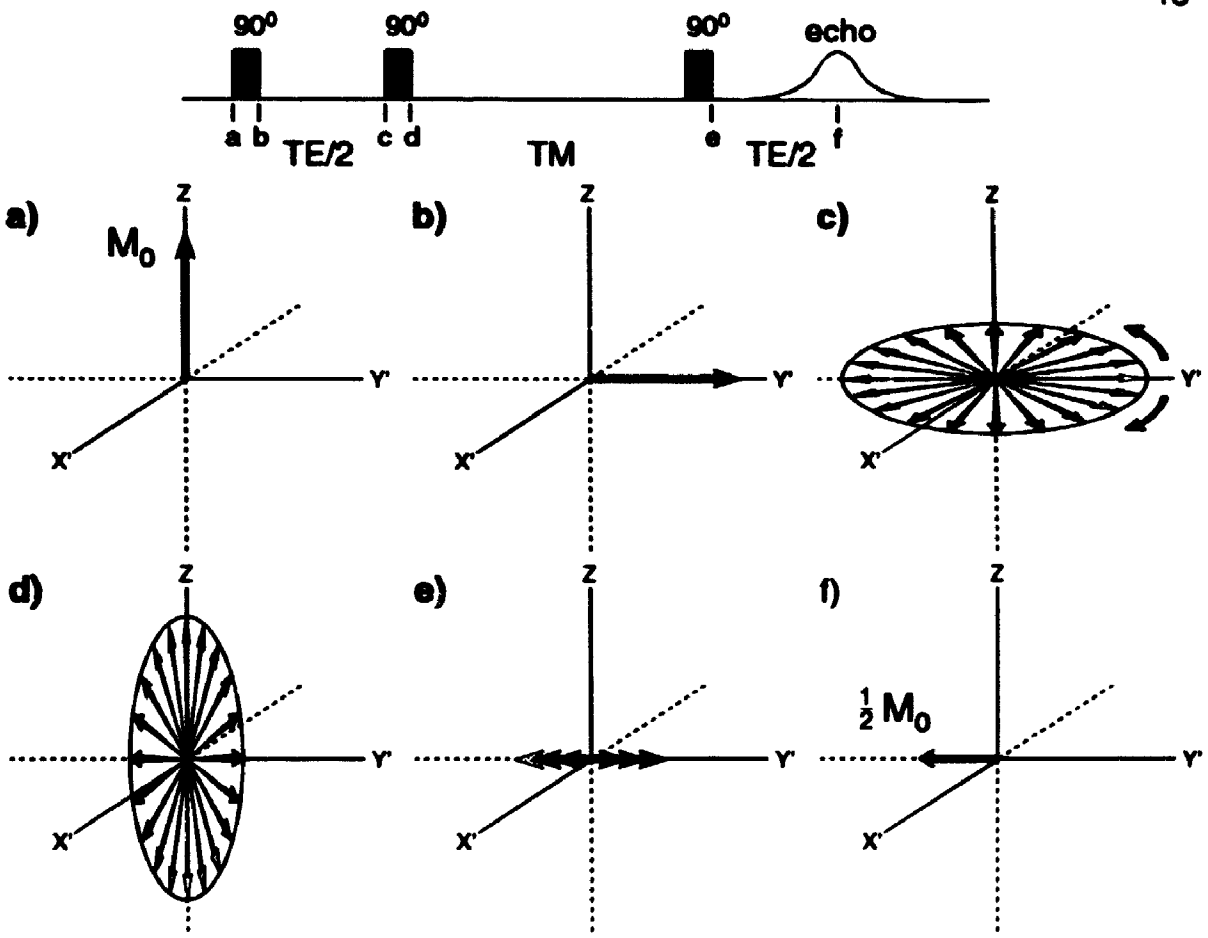

Figure I.5 Time evolution of the stimulated echo sequence. (top) Consists of the pulse train to generate the stimulated echo. The timing position as indicated by the letters, correspond to the appropriate illustrations below. a) At equilibrium, the net magnetization, M_0, is along the z-axis. b) Immediately following the 90° pulse, the magnetization has rotated onto the y'-axis. c) During the TE/2 period the spins have dephased completely. d) All the isochromatic moments have rotated onto the z,x'-plane. e) Immediately after the third RF pulse, the longitudinal magnetization has rotated onto the y'-axis f) At time TE/2 after the third pulse, the spins have refocused the dephased magnetization, $\frac{1}{2}M_0$, which gives rise to the peak of the echo.

maximum amplitude along the y'-axis (arbitrary axis) then decays back to zero.

Figure I.5 is a schematic diagram illustrating the time evolution of the magnetization, M_0, as it is exposed to three 90^0 RF pulses, assuming there is no T_1 or T_2 relaxation. The first 90^0 RF pulse rotates the magnetization onto the x',y'-plane (Figure I.5b) where x' and y' are the axes of the rotating frame of the applied RF field. Immediately following, free precession occurs where the spins dephase due to inhomogeneities in B_0. After a time TE/2, the magnetization (or the individual isochromatic moments as illustrated in Figure I.5c) has averaged to zero in the x',y'-plane. All the isochromatic moments are then rotated onto the z,x'-plane by the second 90^0 RF pulse (Figure I.5d). During the TM period, the projection of the isochromatic moments along the z-axis (the longitudinal magnetization) is unaffected (since it was assumed that there is no T_1 relaxation) and therefore, the longitudinal magnetization maintains its phase and magnitude. The projection of the isochromatic moments along the x'-axis dephase to zero. Immediately following the third pulse, the longitudinal magnetization is rotated back onto the x',y'-plane (Figure I.5e). The spins that are part of the longitudinal magnetization undergo free precession due to inhomogeneities in B_0. After a TE/2 period, these spins have rephased such that the magnetization along the negative y'-axis has refocused to form a stimulated echo (Figure I.5f). Once the maximum amplitude has been reached, these spins dephase and the magnetization along the y'-axis decays to zero (the second half of the echo). Assuming there is no T_1 and T_2 relaxation, the

maximum amplitude of the stimulated echo is ½M_0 which is half the amplitude recovered compared to a spin echo sequence (Hahn 1953). With relaxation, the MR signal would decrease due to T_2 relaxation during the two TE/2 periods, while during the TM period, the longitudinal magnetization would decrease due to T_1 relaxation.

As mentioned, the STEAM pulse sequence requires three 90° excitation pulses to generate a stimulated echo. This is ideal for a localization sequence because these pulses can be defined as three orthogonal slice-selective RF pulses. Consequently, the intersection of these three orthogonal slices defines the VOI, as illustrated in Figure I.4. Figure I.6 is a schematic representation of the STEAM sequence. In addition to these pulses, three Gaussian-shaped RF pulses (chemical shift selective, CHESS, pulses, Haase and Frahm 1985), which are separated by spoiler gradients and have different interpulse delays, are placed at the beginning of the sequence to suppress the water resonance (Figure I.6). The purpose of the spoiler gradients is to enhance the dephasing of the magnetization. Suppression of the water resonance is crucial because the MR signal intensity due to the water resonance is ≈ 10,000 times greater than the intensity of proton-containing metabolites (i.e. the *in vivo* [H_2O] ≈ 55.6M while [proton-containing metabolites] ≈ 10mM) and consequently, the extending "wings" of the water resonance lie over the spectral region of the metabolites under investigation. These CHESS pulses are long in duration and low in amplitude to generate a narrow excitation bandwidth in the

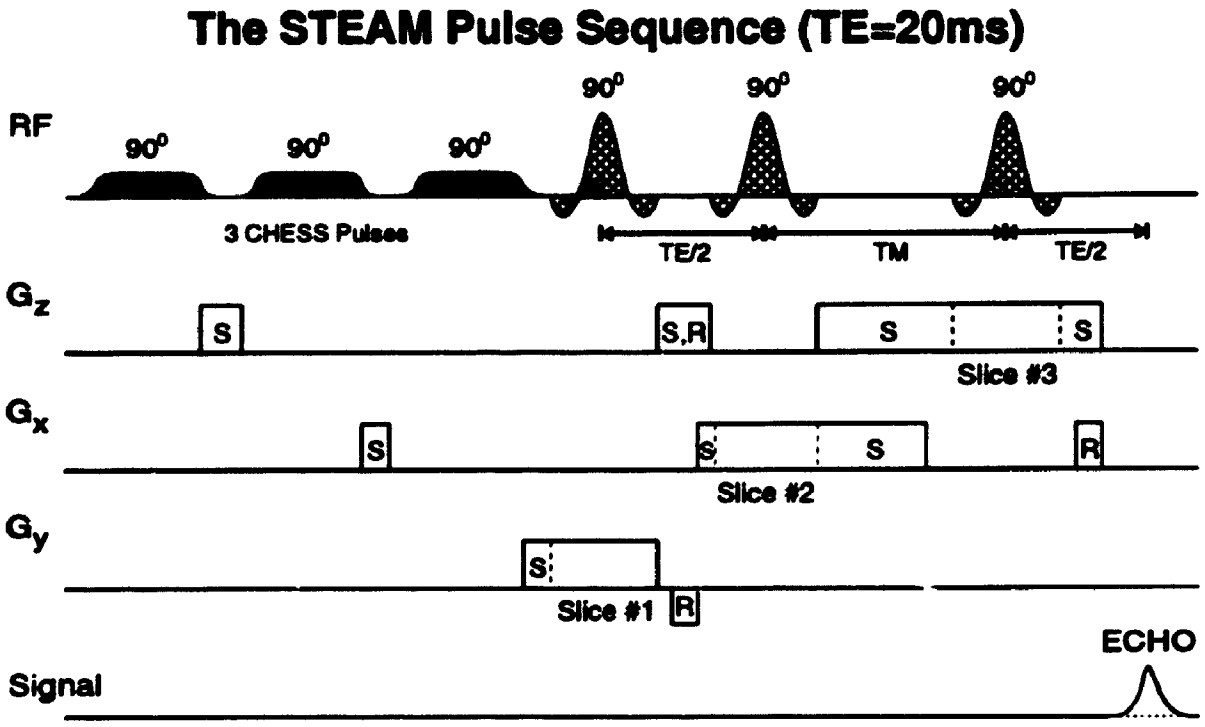

Figure I.6 A schematic representation of a STEAM sequence illustrating the timing of the RF pulses and the magnetic field gradients. At the beginning of the sequence there are three CHESS pulses separated by spoiler gradients to suppress the water MR signal. Following, there are three 90° sinc-shaped slice-selective RF pulses to create the stimulated echo. The S's denote the approximate position of the spoiler gradients and R's denote the location of the slice refocusing gradients.

frequency domain that encompasses the water resonance (Bauer et al. 1984). As a result, the combination of CHESS pulses and spoiler gradients destroys (saturates) most of the longitudinal magnetization of water while leaving the magnetization of the metabolites primarily unaffected and ready for the first 90° excitation pulse.

The STEAM sequence is one of the better single voxel localization techniques for accurately defining the VOI compared to other sequences such as PRESS, a localized single voxel double echo acquisition sequence (Ordidge et al. 1985; Bottomley 1987). 90° sinc-shaped slice-selective RF pulses, which are used in the STEAM sequence, provide better spatial localization than 180° sinc-shaped slice-selective RF pulses (which are used in the PRESS sequence; Moonen et al. 1989). The STEAM sequence uses no phase encoding gradients , therefore, there are no "bleed through artifacts" in the spectra as seen in CSI data (chemical shift imaging; Bottomley 1991). STEAM is also a single-shot acquisition sequence unlike ISIS (image selective *in vivo* spectroscopy; Ordidge et al. 1986) where multiple phase-cycling steps are required.

The STEAM sequence is unique in that it offers control over the degree of T_2 and T_1 relaxation on the acquired MR signal (unlike the PRESS sequence which only has T_2 dependencies). As a result, the STEAM sequence permits shorter echo times (i.e., typically TE= 20ms for STEAM vs TE= 40ms for PRESS). Using a shorter echo time such as a TE=20ms minimizes the overall attenuation of the MR signal (due to T_2 relaxation), increases the MR signal

detection of shorter T_2 species such as glutamate, and minimizes the J-modulation effects (due to spin-coupled resonances; Ernst and Hennig 1991; Wilman and Allen 1993).

In this thesis, the STEAM sequence with TE=20ms and TM=30ms was provided by Siemens. The three 90^0 sinc-shaped slice-selective RF pulses were 2.56ms in length and the slice-selection gradients were $3mTm^{-1}$ in strength. Consequently, the chemical shift uncertainty was ≈0.05cm/ppm. This implies that the signal of NAA (CH_3) with a chemical shift of 2.024ppm would come from a volume that has shifted by 1mm in all three directions relative to the position of the volume from the water signal. The three CHESS pulses were 25.6ms in length, which represents approximately a 60Hz spectral excitation bandwidth, and the spoiler gradients were $3mTm^{-1}$ in strength. The unsuppressed water ^1H spectra were collected by setting the amplitudes of the three CHESS pulses to zero voltage.

I.2.2 The FROGS Pulse Sequence.

FROGS is a spatially defined spectroscopy technique that combines the use of a surface coil with slice-selective RF pulses. This technique takes advantage of the spatially defined RF characteristics of a surface coil where the amplitude of the RF pulse determines the depth of the 90^0 excitation. Addionally, slice-selective RF pulses are used to saturate the MR signal outside the VOI. For example, to acquire a MR signal from the dorsolateral prefrontal cortex, the surface coil is positioned on the forehead and the saturation slice

(which is close to parallel to the coil) is positioned between the coil and the cortex area. The saturation slices eliminate the unwanted MR signal from the scalp and skull, while the surface coil limits the depth of reception of the MR signal to cortical structures. An illustration representing the positioning of the surface coil and saturation slice, and location of the received signal from the cortex area, is shown in Figure I.7. This technique is a single shot acquisition sequence that does not require multiple steps to phase cycle the RF pulses, unlike ISIS (image-selected *in vivo* spectroscopy). The pre-acquisition delay time is determined only by the response time of the receiver and not by additional delays to prepare the spin system, unlike CSI (chemical shift imaging) techniques. Therefore, the FROGS technique is ideal for obtaining MR signal from short T_2 species.

Siemens provided our laboratory with the FROGS pulse sequence. A schematic representation of the FROGS pulse sequence is shown in Figure I.8. The pulse sequence contains two segments: an initial saturation period which consists of ten slice-selective saturation RF pulses, alternating between 90^0 and 180^0, and decreasing in interpulse delay; followed by a nonselective RF excitation pulse. The slice-selective pulses which are acting on the same spatially defined slice, were 2.56ms in length. For a slice thickness of 25mm, a $6mTm^{-1}$ gradient was required, which gave a saturation slice uncertainty of $\approx$0.26mm/ppm. As an extreme case, if the β-ATP resonance was the frequency of the applied RF, the slice defined for the PME signal would be shifted by $\approx$

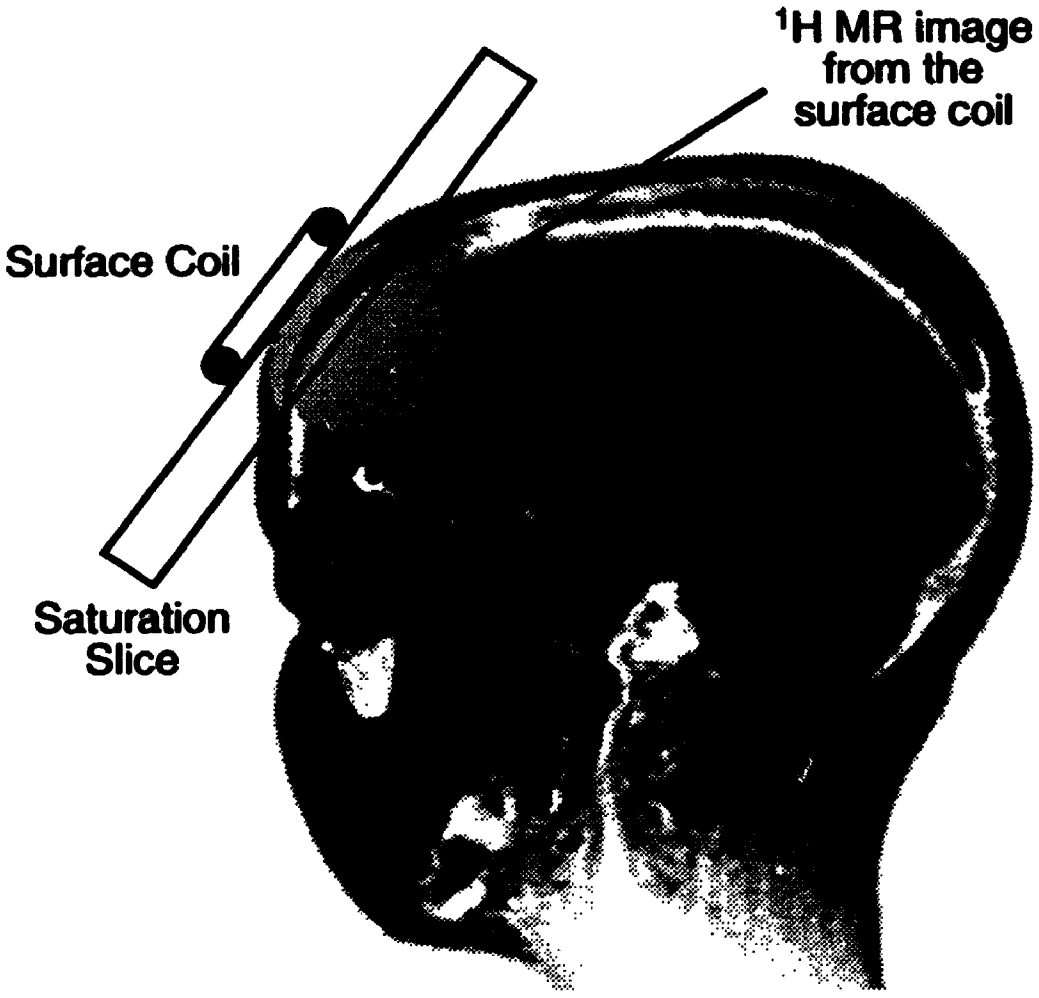

Figure I.7 Positioning of the surface coil and the saturation slice. The figure includes a sagittal ^{1}H image superimposed on an illustration of the surface coil and the saturation slice generated in the FROGS sequence to suppress the signal from the scalp and skull. A super-imposed ^{1}H image acquired with the surface coil is also shown which approximates the mid cross sectional area of the brain tissue measured with ^{31}P MRS.

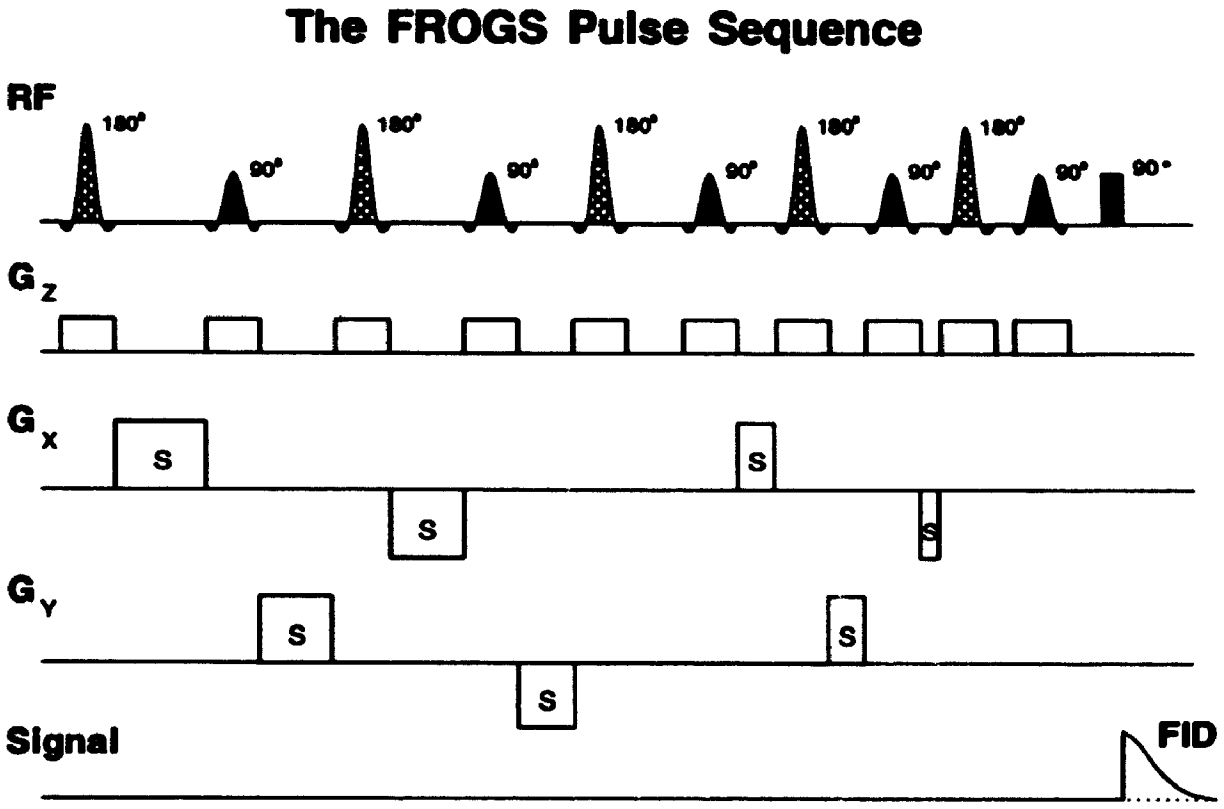

Figure I.8 A schematic representation of FROGS pulse sequence illustrating the timing of the RF pulses and the magnetic field gradients. The first segment of the sequence consists of ten slice-selective RF pulses separated by spoiler gradients. The second part contains a single nonselective rectangular-shaped RF pulse. The S's denote the approximate position of the spoiler gradients.

5.7mm from the position of the defined slice of the β-ATP signal. The spoiler gradients, as indicated in Figure I.8, were 4mTm^{-1} in strength and the pulse width of the nonselective rectangular-shaped RF pulse was 300μs. The total time to execute the ten slice-selective pulses is 153ms. The purpose of multiple slice-selective pulses with varying amplitudes and interpulse delays, in addition to spoiler gradients of random orientation between these RF pulses, is to ensure the longitudinal and transverse magnetization within the spatially defined slice has been destroyed.

I.3 Spectral Information.

I.3.1 Proton MRS.

A ^{1}H MR spectrum contains a wealth of information on metabolites which contain protons and have physiological concentrations of ≈1mmol/kg wet weight or greater. For example, ^{1}H MRS brain studies provide steady-state metabolic levels of neurotransmitters such as glutamate, γ-aminobutyric acid (GABA) and aspartate (Michaelis et al. 1991, Rothman et al. 1992, Wilman and Allen 1993, Provencher 1993). Neuronal cell population can be obtained by quantifying the spectral contribution of NAA, a metabolite which predominately resides in neuronal cells and not in astrocytes (Nadler and Cooper 1972, Birken and Oldendorf 1989, Urenjak et al. 1993). The *in vivo* metabolite levels of glutamine, N-acetylaspartylglutamate (NAAG), glucose, *scyllo*-inositol, choline-containing compounds (Cho_t, which includes phosphorylcholine, PCho, glycerophosphorylcholine, GPCho, and choline, Cho) and phosphocreatine plus

creatine (PCr+Cr) can also be quantified (Frahm et al. 1991; Michaelis et al. 1991; Michaelis et al. 1992; Provencher 1993).

I.3.2 Phosphorus MRS.

For over three decades *in vivo* and *in vitro* ^{31}P MRS has been used to study cellular physiology (Moon and Richards, 1973; Ackerman et al. 1980; Gadian and Radda 1981; Ross et al. 1981; Radda 1986). It has been only in the last decade that *in vivo* ^{31}P MRS has provided physiological information of normal and pathological tissue in the human brain, heart and liver. A typical *in vivo* ^{31}P spectrum of the brain (Figure I.9) includes resonances due to ATP, the main energy source in brain cells; PCr, an important energy store for the cell, and inorganic orthophosphate (Pi) (Gadian and Radda 1981). Phosphomonoesters (PME's) and phosphodiesters (PDE's) can also be observed in a ^{31}P spectrum as indicated in Figure I.9 (Pettegrew et al. 1986; Pettegrew et al. 1987). PCho, phosphorylethanolamine (PE) and phosphorylserine (PS) are the predominant metabolites that contribute to the observed PME signal and they are active mainly in the synthesis of cell membranes (Pettegrew et al. 1986). The observed PDE signal primarily consists of GPCho and glycerophosphorylethanolamine (GPE) which are mainly the breakdown products of cell membranes (Pettegrew et al. 1986). In biological systems, membrane phospholipids play a major role in the structure and function of all cells (Farooqui and Horrocks 1985). Membrane phospholipids basically define the inside/outside compartments of cells and

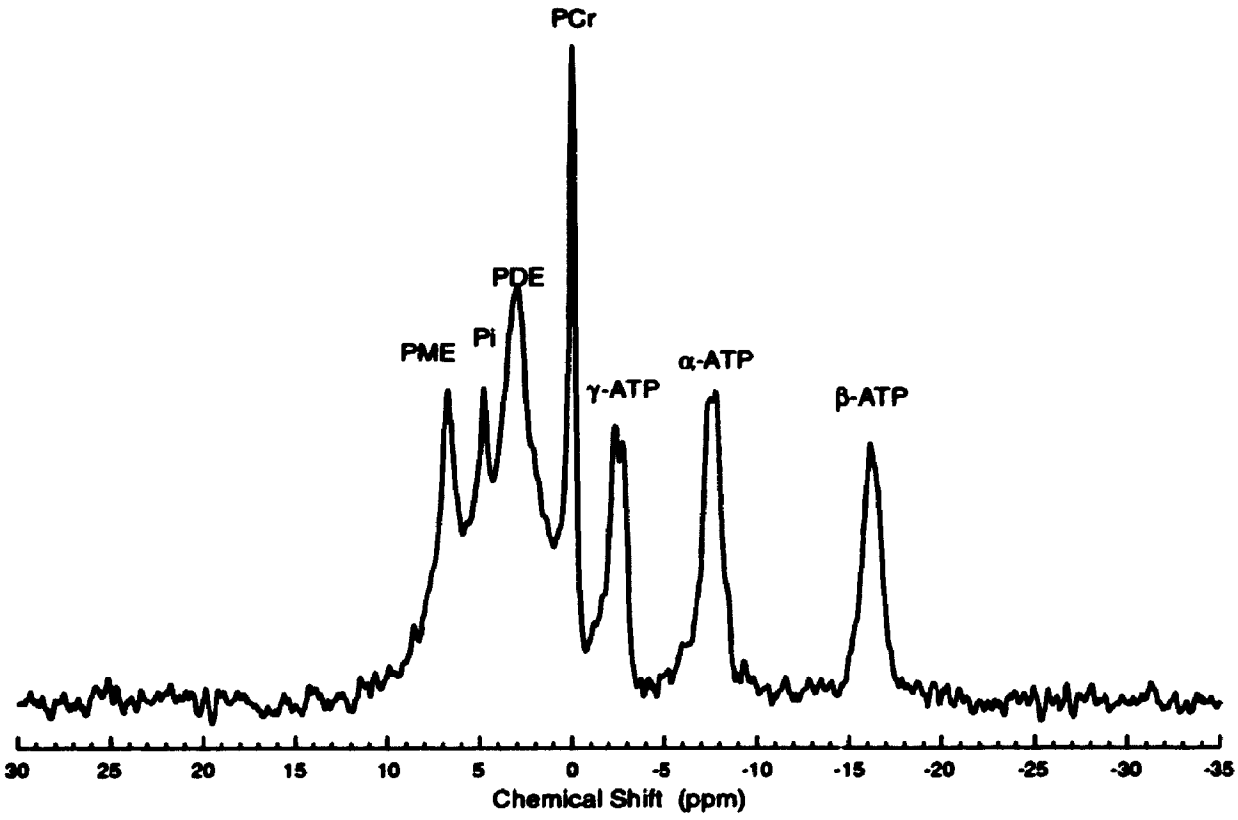

Figure I.9 A typical processed *in vivo* ^{31}P MR spectrum from the left dorsolateral prefrontal cortex of a normal control acquired at 2.0Tesla. The spectral assignments are as indicated.

determine the nature of all cellular comunications between inside and outside compartments. Membrane phospholipids are structured in a bilayer formation as illustrated in Figure I.10. The components of a phospholipid include a phosphate-linked group (i.e., choline, ethanolamine and serine), a phosphate, a glyceryl framework and two fatty acid chains (Figure I.10). A schematic representation of PME's as precursors and PDE's as breakdown products of membrane phospholipids is shown in Figure I.11.

Magnesium (Mg^{2+}) is an important co-factor in many enzymatic reactions in which ATP is a substrate. Consequently, the binding of Mg^{2+} to ATP (primarily the β-ATP site) alters the chemical shift of the β-ATP resonance. Therefore, by determining the chemical shift difference between the α- and β-ATP resonances ($\delta_{\alpha\beta}$, as indicated in Figure I.1), the intracellular free magnesium concentration ($[Mg^{2+}]_{intra}$) can be estimated using the following equation by Gupta et al. (1984):

$$[Mg^{2+}]_{intra} = K_D \cdot \frac{\delta_{ATP} - \delta_{\alpha\beta}}{\delta_{\alpha\beta} - \delta_{MgATP}} \qquad [I.12]$$

where δ_{ATP} = 10.81ppm and δ_{MgATP} = 8.32ppm are the chemical shift values for pure and complex forms of ATP and the dissociation constant is assumed to be K_D = 50μM. Likewise, due to the sensitivity of the chemical shift difference between the Pi and PCr resonances (δ_{PiPCr}, as indicated in Figure I.1), the intracellular pH can be calculated with the following equation (Petroff et al.

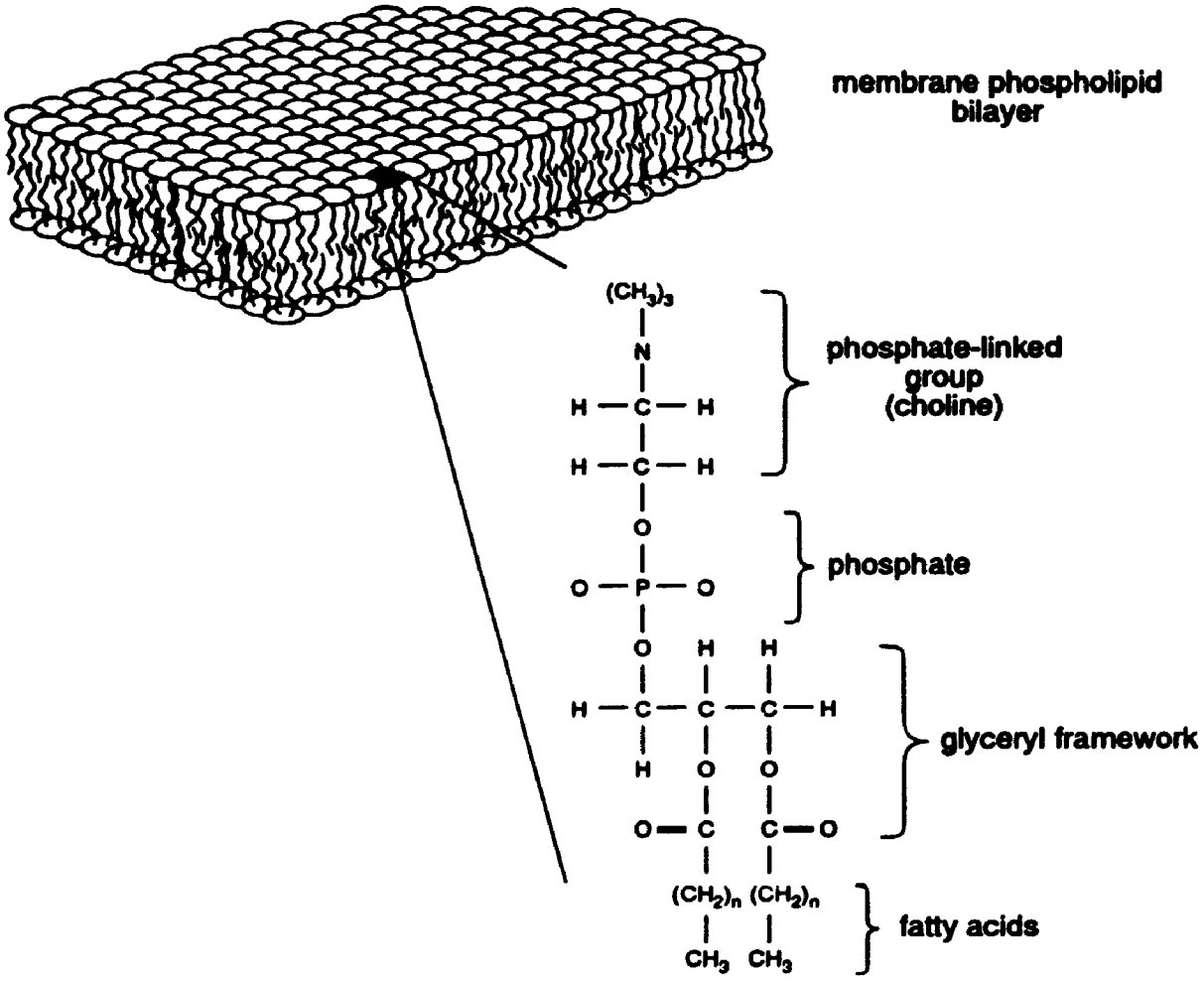

Figure I.10 An illustration of a membrane bilayer (top) and the structure of a phospholipid (bottom). The components of a phospholipid (PtdCho) are as indicated.

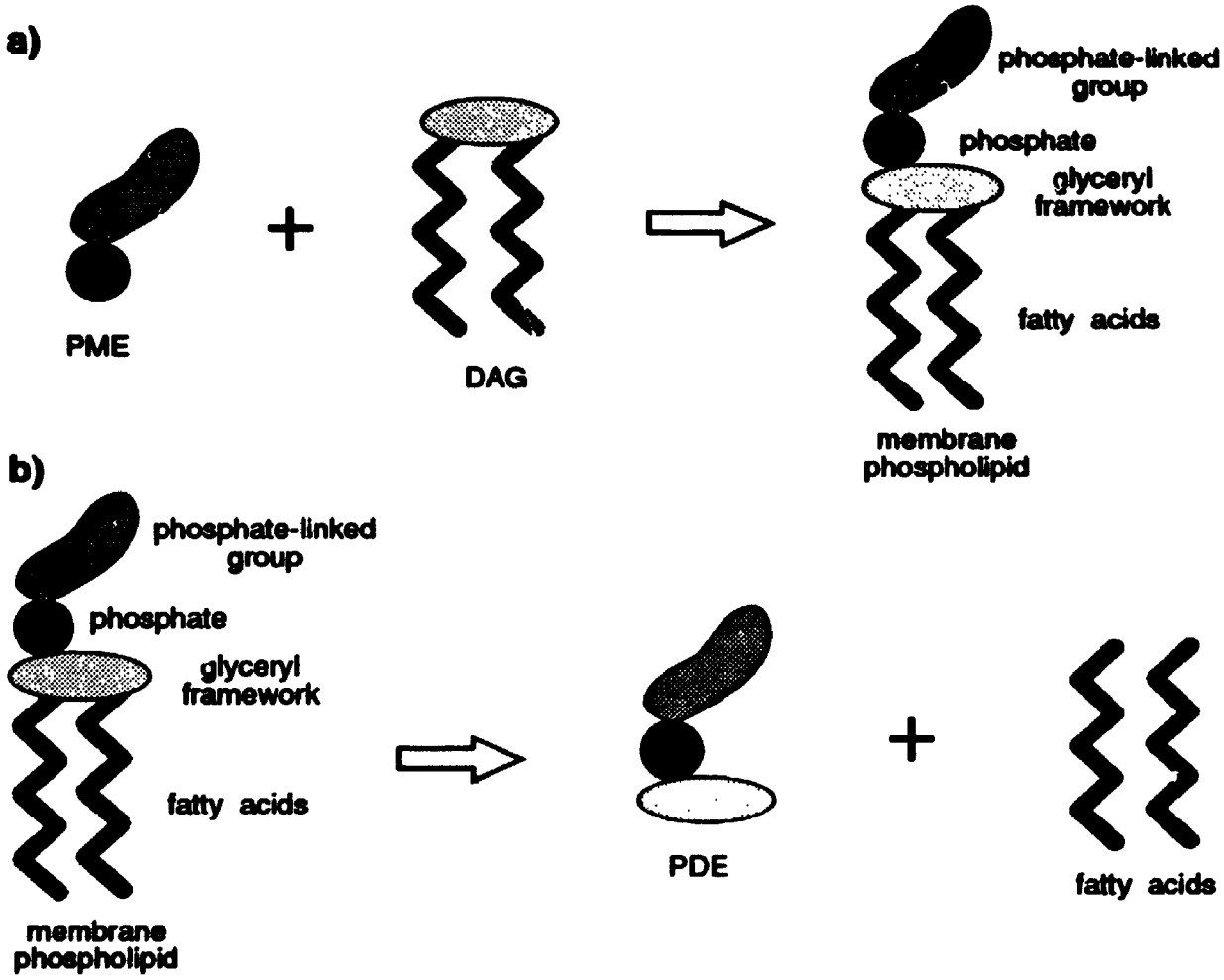

Figure I.11 Membrane phospholipid metabolism. A schematic showing the anabolic (a) and catabolic (b) pathways of membrane phospholipid metabolism.

1985):

$$pH = 6.77 + \log \frac{\delta_{PiPCr} - 3.29ppm}{5.68ppm - \delta_{PiPCr}} \quad . \qquad [I.13]$$

I.4 Quantification of MR Spectra.

The *in vivo* MR signal of metabolites gives rise to single or multiple resonances. This information in a FID, S(t), is in the form of exponentially damped sinusoids:

$$S(t) = \sum_{k=1}^{K} a_k \cdot \exp(i \cdot \phi_k) \cdot \exp(-t / T_{2k}^*) \cdot \exp(i \cdot \omega_k \cdot t) \qquad [I.14]$$

where for resonance k the amplitude is a_k, the phase is ϕ_k, the frequency is ω_k and the exponential decay constant is the inverse of the T_{2k}^* relaxation time. The amplitude of a sinusoid is directly proportional to the number of nuclei associated with that resonance (i.e., CH, CH_2, CH_3, PO_3) and is subsequently proportional to the concentration of that metabolite. In quantifying the MR signal such that the metabolite levels are obtained, the amplitudes of these exponentially damped sinusoids are estimated. There are several different methods available to estimate the amplitudes of damped sinusoids which are based on using modelled functions as in Eq. I.14 (de Beer and van Ormondt 1992). An alternative approach in quantifying the MR signal, is to estimate the metabolite levels in the frequency domain. By applying a Fourier transformation

to the FID, the exponentially damped sinusoids are now of the form of Lorentzian lineshapes with amplitudes a_k, phases ϕ_k, angular frequencies ω_k, and linewidths that are proportional to $(T_{2k}^*)^{-1}$. In this case, the area under the Lorentzian lineshape ($\propto$ amplitude·linewidth) is directly proportional to the number of nuclei associated with that resonance. For example, the NAA molecule gives rise to a singlet due to the CH_3 group and four spectral peaks (i.e., doublet of doublet) due to the CH_2 group. The area ratio between the singlet and the total of the four peaks is 3:2 (assuming there is no relaxation).

For reasons to be discussed in chapter III, the quantification of the *in vivo* ^1H and ^{31}P MRS data was done in the frequency domain where Gaussian and Lorentzian lineshapes were used, respectively, to model the spectral peaks. The ^1H MRS data was modelled with Gaussian lineshapes because a Lorentzian-to-Gaussian transformation was applied in the time domain prior to the Fourier transformation to enhance the spectral resolution.

The Lorentzian lineshape, L(ν), for a spectral peak j has the form

$$L(\nu) = \frac{pa_j}{1 + 4 \cdot \left(\frac{\nu - \nu_j}{w_j}\right)} \qquad [I.15]$$

where pa_j is the spectral peak amplitude, w_j is the full width at half maximum (FWHM) value and ν_j is the centre frequency position of the peak. The area of the Lorentzian lineshape is then determined by

$$\text{area} = \frac{\pi}{2} \cdot pa_j \cdot w_j \ . \qquad [I.16]$$

The Gaussian lineshape, G(ν), for a spectral peak j has the form

$$G(\nu) = pa_j \cdot \exp\left(-\left(\frac{\nu - \nu_j}{W_j}\right)^2\right) \qquad [I.17]$$

where $W_j = (2\sqrt{\ln 2})^{-1} \cdot w_j$ and the area of a Gaussian lineshape is calculated by

$$\text{area} = \sqrt{\pi} \cdot pa_j \cdot W_j \ . \qquad [I.18]$$

The fitting routine varies the amplitude, peak position and the FWHM until the difference between the model spectrum and the acquired spectrum is minimized (i.e., the sum of the chi squares of each data point is minimized).

I.5 The Software and Hardware Equipment.

All *in vitro* and *in vivo* MRS experiments were conducted on a whole body MR spectrometer (Helicon SP system, Siemens AG, Erlanger, Germany). Software to collect and display spectroscopy and imaging data was provided by Siemens (i.e., "NUMARIS", Siemens' operating system, version A2.5). This thesis required the acquisition of both ^{1}H and ^{31}P MRS data on the subjects. Consequently, for the study in Chapters IV and V, the ^{1}H MRS protocol was conducted first. It took approximately 45-60 minutes to collect one localized

spectrum with the STEAM sequence. The ^{31}P MRS protocol was then carried out, which required a change in the static magnetic field from 1.5Tesla to 2Tesla. By collecting the ^{31}P data at 2Tesla, the S/N improves by approximately 32% compared to the S/N of the data collected at 1.5Tesla (Boska et al. 1990). This increase in the S/N is beneficial because the inherent sensitivity of the ^{31}P nuclei is 1/15 of the ^{1}H nuclei. This process required approximately 40 minutes to re-establish stability of the static magnetic field. The subject was re-positioned in the magnet and the time required to acquire the ^{31}P data was approximately 40-60 minutes.

For the ^{1}H MRS experiments, a circularly polarized head coil (a product of Siemens) was used to transmit the RF pulses and receive the ^{1}H MR signal. This coil provided adequate B_1 homogeneity over a field of view of at least 240mm which is required for volume excitation pulse sequences (i.e., collecting ^{1}H STEAM and imaging data). For the ^{31}P MRS experiments, a 5cm transmit/receive surface coil (a product of Siemens) was used. This coil was able to operate at either the ^{1}H or ^{31}P frequency.

The low-pass filter used in the receiver, was a Tschebbyscheff for the ^{1}H STEAM and imaging experiments, and a Bessel function for the ^{31}P MRS experiments. The Tschebbyscheff filter provides a sharp frequency cutoff at the expense of a slow response time and a large overshoot in the response. This filter was adequate with the bandwidth used to collect the STEAM data. However, the ^{31}P data was more sensitive to the response time of the filter.

Therefore, the Bessel function provided a fast response time, a linear phase behaviour, and minimal overshoot in the response at the expense of a gradual frequency cutoff.

All of the processing and fitting of the data was done offline on a personal computer. Therefore, the data files were transferred from the VAX computer system to a personal computer via the hospital's ethernet system. All the steps taken to process both the ^{1}H and ^{31}P data were done using the NMR-286 commercial software package (Soft Pulse Software, Box 504, Guelph, Ontario, CANADA, N1H 6K9). The fitting of the ^{31}P data was also done using the NMR-286 package, however, fitting the STEAM data with *a priori* knowledge was done using an in-house software package. With the help of John Potwarka (hired as a summer student) to write the software, this in-house fitting software package was developed in our laboratory which enabled complete control by the operator to input *a priori* knowledge into the fitting algorithm.

The statistical analysis was done using the SPSS for Windows software package (SPSS Inc.).

CHAPTER II

The Illness of Schizophrenia

Schizophrenia is no longer regarded as a "functional psychosis" which implies that the delusions, hallucinations and cognitive impairments that schizophrenic patients endure arise from disorderly activity of neurons due to structural and/or functional abnormalities in the brain. The illness of schizophrenia affects about one in every 100 Canadians. The lifelong risk of someone developing schizophrenia is 1%, a prevalence five times greater than multiple sclerosis. The onset of symptoms appear between the ages of 15 and 45 years for 90% of the cases. Approximately 40% of the patients affected with schizophrenia result in having a lifelong debilitating illness (Crow and Johnstone 1987). For these reasons, the social and economical cost for the care of patients with schizophrenia in 1985 was estimated at approximately $40 billion in the United States (McGuire 1991).

Over the years, research in schizophrenia has encompassed many different avenues including studies in social, genetic and obstetric factors, neuropathology, *in vitro* neurochemistry, *in vitro* brain morphology and functional imaging, yet this brain disease is not fully understood in terms of its pathophysiology. It is unclear what neuronal circuitry or neurophysiological process underlies the illness of schizophrenia. Additionally, it is unclear at what point in life this illness develops. This raises many questions, including: are

genetic factors involved? (Owen and Mullan 1990; Jones and Murray 1991); are there abnormalities in the neurodevelopment? (Weinberger 1987; Nasrallah 1993); is schizophrenia a neurodegenerative illness?

MRS is not the definitive technique to study the illness of schizophrenia, however, it does provide *in vivo* information on the biochemistry of a specified region of interest which is not possible with any other technique. This includes information on *i)* metabolite levels of excitatory and inhibitory neurotransmitters, *ii)* neuronal cell viability, *iii)* membrane phospholipid metabolism and *iv)* high-energy phosphate metabolism (Chapter I). Therefore, obtaining an *in vivo* biochemical analysis on patients with schizophrenia offers a new dimension towards the understanding of the neurobiological underpinnings of schizophrenia.

Techniques measuring brain function and brain structure of schizophrenic patients have resulted in implicating three main brain regions, the frontal lobes, the temporal lobes and the basal ganglia (Buchsbaum 1990). This suggests that the abnormality causing these symptoms of delusion, hallucination and cognitive impairments in schizophrenia involves several brain regions. It is for this reason that schizophrenia could be considered as an abnormality involving a neuronal pathway or different neuronal pathways connecting these brain regions. In the human brain, the neurotransmitter system is composed of predominantly excitatory glutamatergic and inhibitory GABAergic pathways, which may be implicated (Curtis and Johnston 1974; Fagg and Foster 1983,

Erecińska and Silver 1990). This emphasizes the importance of obtaining *in vivo* biochemical analyses on schizophrenic patients, since ^{1}H MRS is capable of quantifying *in vivo* levels of neurotransmitters including glutamate. Recently, attention has focused on the excitatory amino acid (EAA) system of schizophrenic patients as several studies have observed abnormalities in the glutamatergic system (Wachtel and Turski 1990; Ulas and Cotman 1993).

As these issues dealing with functional and anatomical aspects and the glutamatergic system are of interest to this MRS study, the following includes a literature review of past and present studies on schizophrenia involving these matters. A discussion will then follow on previous MRS studies in schizophrenia and their results. The objectives, hypotheses and outline of this thesis will then follow.

II.1 Functional and Anatomical Studies in Schizophrenia.

Abnormalities in the frontal lobe activity of schizophrenic patients during cognitive tasks have consistently been cited. With quantitative studies involving electroencephalogram (EEG) measures (Hoffman et al. 1991; Morrison-Stewart et al. 1991), cerebral blood flow (Berman et al. 1986; Weinberger et al. 1986; Berman et al. 1988; Weinberger et al. 1988), and positron emission tomography (PET) (Cohen et al. 1987; Volkow et al. 1987; Buchsbaum 1990; Buchsbaum et al. 1990; Andreasen et al. 1992; Buchsbaum et al. 1992), a reduction in activity has been demonstrated in the frontal lobes of schizophrenic patients during these frontal lobe tasks.

MRI techniques provide anatomical images with spatial resolution of ≈ 1mm which is ideal for volumetric measurements of brain structures. However, volumetric results from the prefrontal region have not been consistent, even with the recent improvement of using thinner cross-sectional slices to obtain these volumes. Zipursky et al. (1992) have observed a reduction only in grey matter volume while Breier et al. (1992) and Buchanan et al. (1993) have observed a decrease in white matter volume from the prefrontal region of schizophrenic patients compared to controls. T_2 relaxation time constants, which reflect the water environment in tissue, can also be obtained from the MRI images. Williamson et al. (1992) have observed an increase in T_2 values in the left prefrontal white matter of patients compared to controls.

In most cases, studies of the temporal lobes in schizophrenic patients have resulted in observing structural abnormalities as opposed to functional deficits during cognitive tasks. Reduced temporal and hippocampal volumes, estimated from MRI techniques, have been observed in patients with schizophrenia compared to controls by many research centres (Suddath et al. 1989; Barta et al. 1990; Bogerts et al. 1990; Dauphinais et al. 1990; Rossi et al. 1990; Suddath et al. 1990; Shenton et al. 1992). However, several volumetric studies of the temporal lobes in schizophrenic patients using MRI have reported no significant differences in volumes compared to controls (Kelsoe et al. 1988; DeLisi et al. 1991; Young et al. 1991) and Zipursky et al. (1992) reported there was a widespread cortical loss in schizophrenic patients.

Structural abnormalities in the basal ganglia (which includes the striatum, substantia nigra and the subthalamic nucleus, figures II.1, II.2 and II.3) of schizophrenic patients have been observed in several studies. Enlargement of the lenticular nucleus (i.e., the putamen and the globus pallidus, figures II.1 and II.2) has been observed in schizophrenic patients compared to controls using MRI (Jernigan et al. 1991; Swayze et al. 1992). This increase in volume coincides with a post-mortem study where the volume of the striatal region (figures II.1 and II.2) was also increased in the patient group compared to controls. Increased T_2 relaxation times have been reported in the lenticular nucleus but on the left side only of patients with schizophrenia compared to controls (Williamson et al. 1992).

II.2 Evidence Implicating Glutamatergic System.

The central dopaminergic system has been implicated in schizophrenia for almost 20 years (Angrist et al. 1971; Carlsson and Lindquist 1963; Stevens 1973). This classical dopamine hypothesis states that there is an increased activity of dopamine neurotransmission in schizophrenic patients (Meltzer and Stahl 1976; Seeman 1987). Evidence was based on several observations: *i)* conventional anti-psychotic medication targets the dopamine system by blocking the central dopamine D_2 receptors, *ii)* the correlation of the effectiveness of anti-psychotic drugs and the degree of D_2 receptors blockage, *iii)* increased density of D_2 receptors in schizophrenic patients and *iv)* the administration of amphetamine, a dopamine agonist, induces psychotomimetic symptoms

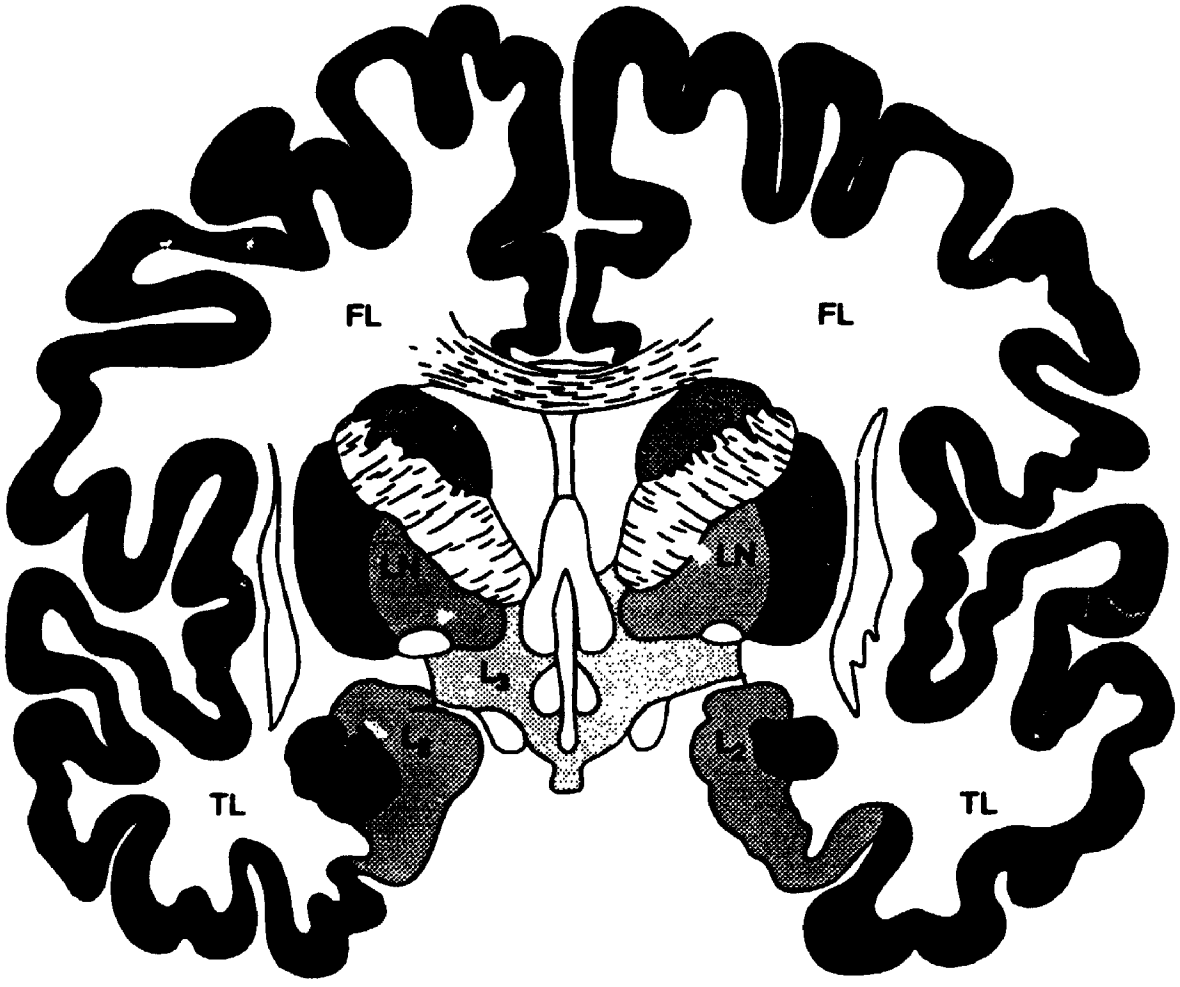

Figure II.1 Illustration of a coronal cross-section through the frontal (FL) and temporal (TL) lobes. The striatum consists of the caudate nucleus (S_1) and the putamen (S_2). The lenticular nucleus includes the putamen (S_2) and the globus pallidus (LN). The amygdala (L_1), parahippocampal gyrus (L_2) and hypothalamus (L_3) are structures that are part of the limbic system.

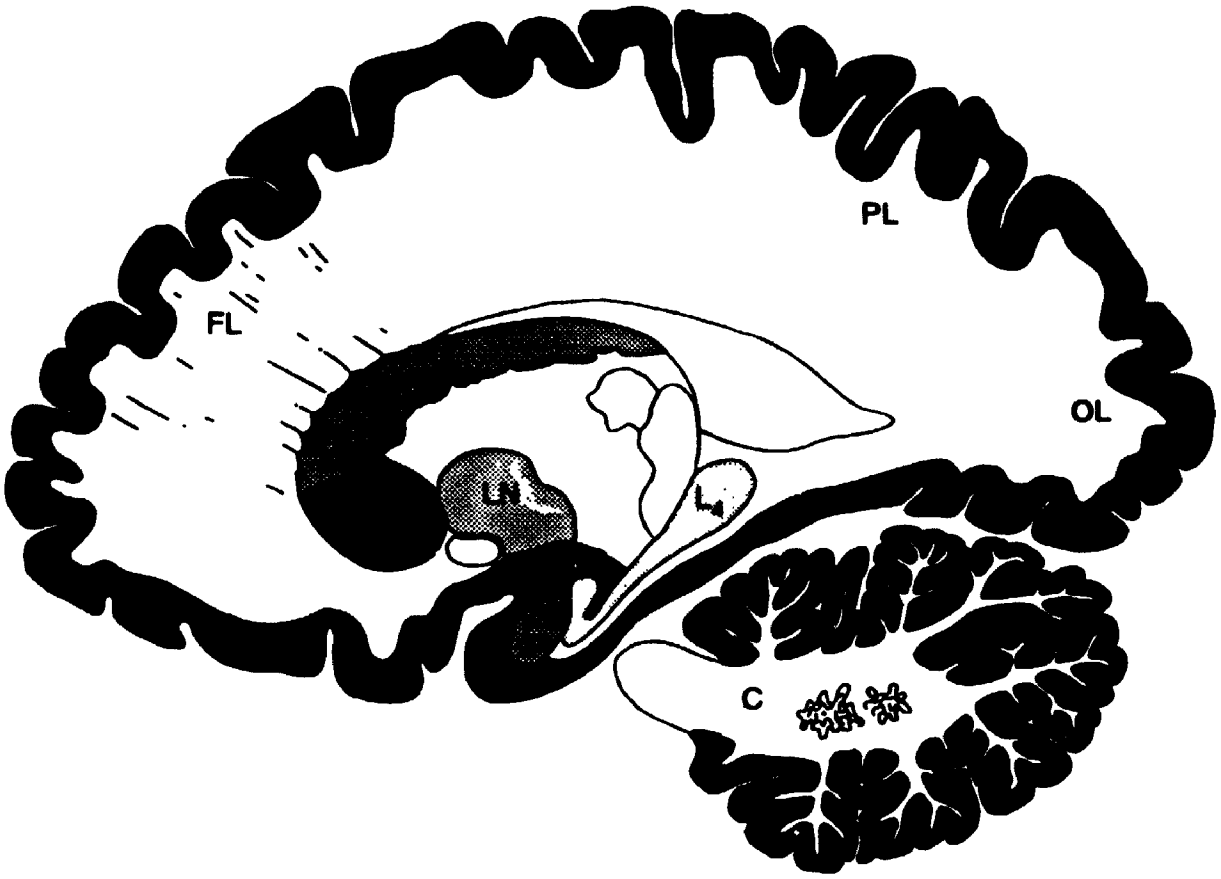

Figure II.2 Illustration of a sagittal cross-section through the frontal (FL), parietal (PL) and occipital (OL) lobes. The striatum consists of the caudate nucleus (S_1) and the putamen (S_2). The lenticular nucleus includes the putamen (S_2) and the globus pallidus (LN). Structures that are part of the limbic system include the amygdala (L_1), and the hippocampus and dentate (L_4).

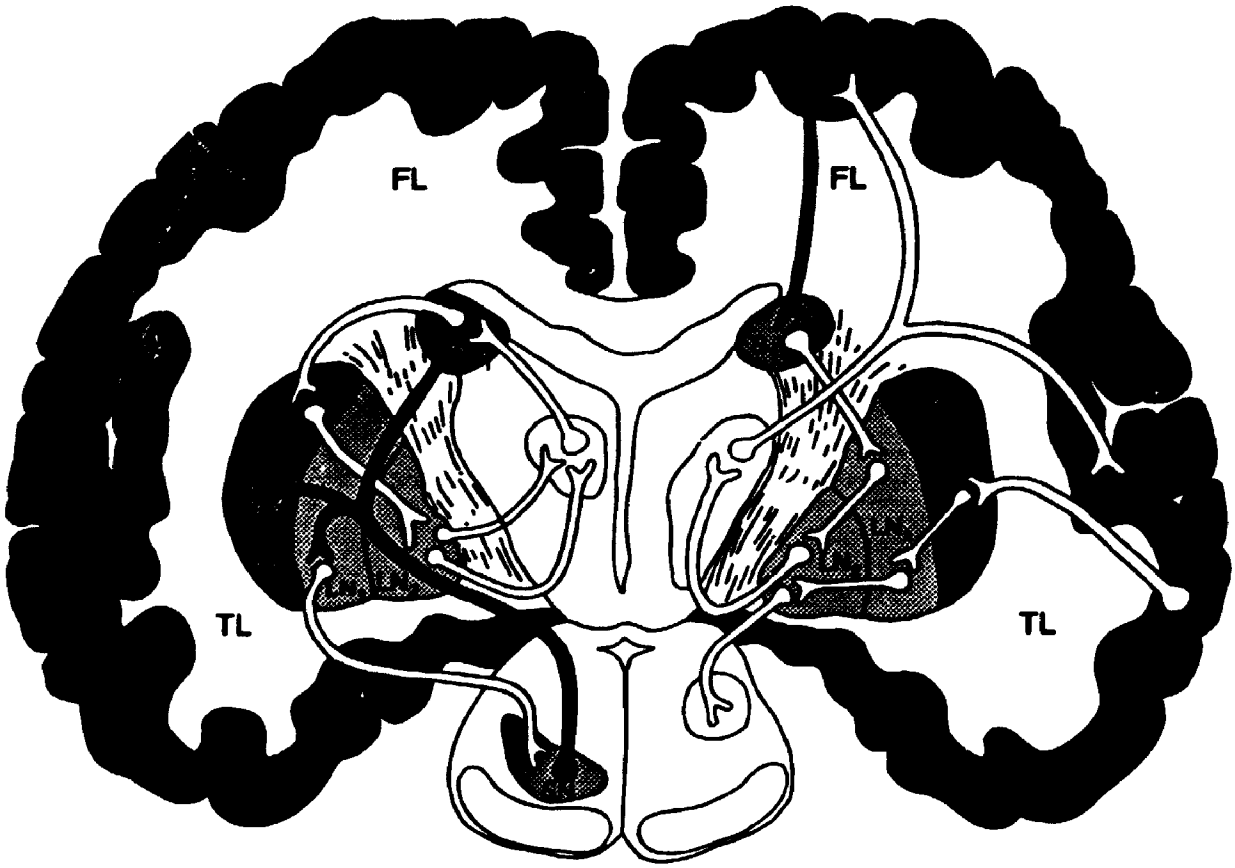

Figure II.3 Neuronal circuitry in the basal ganglia. The afferent connection from the frontal lobe to the striatum (i.e., the caudate, S_1) is the corticostriatal glutamatergic pathway as indicated in black. The afferent connection from the substantia nigra to the striatum (i.e., the caudate, S_1, putamen S_2, and lateral segment of the globus pallidus, LN_1) is the nigrostriatal dopaminergic pathway as indicated in black. The additional structure indicated is the medial segment of the globus pallidus, LN_2.

(Seeman 1987). However, recent studies have failed to provide unequivocal evidence of dopamine hyperactivity either *in vivo* or in post-mortem brain tissues (Carlsson 1988; Crow 1987; Healey 1991; Reynolds 1989). Even more disappointing was the absence of a linkage between the D_2 and D_4 dopamine receptor gene region and the incidence of schizophrenia (Moises et al. 1991; Macciardi et al. 1994).

Glutamate is the most abundant amino acid in the brain and important for a variety of cellular functions (Szerb 1988). As a consequence, glutamate serves as the major EAA neurotransmitter in the central nervous system, playing a vital role in neuronal development, memory, learning and behaviour (Collingridge 1987; Fagg 1985). Thus, it follows that glutamate may be involved in schizophrenia in some way.

The first evidence implicating glutamate in schizophrenia was reported by Kim et al. (1980). In this study, decreased glutamate levels in cerebrospinal fluid (CSF) of schizophrenic patients were observed when compared to a control group. Unfortunately, subsequent investigations have been unable to confirm this observation (Gattaz et al. 1985; Korpi et al. 1987; Perry 1982). The most convincing evidence of a glutamatergic hypothesis comes from the drug phencyclidine (PCP, "angel dust"), which is the most effective drug to induce both negative (flattened affect, social withdrawal, lack of motivation) and positive (hallucinations, delusions) schizophrenic symptoms (Javitt 1987; Johnson 1983; Snyder 1980). PCP is a specific, non-competitive antagonist of

N-methyl-D-aspartate receptors (NMDA, a glutamate subtype receptor). Therefore, the induction of schizophreniform symptoms via the binding of PCP and subsequently PCP blocking the NMDA ion channel have suggested a dysfunction of NMDA receptor-mediated neurotransmission in schizophrenia (Javitt and Zukin 1990).

Numerous EAA receptor studies on post-mortem brain from schizophrenic patients have been conducted and have revealed inconsistencies with the implication of glutamate (Ulas and Cotman 1993). Suga et al. (1990) have observed an increase in NMDA receptor density in the temporal and parietal cortex of schizophrenics. In the putamen (figures II.1 and II.2), Kornhuber et al. (1989) have observed an increase and Suga et al. (1990) and Weissman et al. (1991) have found no change in the NMDA receptor densities. The distribution of the binding sites of NMDA showed no differences in the hippocampus (figure II.2) of schizophrenics compared to controls (Kerwin et al. 1990). Kurumaji et al. (1990) have observed no differences in the binding of glutamate subtype receptors, quisqualate, in the frontal, temporal and parietal cortex in schizophrenics. In terms of kainate receptor binding (glutamate subtype receptor), Deakin et al. (1989) and Nishikawa et al. (1983) have observed an increase in the frontal cortex while Kerwin et al. (1988) observed a decrease and Deakin et al. (1989) observed no change in the hippocampus of schizophrenic patients. Post-mortem studies have offered two other lines of evidence for glutamate dysfunction in schizophrenia. In the frontal and

temporal cortex of schizophrenics, a decrease in the release of glutamate and in the glutamate decarboxylase activity were observed by Sherman et al. (1991). Harrison et al. (1991) have observed a striking and specific loss of messenger RNA (ribonucleic acid) that encodes a non-NMDA glutamate receptor in the hippocampal tissue of patients compared to controls.

The relationship of these post-mortem studies with the proposed glutamatergic deficiency state in schizophrenia is uncertain. Some inconsistencies might be explained by the use of the autoradiography markers for different receptor subtypes and the effects of medication which have been shown to increase glutamate levels (Deutsch et al. 1989). Post-mortem studies also generally reflect the chronic stage of the illness and may not be related to the original pathophysiology.

II.2.1 The Effect of Neuroleptic Medication on Glutamate.

In the striatum, there are afferent glutamatergic neurons from the prefrontal cortex (i.e., the corticostriatal glutamatergic pathway) and afferent dopaminergic neurons from the substantia nigra (i.e., the nigrostriatal dopaminergic pathway) as illustrated in figure II.3. Evidence has shown that these two systems are behaviourally antagonistic (Scatton et al. 1982, Kerkerian et al. 1987; Kerwin et al. 1984; Nieoullon et al. 1983) Additionally, it is these two pathways that several investigaters have based their hypothesis for schizophrenia (Kim et al. 1980; Kornhuber and Kornhuber 1986; Schmidt 1986; Carlsson 1988; Deutsch et al. 1989; Grace 1991; Javitt and Zukin 1991;

Riederer et al. 1991). For these reasons, it would be expected that neuroleptic medication, which block dopamine receptors, would alter the function of the afferent glutamatergic neurons (Deutsch et al. 1989). However, there have been several *in vitro* studies where the effect of neuroleptic medication on glutamate was investigated and none of them implicated the glutamate in the prefrontal region. Following chronic (12 days) administration of neuroleptic medication (sulpiride) in rats, the glutamate level was increased in CSF, decreased in the striatum and hippocampus, and normal in the cortex (Kim et al. 1983). Perry et al. (1979) investigated the glutamate content in the mesolimbic area (which includes the amygdala, hippocampus, dentate and the hypothalamus, figures II.1 and II.2) after chronic (100 days) administration of neuroleptic medications (chlorpromazine and haloperidol) in rats and found no differences. The glutamate release from *in vitro* synaptosomes prepared in the presence of neuroleptic medication, was investigated (Sherman and Mott 1984). The synaptosomes were from rat tissue samples of the cortex, hippocampus, striatum, and amygdala. The only significant difference was a decrease in glutamate release in the synaptosomes from the amygdala.

II.3 MRS and Schizophrenia.

The first *in vivo* ^{31}P MRS study on first episode drug-naive (DN) schizophrenic patients was reported by Pettegrew et al. (1991). In this study, the ^{31}P MR signal was acquired from the dorsal prefrontal region (left and right side combined) with a surface coil in these patients and normal controls. A

significant decrease in the PME and Pi levels and a significant increase in the PDE and ATP levels were observed. Pettegrew and colleagues have suggested that these differences are due to alterations in the membrane phospholipid metabolism and a reduction in metabolic activity in the dorsal prefrontal cortex.

O'Callaghan et al. (1991) reported results on an *in vivo* ^{31}P MRS study of the left temporoparietal region in chronic schizophrenic patients and controls. The localization technique used was the surface coil. There were no significant differences observed between the ^{31}P metabolite levels of the patients and that of the controls. However, the pH level was higher in the patients compared to the controls. It was suggested that this difference was due to tissue damage in this region.

In a study by Calabrese et al. (1992), the ISIS localization sequence was used to acquire *in vivo* ^{31}P MR spectra from the left and right temporal region (4.5x5.5x3.5cm^3) of chronic schizophrenic patients and controls. The ^{31}P metabolite levels of these patients were not significantly different from the levels of the controls on both sides.

To date, there are no published ^{1}H MRS studies in schizophrenia except for preliminary studies reported as abstract. In a pilot study by Nasrallah et al. (1992), ^{1}H MR spectra were acquired from either the left or right hippocampus region of 11 chronic schizophrenic patients and 11 controls. All experiments were done on a 1.5Tesla GE Signa system using a STEAM sequence (TE=

50ms, TR= 2sec, 200 acquisitions). The chosen VOI was 12ml, which is quite large for the hippocampus. However, the intensity ratios of NAA/Cho_t and NAA/(PCr+Cr) were significantly reduced by 30% in the right hippocampus of the schizophrenic patients compared to the controls. The glutamate levels were not reported. The author has attributed this deficit of NAA in the right hippocampus of the patient group to neuronal cell loss, possibly due to hypoplasia or degeneration.

Moore et al. (1992) have reported metabolite levels in the left temporal and frontal lobes of 30 schizophrenic patients (of which 5 were neuroleptic-naive patients suffering from acute schizophreniform psychosis) and 20 age matched controls. A STEAM sequence (TE= 68ms, TR= 3sec, 256 acquisitions) was used to localize a 11ml VOI. Only the metabolites NAA, PCr+Cr and Cho_t were examined and no significant differences were observed in these levels between the patient group and the controls in either the left temporal or frontal lobes.

Left and right temporal lobes were investigated by localized *in vivo* ^1H MRS on 15 chronic schizophrenic patients and 14 controls by Yurgenlun-Todd et al. (1993). ^1H MR spectra were acquired from a 3.0x2.0x2.0cm^3 VOI positioned in the centre of the lobes with the STEAM sequence (TE= 30ms, TR=2sec, 400 acquisitions) on a 1.5Tesla GE Signa system. A significant reduction in the NAA/(PCr+Cr) ratio was observed in the left and right temporal lobes of these patients compared to controls. The authors have attributed the

decrease in ratio due to a decrease in NAA concentration. The contribution of glutamate to the spectra was not measured.

In summary, the ^{31}P and ^{1}H MRS studies thus far on schizophrenia have concentrated on observing metabolite differences in chronic patients compared to controls, except for the study by Pettegrew et al. (1991) where DN patients were investigated. Therefore, information on the ^{1}H metabolites of schizophrenic patients early in illness has yet to be obtained. In the ^{1}H MRS studies, none have quantified all the spectral information, including glutamate, observed in spectra that have been acquired with a short echo STEAM sequence. With a fitting routine to model the spectral peaks of the amino acids (i.e, glutamate) with *a priori* knowledge, these metabolites can now be quantified. Furthermore, none of the studies acquired both ^{1}H and ^{31}P MRS data on the same subject groups. Correlating results from both the ^{1}H and ^{31}P MRS may gives additional insight into the possible physiological interdependencies between these metabolites.

II.4 Objectives of Thesis.

The quantification of *in vivo* metabolites such as glutamate (in ^{1}H spectra acquired with a short echo time) has recently been shown to be feasible with the use of *a priori* knowledge (de Graaf and Bovée 1990a; Provencher 1993). This *a priori* knowledge, which is obtained from *in vitro* experiments, contains information on the spectral peak arrangement for each metabolite. However, issues dealing with reproducibility and reliability of quantifying these metabolites

as a function of spectral S/N have yet to be investigated. Therefore, the objectives of this thesis were to:

i) Develop an in-house software package that would enable us to quantify *in vivo* short echo ^{1}H spectra in the frequency domain with *a priori* knowledge.

ii) Present a quantitative analysis on the accuracy and precision of quantifying simulated *in vivo* ^{1}H spectra as a function of S/N and with different relative metabolite levels.

iii) Investigate the efficacy of this modelling technique by quantifying repeated *in vivo* measures of two different volume sizes on an individual. In addition, the differences in metabolite levels between the two volumes and the differences in grey/white matter ratios within the volumes should reflect the regional distribution of metabolite levels as observed in previous *in vivo* and *in vitro* studies of the brain.

In addition, this thesis embodies the first comprehensive *in vivo* study on schizophrenia. Both, *in vivo* ^{1}H and ^{31}P MR spectra of schizophrenic patients representing different stages of illness, (first episode DN, newly-diagnosed medicated (NDM) and chronic medicated (CM) patients), were acquired and compared to controls. The localized region under investigation in these patients was the left dorsolateral prefrontal region. Additional objectives of this thesis were to investigate:

iv) Possible abnormalities in these *in vivo* measures of patients with

schizophrenia, specifically in the glutamate level.

v) Possible changes in the metabolite levels as the illness progresses from early onset of symptoms to the chronic stage. Are there signs of neurodegeneration in the chronic patients?

vi) The effect of medication on the *in vivo* measures. Does neuroleptic medication alter the glutamate level in the prefrontal region?

vii) If the abnormalities in the membrane phospholipid metabolism observed in the DN patients by Pettegrew et al. (1991) are reproduced in this study.

II.5 Hypotheses.

We hypothesize that:

i) Glutamate levels are altered in the left dorsolateral prefrontal region of first episode DN schizophrenic patients.

ii) The initial administration of neuroleptic medication to the NDM patients will not alter the glutamate level in the prefrontal region.

iii) Evidence of neurodegeneration will be observed in the CM patients (i.e., decreased levels in NAA and PCr+Cr, and increased levels in Cho_t).

iv) The increase in breakdown of membrane phospholipid will only be present early in the illness suggesting that an abnormal neurodevelopment in the prefrontal region may be present.

II.6 Outline of Thesis.

Chapter III contains the main body of a manuscript written by Jeff A.

Stanley entitled "The Use of *a Priori* Knowledge to Quantify Short Echo *in Vivo* ^{1}H MR Spectra". The additional authors are Dick J. Drost, Peter C. Williamson and R. Terry Thompson. The manuscript has been accepted for publication in ***Magnetic Resonance in Medicine*** with minor revisions. The quantification technique used to obtain the metabolite levels from *in vivo* ^{1}H spectra is outlined. The accuracy and precision of this technique was tested on simulated *in vitro* data. In addition, the reproducibility of quantifying the *in vivo* ^{1}H metabolite levels was investigated by repeated measures on a normal individual. I created the protocol of the study and developed the quantification method. I did all the data collection, data processing, spectral quantification and statistics. Dr. Thompson and Dr. Drost provided helpful discussions. The computer programming for the in-house quantification software was done by John Potwarka, a hired summer student.

Chapter IV consists of the main body of a manuscript written by Jeff A. Stanley entitled "An *in Vivo* Proton Magnetic Resonance Spectroscopy Study of the Prefrontal Region of Schizophrenic Patients at Different Stages of Illness". The additional authors are Peter C. Williamson, Dick J. Drost, R. Jane Rylett, Tom Carr, Ashok Malla and R. Terry Thompson. This manuscript has been submitted for publication in ***Schizophrenia Bulletin.*** In this study, localized *in vivo* ^{1}H MR spectra from the prefrontal region of schizophrenic patients were acquired and compared to control subjects. Schizophrenic patients and control subjects were recruited by Dr. Williamson, Dr. Malla and by psychiatrists from

the local area. Dr. Carr assisted in the collection of MR images and positioning of the volume of interest for spectroscopy. I designed the protocol for data collection. The data collection was shared by Dr. Drost and myself. The quantification method from chapter III that I developed was used to analyze the data. I processed and analysed the ^{1}H spectra and I performed the statistical tests on the data. Dr. Williamson and Dr. Rylett provided valuable discussions on the psychiatric and physiological interpretation of the results, respectively.

Chapter V is, in part, the main body of a manuscript written by Jeff A. Stanley entitled "An *in vivo* Study of the Prefrontal Cortex of Schizophrenic Patients at Different Stages of Illness via Phosphorus Magnetic Resonance Spectroscopy". The additional authors are Peter C. Williamson, Dick J. Drost, Tom Carr, R. Jane Rylett, Ashok Malla and R. Terry Thompson. This manuscript has been accepted for publication in the ***Archives of General Psychiatry*** with minor revisions. In this study, ^{31}P MRS was used to investigate possible metabolic abnormalities in the prefrontal cortex of schizophrenic patients. Schizophrenic patients and control subjects were recruited by Dr. Williamson, Dr. Malla and by psychiatrists from the local area. Dr. Carr assisted in the acquisition of MR images and positioning of the volume of interest for spectroscopy. Dr. Drost and I shared the collection of the data. I created the quantification protocol. I processed and analysed the ^{31}P spectra and I performed the statistical tests on the data. Dr. Williamson and Dr. Rylett provided valuable discussions on the psychiatric and physiological interpretation

of the results, respectively.

Chapter VI contains the general discussion and conclusion on the differences of the *in vivo* ^{1}H and ^{31}P measures observed between the schizophrenic patients and controls. An attempt to correlate the findings of both studies is made. A discussion on the effect of medication and stage of illness on the *in vivo* measures is also presented. Furthermore, this chapter includes a discussion of additional experiments for future work that can be conducted on schizophrenic patients to further comprehend this illness.

Appendix A provides brief explanations of the main terminologies that are used in this thesis.

Appendix B includes details on: *i)* a technique used on the ^{1}H MR data to restore the spectral peaks to pure Lorentzian lineshapes and *ii)* obtaining absolute levels of the ^{1}H metabolites.

Appendix C contains the main body of a manuscript written by Jeff A. Stanley entitled "Membrane Phospholipid Metabolism and Schizophrenia: an *in Vivo* ^{31}P MR Spectroscopy Study" by Jeff A. Stanley, Peter C. Williamson, Dick J. Drost, Tom Carr, R. Jane Rylett, Sandra Morrison-Stewart and R. Terry Thompson. This manuscript has been accepted for publication in ***Schizophrenia Research*** (in press, 1994). Localized *in vivo* ^{31}P MRS was used to investigate metabolic differences in the prefrontal cortex between medicated schizophrenic patients and control subjects. Unlike the study in Chapter V, the data was analysed unblind and the spectral processing procedure did not have

the improved non-interactive method to cope with the pre-acquisition time delay. The authors' contribution to this study is identical to Chapter V.

CHAPTER III

The Use of a Priori Knowledge to Quantify in vivo ^{1}H MR Spectra

III.1 Introduction.

Quantifying the *in vivo* glutamate level from a specified brain region in schizophrenic patients has the potential to provide important information in the understanding of the pathophysiology of schizophrenia. Chapter II reviewed important findings where glutamate has been implicated in schizophrenia. ^{1}H MRS is a technique that is capable of accessing the *in vivo* glutamate level in a localized region of the brain which is not possible with any other technique. In this study, a spectroscopy protocol was developed to properly collect localized *in vivo* ^{1}H MR spectra of the brain and to quantify the ^{1}H metabolites with an accurate and precise technique. The following includes the decision process used to establish an appropriate protocol to quantify the *in vivo* ^{1}H metabolite levels.

The STEAM pulse sequence, which is a single voxel localization technique, was used to collect MR data. A single voxel localization technique was chosen over a multiple voxel technique for several reasons. The homogeneity of the static magnetic field which reflects the spectral resolution, increases as the size of the VOI decreases. Hence, with a single voxel MRS technique, the spectral resolution should be better and easier to achieve compared to a multiple voxel technique. This increase in spectral resolution,

facilitates a more efficient suppression of the water resonance. Additionally, working with a single and smaller VOI reduces any magnetic field susceptibility effects, due to differences in the tissue environment, and consequently, improves spectral resolution. The advantages of STEAM over other single voxel techniques is discussed in Chapter I.

The ^{1}H MR spectra of glutamate consists of multiple resonances due to scalar spin-spin coupling (see Appendix A) and the T_2 of glutamate is relatively shorter. Therefore, to observe the ^{1}H MR signal of glutamate, the data must be collected with a pulse sequence that has a short echo time. This is feasible with the STEAM sequence. A shorter echo time minimizes the T_2 relaxation of the metabolites and the J-modulation effect on the multiplet structures. With minimal signal loss: *i)* the size of the VOI may be reduced to improve the spatial and spectral resolution, *ii)* the number of averaged acquisitions may be reduced to decrease the total experimental time and hence, the probability of introducing motion artifacts and *iii)* the *in vivo* metabolites with relatively smaller concentrations may be better resolved. Minimizing the J-modulation effect will ensure that the amplitudes of the spectral peaks are all positive and near in-phase to each other. Negative amplitudes or out of phase peaks will subtract from the amplitudes of overlapping spectral peaks and the apparent spectral lineshapes will appear less intense. Furthermore, acquiring *in vivo* ^{1}H MR data of the brain with a short echo time pulse sequence enables the observation of other metabolites with short T_2's such as glutamine, GABA, and glucose (Figure

III.1) (Frahm et al. 1989a; Frahm et al. 1990; Michaelis et al. 1991; Gruetter et al. 1992).

Short echo ^{1}H MR spectra have limited chemical shift dispersion due to the relatively low magnetic field strengths available for whole body MRS on humans and the resonances have broad linewidths due to their short T_2^*'s. Consequently, short echo ^{1}H MR spectra consist of complex overlapping resonances especially in the 2.0ppm to 2.7ppm region. Figure III.2 contains individual *in vitro* ^{1}H MR spectrum of NAA, glutamate, glutamine, GABA, choline, and aspartate which illustrates the degree of overlapping resonances observed in Figure III.1. This makes, the quantification of these metabolites problematic and standard spectral quantification methods which employ peak heights, triangulation and computer integration are not adequate in modelling the individual metabolites (Tofts and Wray 1988, Bottomley 1989). The main criticism of these fitting techniques is that they do not account for the degree of overlap between the spectral peaks (de Beer and van Ormondt 1992), therefore, these techniques were not attempted in this study. The concept of quantifying MR data is reviewed in Chapter I.

In selecting a method to quantify short echo ^{1}H MR data , the technique should be sensitive in resolving overlapping resonances, effective in maintaining its accuracy even with poor S/N and operator independent or near operator independent. To effectively resolve overlapping resonances, the relationship of the individual multiplet structures as observed in Figure III.2 must be maintained

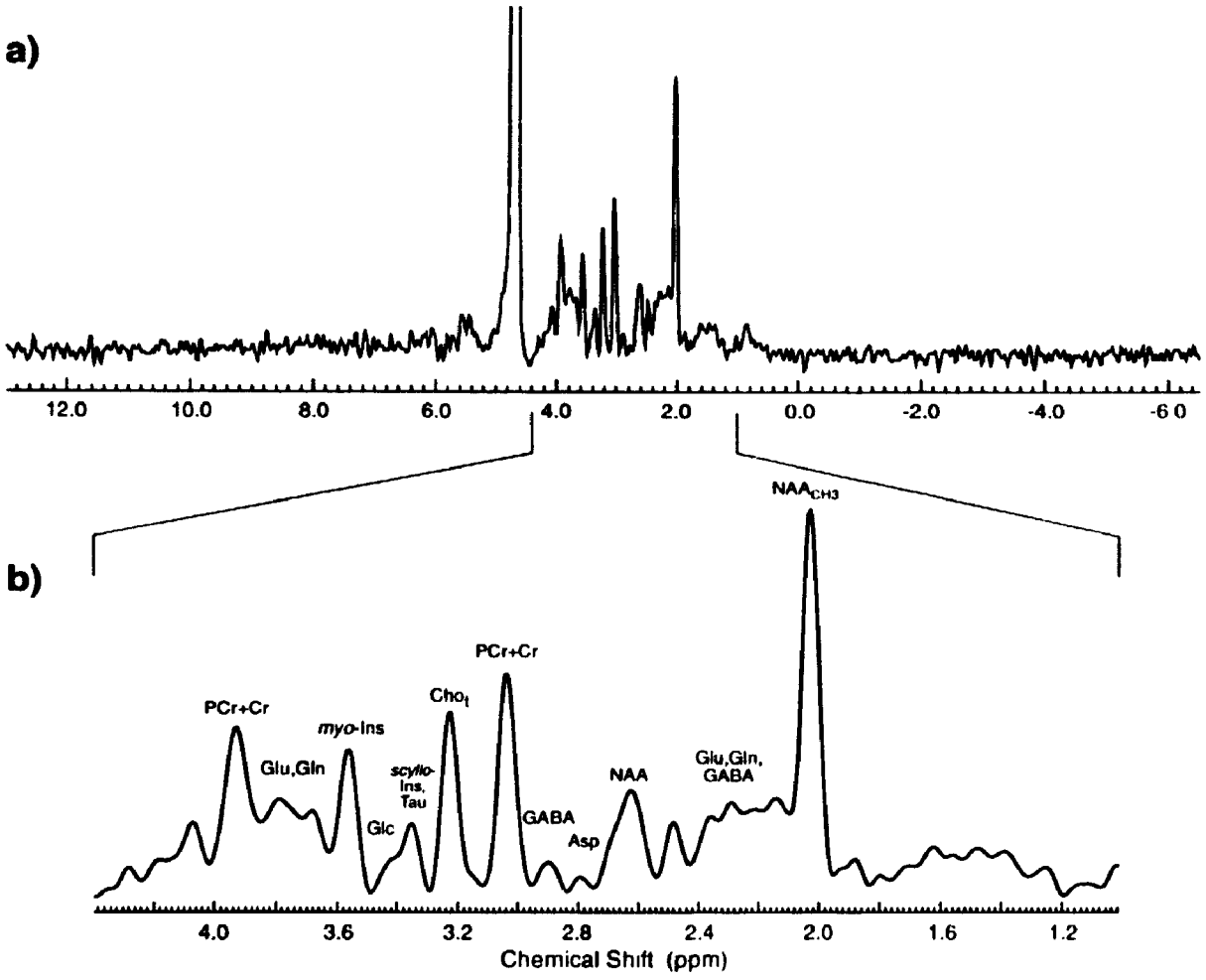

Figure III.1 A typical processed *in vivo* ^{1}H MR spectrum. (a) Contains a spectrum acquired from the left dorsolateral prefrontal region with STEAM sequence (TE=20ms) at 1.5Tesla and (b) shows the same spectrum with the central frequency region expanded.

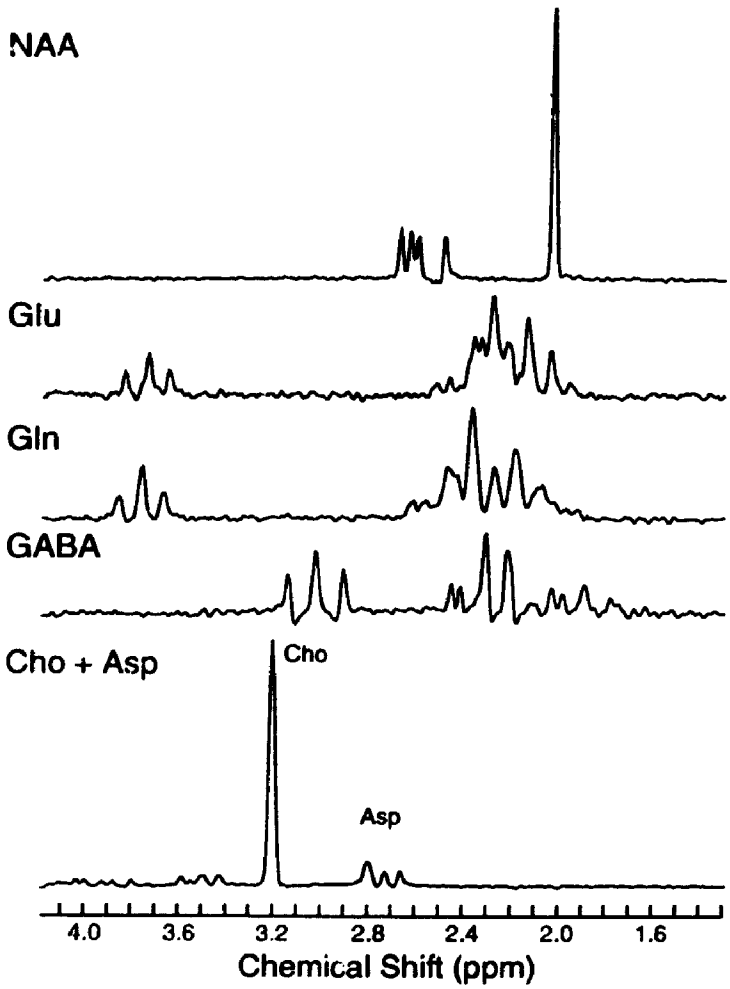

Figure III.2 Individual in vitro ^{1}H MR spectrum of NAA, glutamate (Glu), glutamine (Gln), GABA, choline (Cho) and aspartate (Asp) in aqueous solution, acquired with the STEAM TE=20ms sequence at 1.5Tesla.

in the quantification. We can assume that the chemical shifts and the relative amplitudes and linewidths of each metabolite will remain constant from spectrum to spectrum as long as the experimental protocol is identical for all. Therefore, information pertaining to constraints on the multiplet structures can be incorporated into the fitting model as *a priori* knowledge. De Graaf and Bovée (1990) first introduced this concept of incorporating *a priori* knowledge to quantify *in vivo* ^{1}H MR brain spectra of rats collected on a 7 Tesla system. The *a priori* knowledge was obtained from *in vitro* experiments of single metabolites in aqueous solution. The complexity of the quantification of these overlapping resonances was greatly reduced due to the significant reduction in the number of degrees of freedom in the model. As a result, the overlapping resonances were more consistently resolved. To be able to incorporate *a priori* knowledge into a quantification method, the fitting algorithm must be nonlinear and in this case the Marquardt nonlinear least-squares algorithm was used (Marquardt 1963). This algorithm is flexible such that *a priori* knowledge about the chemical shifts, amplitudes and linewidths can easily be implemented.

The last decision to make on the quantification technique was to either model the MR data in the frequency domain or in the time domain as discussed in Chapter I. In this thesis, the short echo ^{1}H MR data was quantified in the frequen y domain with model lineshapes for the following reasons: *i)* it is easier to visualize the fit of spectral peaks than the fit of damped sinusoids in the time domain, *ii)* it is easier to determine the initial starting values of the parameters,

and *iii)* it does not require the added step of physically subtracting the water resonance prior to the fit as in the time domain method (van Dijk et al. 1992) because a specific spectral region can be selected to model the spectral peaks and consequently the water resonance is ignored. Furthermore, from preliminary unpublished results, modelling the data in the time domain with *a priori* knowledge appears to be less sensitive in resolving the similar overlapping resonances of glutamate and glutamine, (Figure III.2), compared to the results from the frequency domain fit. The main disadvantage of modelling in the frequency domain is that after the Fourier transformation of the FID is applied, the spectral peaks must be manually phased prior to the modelling, which is operator dependent. There are techniques that have been developed to automatically phase the spectra (Sotak et al. 1984), however, these methods are not effective when overlapping resonances are present in the spectra.

At the same time that this quantification technique was first presented (Stanley et. al 1993), Provencher (1993) reported on results where *in vivo* STEAM spectra of the brain were quantified with the incorporation of *a priori* knowledge in a Linear Combination Model Method (Marquardt 1963). Provencher's technique is similar to the one presented in this chapter, except in his, the baseline was also modelled simultaneously with N-cubic splines. Peak distortion due to eddy currents and inhomogeneities in field, and unknown background signal from protons that are not accounted for contributed to the modelling of the baseline. It is unclear if the approach of estimating the

baseline contribution is valid because of the lack of understanding of the background signal.

Neither studies by de Graaf and Bovée (1990) or Provencher (1993) presented a quantitative analysis on the effectiveness of their quantification method in modelling *in vivo* spectra with different S/N's. Poor S/N's can also impair the quantification of *in vivo* ^{1}H MR spectra. To maintain accurate, precise results in modelling with *a priori* knowledge, a reasonable lower limit on the S/N for ^{1}H MR data must be determined. Therefore, one objective of this study was to investigate the accuracy and precision of modelling simulated short echo ^{1}H MR spectra as a function of the S/N and at different relative metabolite levels. The quantification technique includes modelling the short echo spectra in the frequency domain with the incorporation of *a priori* knowledge as described above. The spectral resolution, relative metabolite levels and S/N's were similar to those encountered in the brain.

The efficacy of modelling *in vivo* ^{1}H MR spectra with *a priori* knowledge was also investigated. Two localized *in vivo* ^{1}H MR spectra of the dorsolateral prefrontal cortex from a normal subject were acquired and repeated on 10 different occasions. The first VOI was 8cm^3 and the second was 4cm^3. However, the 4cm^3 VOI was positioned within the 8cm^3 VOI such that the 4cm^3 volume contained a larger proportion of grey matter as estimated from ^{1}H MR images. The repeated measures provided a quantitative assessment on the reproducibility of the *in vivo* metabolite levels for different volume sizes and

the S/N within an individual. In addition, the differences in the quantified metabolite levels between the two VOI's with the differences in the estimated grey/white matter ratios should reflect the regional distributions of metabolite levels that have been observed in previous *in vivo* ^{1}H MRS studies on human brains (Frahm et al. 1989b; Narayana et al. 1989; Hennig et al. 1992; Kreis et al. 1993; Michaelis et al. 1993; Provencher 1993).

III.2 Method.

III.2.1 Sample Preparation and Subject.

N-acetyl-L-aspartic acid, L-glutamic acid, L-glutamine, γ-amino-n-butyric acid, L-aspartic acid, D-glucose, taurine, *scyllo*-inositol and NAAG, (Sigma Chemical Co., St. Louis, MO, USA) were dissolved separately in individual 50ml wide polypropylene tubes to a concentration of 20mM in H_2O containing sodium 3-trimethylsilylpropionic acid (TSP, the internal reference for the calibration of the resonant frequencies). The pH of each solution was adjusted to 7.00±0.10 using hydrochloric acid (HCl) or sodium hydroxide (NaOH). The 50ml tube was placed inside a water filled 20cm diameter sphere. The water in the sphere contained manganese chloride ($MnCl_2$) such that its load in the coil was similar to the load of a human head.

For the *in vivo* ^{1}H MRS study, a normal healthy 28 year old female volunteered. The repeated measures were acquired at the same time of day ± three hours, over a period of three weeks.

III.2.2 ^{1}H MR Spectroscopy.

All *in vitro* and *in vivo* ^{1}H MRS experiments were conducted at 1.5Tesla using a circularly polarized head coil. The STEAM sequence with TE= 20ms and TM= 30ms was used for the spatial localization technique (Chapter I). Water suppression was achieved with three CHESS pulses and spoiler gradients. A non-localized shim was followed by a localized VOI shim to maximize the homogeneity of the magnetic field. Positioning of the VOI was determined from a set of sagittal and coronal ^{1}H MR images. A total of 4,096 complex data points were used to digitize 1 second of the second half of the stimulated echo (i.e., spectral bandwidth ±2.0kHz) and the TR was 1,500ms. For each *in vitro* solution, three STEAM ^{1}H MR spectra of 256 acquisitions were acquired with a VOI of 7.7cm^3 (i.e., 1.6x3.0x1.6cm^3).

In the *in vivo* experiments, two consecutive STEAM ^{1}H MR measurements with a VOI of 2.0x2.0x2.0= 8cm^3 (450 acquisitions) and 1.6x1.6x1.6= 4cm^3 (550 acquisitions) were acquired. This was repeated 10 times over a period of three weeks. The 8cm^3 VOI was positioned over the left dorsolateral prefrontal cortex and the 4 cm^3 VOI was positioned within the 8cm^3 VOI where the lateral, anterior, and superior sides of both VOI were the same. Ten different *in vivo* STEAM spectra of noise (i.e., the voltages of the excitation pulses = 0.0 volts) were acquired under identical *in vivo* conditions. A water unsuppressed STEAM ^{1}H MR spectrum was collected for each water suppressed spectrum acquired.

III.2.3 Volumetric Measurements.

Sagittal and coronal spin echo MR images (TR= 600msec, TE= 20msec, slice thickness= 5mm, 0.5mm gap between slices, 256 phase encoding steps, field of view= 240mm) were acquired to estimate the grey matter, white matter and CSF volume within the VOI of the acquired *in vivo* spectroscopy data. Volumetric measurements were determined using the Analyze software package (Robb 1990) and in-house software on a UNIX system. For each image, the pixel intensity values from grey matter, white matter and CSF within the VOI were segregated by manual intensity thresholds determined by visual inspection. Volumes for slices with partial thickness outside the VOI were weighted by the fraction within the VOI. The grey matter, white matter and CSF volumes of each slice within the VOI were added. The results from the set of sagittal and coronal images were averaged and then normalized (i.e., expressed as a % volume). In estimating the % volumes, the true excited VOI's in the ^{1}H MR experiments were assumed equal to the specified dimensions of the VOI's.

III.2.4 Post-Spectral Processing.

All *in vitro* and *in vivo* ^{1}H MR data were processed in an identical manner. The time domain deconvolution technique, QUALITY (de Graaf et al. 1990), was applied to the FID followed by multiplying the time domain signal by h(t), a Lorentzian-to-Gaussian transformation to enhance the spectral resolution (Ferrige and Lindon 1978) ($h(t)= \exp(-\pi \cdot a \cdot t + \pi \cdot a \cdot t^2/(4 \cdot b))$ where b=42/4,096 and

a=-0.03 for minimal filtering and a=-0.6 for the *in vivo* data). The ^{1}H MR signal was zero filled (from 4,096 to 8,192 complex data points), Fourier transformed and phased using the 0th order and 1st order within ± ½ a dwell period (the time between digitized points).

III.2.5 Obtaining the *a Priori* Knowledge.

Information on the resonances of NAA, glutamate, glutamine, GABA, Aspartate, NAAG, glucose, *scyllo*-inositol and taurine were first obtained by modelling their respective *in vitro* ^{1}H MR spectra with minimal filtering. A frequency domain nonlinear least-squares fitting algorithm (Marquardt 1963) was used to model the spectral peaks with Gaussian lineshapes. The appropriate number of spectral peaks for each metabolite incorporated in the model was confirmed with previous high resolution ^{1}H MRS studies (Behar and Ogino 1991; Michaelis et al. 1991; Holowenko et al. 1992). Only the spectral peaks with resonances between 1.88 and 3.45ppm were considered in the model. The amplitudes (allowing only positive values), chemical shifts and linewidths were allowed to vary. The linewidths were kept equal to each other with the assumption that the J-modulation on the multiplet structures is minimal with a stimulated echo time of 20ms and the T_2's of the protons within the metabolite are equal to each other (de Graaf and Bovée 1990). The average relative amplitudes and chemical shifts of the three spectra for each metabolite were used for the a priori knowledge of each metabolite.

The linewidths were inter-linked between the various metabolites with

constants reflecting their relative linewidth difference. These constants were obtained by fitting the three spectra of each metabolite a second time. However, this time the spectra were filtered to simulate the linewidth resolution found *in vivo* and the spectral peaks were linked with relative amplitude scaling constants and chemical shift values, which were determined from the above. The resulting linewidth of each metabolite was normalized to the linewidth of the internal standard TSP (assuming the T_2 of TSP was the same for all the solutions). The average value was used as a priori knowledge.

In summary, for this fitting algorithm:

i) the relative amplitude of the spectral peaks within each metabolite were maintained with amplitude scaling constants

ii) the position of the peaks were linked with chemical shift constants and

iii) the relative linewidth differences between the metabolites were maintained.

The latter point does however render the model insensitive to T_2 changes for the *in vivo* metabolites. In addition, relative T_2 differences between the metabolites in aqueous solution were assumed to be similar to the relative T_2 differences *in vivo*. No *a priori* knowledge was needed to quantify the resonances of PCr+Cr and Cho_t except that a single peak was used to model each resonance.

III.2.6 Quantifying *in vitro* ^{1}H MR Spectra.

The accuracy and precision of modelling the overlapping resonances in *in vitro* ^{1}H MR spectra with different S/N's and with different relative metabolite

levels was investigated. Four different spectra were generated by adding the individual *in vitro* ^{1}H MR spectra of NAA, glutamate, glutamine, GABA and aspartate at different, comparable *in vivo* concentrations with the *in vivo* filtering level. The S_{NAA}/N_{rms}'s were greater than or equal to 220 (S_{NAA} refers to the maximum amplitude at ≈ 2.024ppm, the NAA_{CH3} resonance, and N_{rms} is the root mean square of the noise). Eight different representations of *in vivo* noise were added individually to each of the four different composite spectra to generate 32 spectra (i.e., 8 times 4) with the S_{NAA}/N_{rms} reduced to ≈54. In addition, ten different representations of *in vivo* noise were added individually to one of the four composite spectra to generate ten simulated ^{1}H MR spectra at different S_{NAA}/N_{rms}'s ranging from 23 up to 220.

The acquired *a priori* knowledge was used to model the above generated *in vitro* ^{1}H MR spectra such that the amplitudes, linewidths and chemical shifts varied under the constraints of the inter- and intra-linking constants. The expected areas of individual metabolites were determined by integrating the areas (with 3.4 and 1.4ppm as boundaries) before generating the simulated spectra. The accuracy of the model was determined by calculating the difference between the modelled areas and the expected areas. To quantify the precision of the modelled areas the standard deviations were extracted from the variance covariance matrix of the fitting routine.

III.2.7 Quantifying *in vivo* ^{1}H MR Spectra.

The quantification procedure used for the *in vitro* data was also used to

quantify the 20 different *in vivo* ^{1}H MR spectra. In addition, the unsuppressed water ^{1}H MR spectra was utilized as an internal standard to derive relative^{1}H metabolite levels (Appendix B). This enabled direct comparison of metabolite levels between the data collected with 8 and 4cm^3 VOI. The relative metabolite levels (RML) were determined by substituting the quantified metabolite spectral peak area (A_{met}), the number of protons associated with the peak (P_{met}), the integral value of the unsuppressed tissue water spectral peak (A_{H2O}), P_{H2O}=2, and the volume fractions of grey matter and white matter within the VOI (f_{grey} and f_{white}) that were estimated from the volumetric measurements performed on the ^{1}H images into Eqs. [B.8] and [B.9]. No attempt was made to correct for the attenuation of the MR signal due to T_1 and T_2 relaxation. Since the fraction of CSF volume was estimated within the VOI, the excitation volume of the unsuppressed water ^{1}H spectrum (V_{H2O}) was corrected for CSF contamination by adding the $(1-f_{CSF})^{-1}$ term in Eq. [B.9].

III.3 Results and Discussion.

III.3.1 The Dependence on the S/N.

An example of a generated *in vitro* spectrum of comparable *in vivo* resolution and relative metabolite concentrations is shown in Figure III.3. The spectrum (#1 of 4) consists of the following metabolite area ratios: NAA= 8: Glu= 4: Gln= 3: GABA= 3: Asp= 1: NAAG=0. The result of modelling this spectrum with *a priori* knowledge is displayed as a sum of all peaks. For

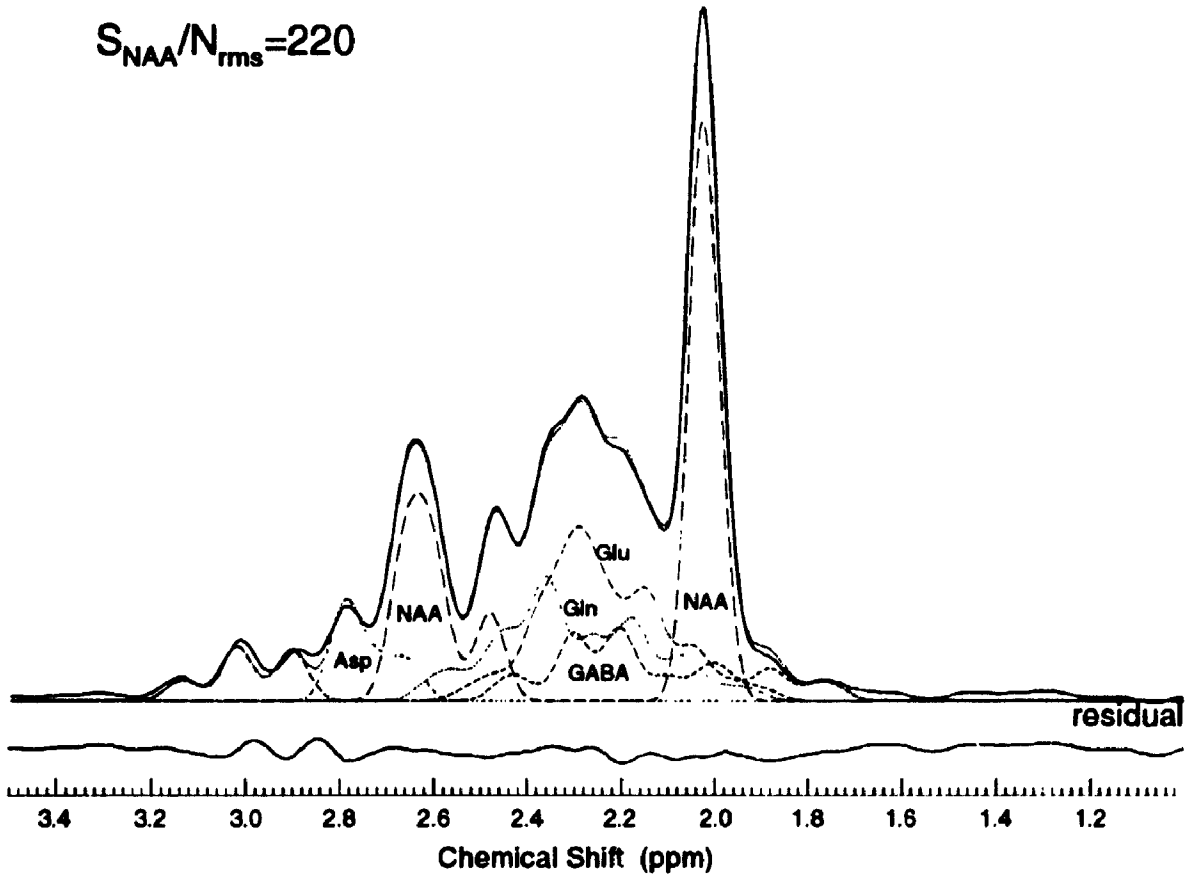

Figure III.3 Generated *in vitro* spectrum (#1, solid) superimposed on the modelled spectrum (smallest dashes) and the sum of the modelled peaks for NAA, glutamate (glu), glutamine (Gln), GABA and aspartate (Asp) (various dashes).

comparison the sum of peaks for each metabolite is also displayed in Figure III.3. Under the singlet resonance of NAA_{CH3}, it is interesting to note the relative degree of overlap from the resonances of $Glu_{\beta\text{-}CH2}$, $Gln_{\beta\text{-}CH2}$ and $GABA_{\beta\text{-}CH2}$ (it includes $NAAG_{CH3}$ which is not shown). For this reason it would be inaccurate to use methods such as integration to quantify the NAA_{CH3} resonance in short echo *in vivo* ^{1}H MR spectra.

The results of modelling the above spectrum with different S_{NAA}/N_{rms}'s (ranging from 23 up to 110) are displayed in Figure III.4. This figure includes the individual spectrum superimposed on the modelled spectrum, and the residual. In Figure III.5, the modelled areas for each metabolite are plotted as a function of the S_{NAA}/N_{rms}. For the S_{NAA}/N_{rms} of 54, eight spectra with different representations of *in vivo* noise were modelled and their areas are expressed as a mean, Figure III.5. In modelling NAA with its relatively intense resonance at 2.024ppm, the bias (the percentage difference between the expected level and the measured level) did not deviate greater than 3% from its expected value. In general, the bias was not greater than the standard deviation of the modelled NAA area. Only for a S_{NAA}/N_{rms} >41, was the deviation of glutamate <7%. The modelled areas of glutamine were all within 10% of the expected area. The bias of GABA exceeded 10% for S_{NAA}/N_{rms}'s of 48, 56 and 83 while the bias of aspartate exceeded 10% for 5 different S_{NAA}/N_{rms}'s. These large deviations in the modelled areas of GABA and to a greater extent aspartate suggest that with these relative levels, these metabolites are less reliable to

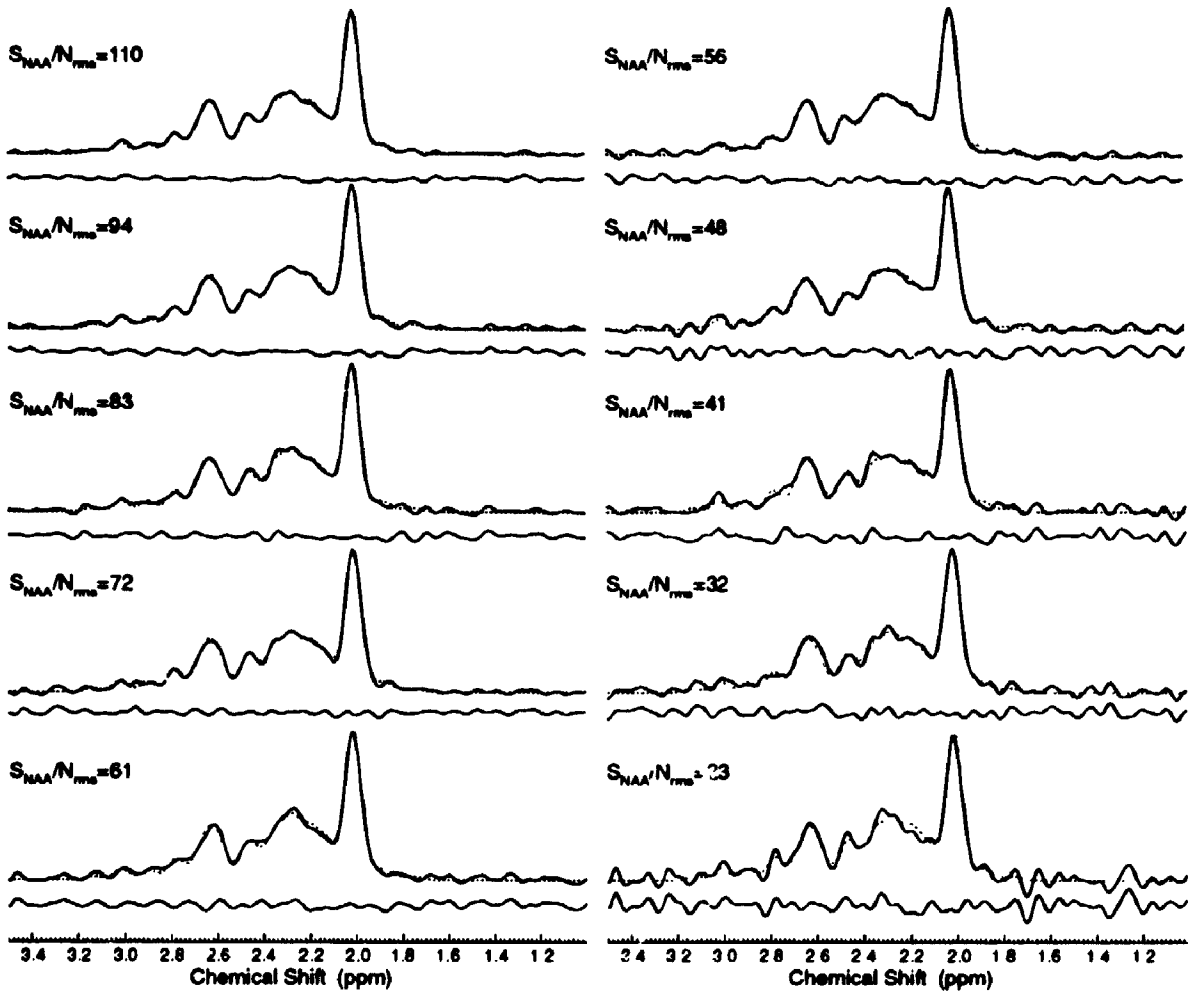

Figure III.4 Generated *in vitro* ^{1}H MR spectra with different S_{NAA}/N_{rms}'s are shown (solid) along with the modelled spectra (dotted) and the residual (solid, below the spectrum).

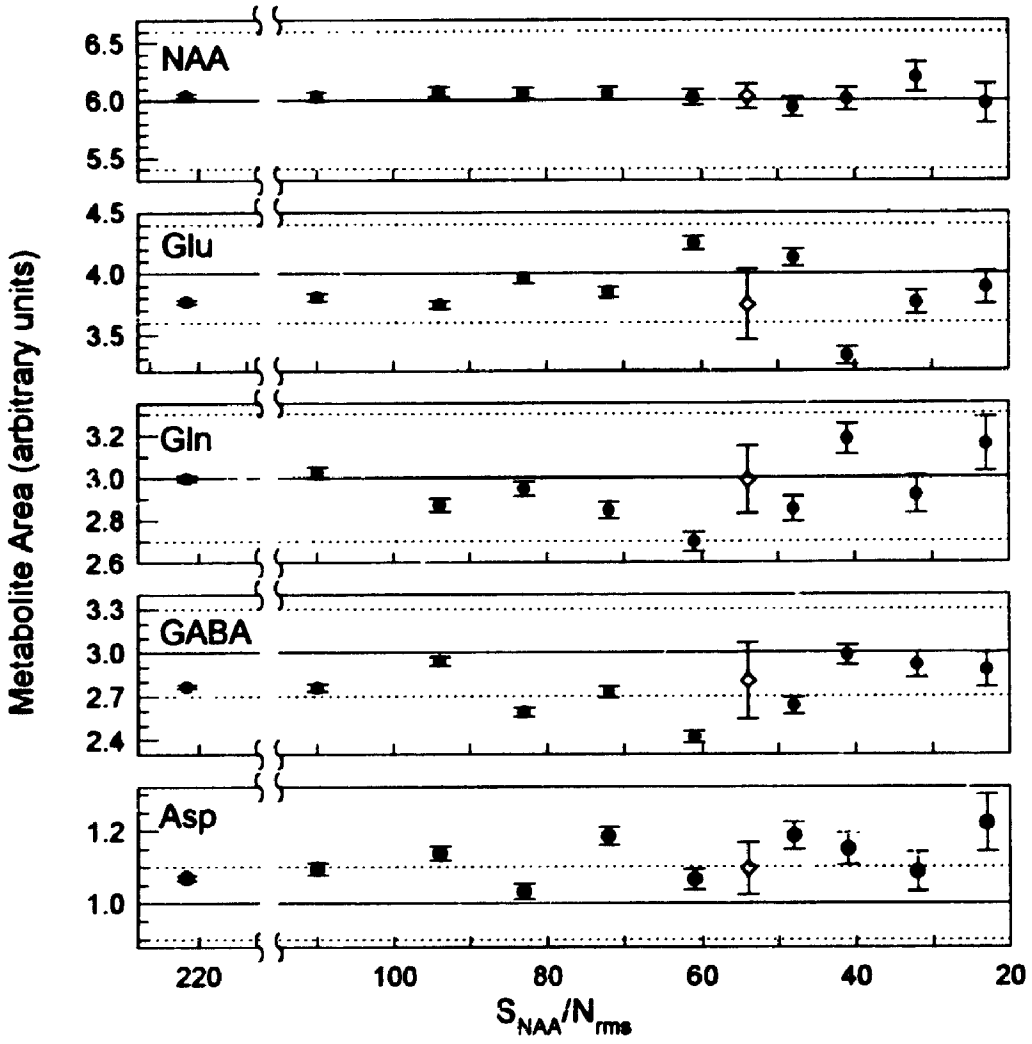

Figure III.5 The dependence of the quantified areas of NAA, glutamate (glu), glutamine (gln), GABA and aspartate (Asp) on the S_{NAA}/N_{rms}'s. ● represents the quantified area±1 standard deviation (from the variance covariance matrix in the fit routine); ◊ denotes the mean area±1 standard deviation from a population of 8 quantified spectra containing different *in vivo* noise representations; the expected area is indicated by the solid line and the dotted line represents ±10% of the expected area.

quantify (i.e., with bias of greater than 10%). Furthermore, on average the modelled areas for NAA and aspartate were overestimated while the modelled areas for glutamate, glutamine and GABA were underestimated.

III.3.2 The Dependence on Relative Metabolite Concentrations.

The remaining 3 of the 4 generated *in vitro* ^{1}H MR spectra had the following metabolite area ratios: spectrum #2, NAA= 6: Glu= 4: Gln= 2: GABA= 2: Asp=1: NAAG=1; spectrum #3, 6:3:3:2:0.5:2; and spectrum #4, 6:2:4:3:0.5:0. The mean (i.e., from a population of 8 spectra of S_{NAA}/N_{rms}=54 but with different representations of *in vivo* noise) quantified metabolite areas for each composite *in vitro* spectrum are plotted in Figure III.6. The mean areas of glutamate, glutamine and GABA were all within one standard deviation of the mean from the expected values. Even the spectra where the glutamate:glutamine were reversed from 4:2 to 2:4 (spectrum #2 and #4, respectively, Figure III.6), the bias which was <10% did not exceed the standard deviation of the mean. In modelling aspartate, the bias was greater than the SD of the mean for three of the four spectra. This confirms the earlier result that aspartate is less reliable to quantify (i.e., with a bias of greater than 10%).

In estimating NAA, the bias was well under 1% from its expected value except for spectra #2 and #3, which also included contributions of NAAG in the generated spectra (Figure III.6). In these two cases, the NAAG areas were well underestimated in the model and due to the similar resonances of NAAG and NAA, it appears that the mean areas of NAA were overestimated by

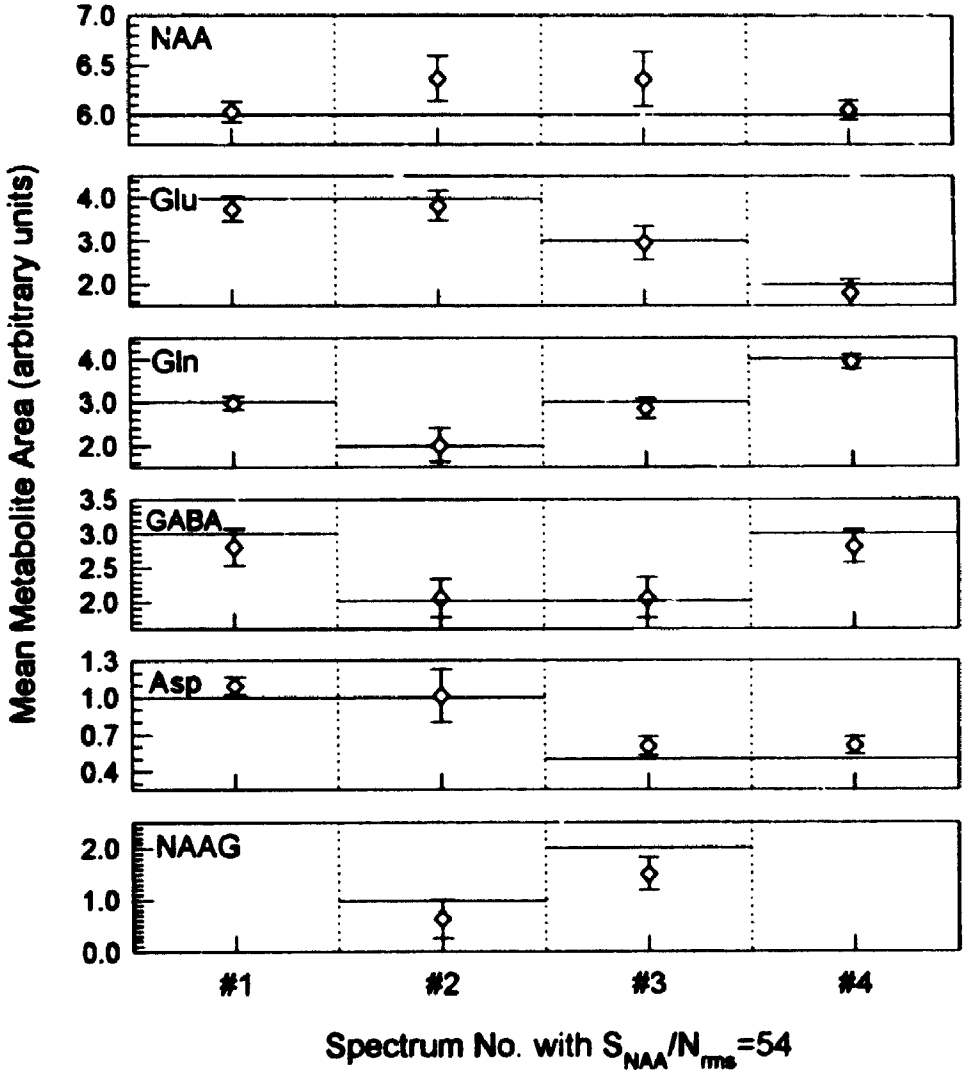

Figure III.6 The mean (◊) quantified areas±1 standard deviation of NAA, glutamate (Glu), glutamine (Gln), GABA and aspartate (Asp) (N=8 *in vitro* ^{1}H MR spectra generated with the same metabolite areas but different *in vivo* noise representations) for the four sets of spectra containing different levels of these metabolites. The solid line represents the expected metabolite area.

approximately that difference. NAAG has a predominant singlet resonance at 2.057ppm due to the CH_3 group which is next to the 2.024ppm resonance of NAA_{CH3}. For this reason and the fact that the *in vivo* concentration of NAAG in white matter is approximately 4 to 9 times lower than the concentration of NAA (Frahm et al. 1991), the quantification of NAAG appears to be unreliable. NAAG has the potential to be underestimated due to the much larger spectral contribution of NAA.

III.3.3 Brain Matter Volume Estimations.

The estimated % grey matter volume within the $8cm^3$ VOI's ranged from 21 to 35% and from 28 to 56% for the $4cm^3$ VOI's, Table III.1. In a two-tailed paired t-test, the $4cm^3$ VOI contained significantly greater amounts of grey matter compared to the $8cm^3$ VOI ($p<0.001$, Table III.1). The CSF contribution within the VOI's ranged from 0.9% to 5.5%. A significantly greater % CSF volume was observed in the $4cm^3$ VOI compared to the $8cm^3$ VOI ($p= 0.029$, Table III.1). Since the timing parameters of the imaging sequence were not optimal for CSF discrimination, the %CSF volume may be underestimated. Ernst et al. (1993) have observed 10-20% lower estimated CSF values derived from images compared to CSF values calculated from the extraction of different T_2 compartments.

III.3.4 *In vivo* ^{1}H MRS.

Figure III.1 consists of a processed *in vivo* ^{1}H MR spectrum acquired from the left dorsolateral prefrontal cortex with a $8cm^3$ VOI. The spectrum

Table III.1. Results of the Brain Matter Volume Estimation for the VOI's.

		% Volume								
		Grey Matter			White Matter			CSF		
VOI	No.	Mean±SD	min	max	Mean±SD	min	max	Mean±SD	min	max
$8cm^3$	10	30±5	21	35	68±5	62	78	1.9±0.6	0.9	2.9
$4cm^3$	10	41±8[a]	28	56	56±9[a]	39	70	2.8±1.4[b]	1.3	5.5

[a] Significantly different from the $8cm^3$ VOI (two-tailed paired t-test, $p<0.001$).

[b] Significantly different from the $8cm^3$ VOI (two-tailed paired t-test, $p=0.029$).

contains no dominating broad spectral resonances that underlie the baseline noise. Spectral resonances of NAA, PCr+Cr, Cho_t, *myo*-inositol, glutamate, glutamine, GABA, aspartate, glucose, *scyllo*-inositol and taurine (Figure III.1), were all resolvable with the STEAM acquisition sequence (TE time of 20ms). Only the resonances between 1.88 and 3.45ppm were modelled to ensure that the residual from the "wings" of the H_2O resonance would not interfere in the model. The mean S_{NAA}/N_{rms} for the ^1H MR spectra collected with the $8cm^3$ VOI was 72±15 (ranging from 49 to 97) and with the $4cm^3$ VOI it was 51±9 (ranging from 36 to 62). Therefore, a S_{NAA}/N_{rms} of 54 which was used to evaluate the simulated *in vitro* spectra represents the typical S/N of a $4cm^3$ VOI spectra. Furthermore, the mean quantified metabolite areas for all 20 *in vivo* spectra had the following metabolite area ratios: NAA = 6: Glu = 3.4: Gln = 1.8: GABA = 1.8: Asp = 0.5: NAAG = 0.7. Therefore, the spectral resolution and relative amplitudes of the metabolites within the 2.0 and 2.66ppm spectral region (Figure III.3) were similar to the simulated *in vitro* spectra (Figure III.1).

A modelled *in vivo* ^1H MR spectrum which includes the sum of all the modelled peaks superimposed on the acquired spectrum is shown in Figure III.7a along with the residual. In addition to the quantified metabolites used in the *in vitro* study, PCr+Cr, Cho_t, glucose, *scyllo*-inositol, and taurine were also included in modelling the *in vivo* spectra. Any relatively broader resonances upfield from the NAA_{CH3} resonance were modelled with a single resonance to account for the overlap to the NAA_{CH3} resonance (Figure III.7). Overall, a

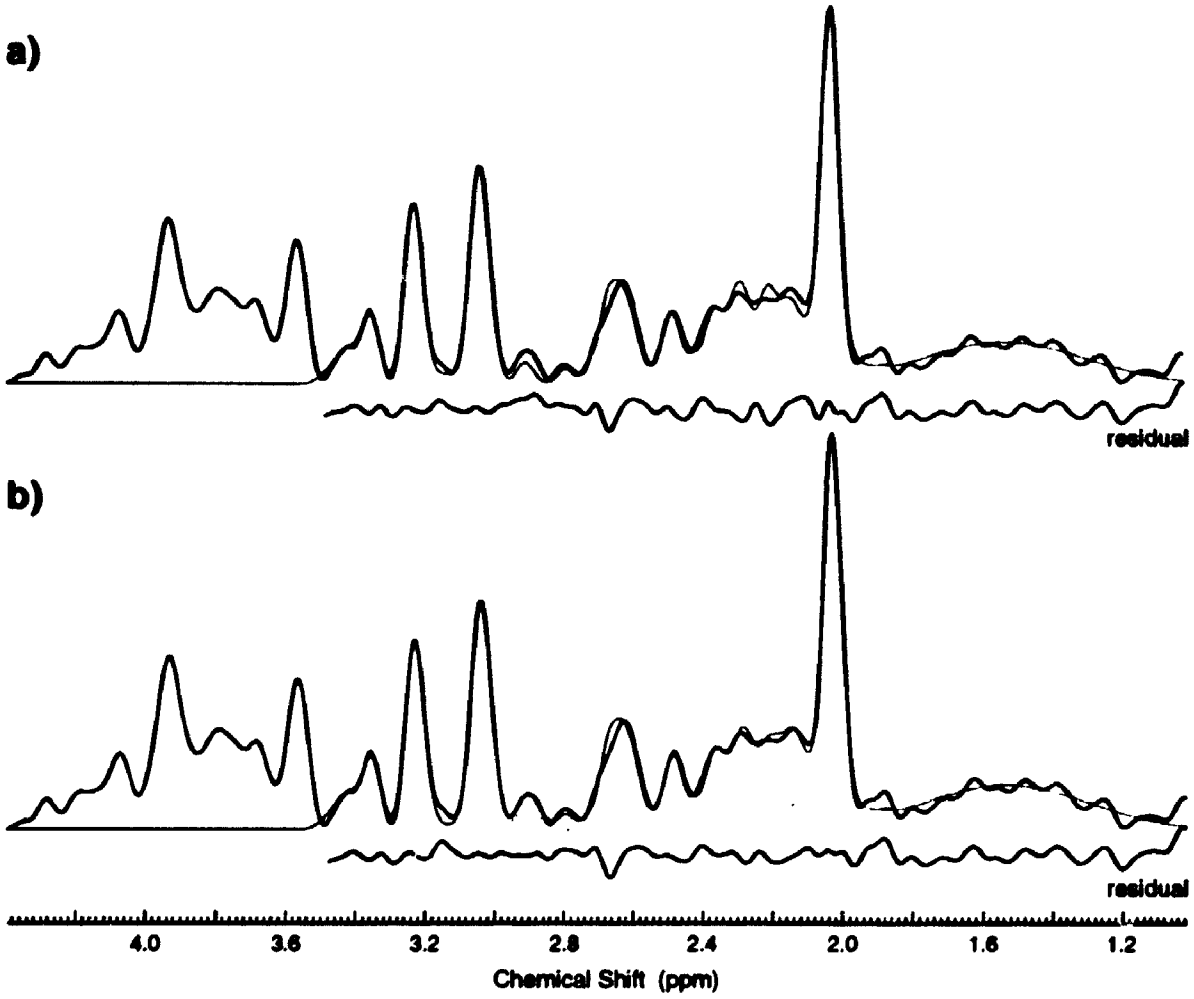

Figure III.7 The result of modelling a typical *in vivo* spectrum using the *a priori* knowledge. The thick line is the acquired spectrum and the thin line is the modelled spectrum. (a) In the overlap region of glutamate, glutamine and GABA, there are differences between the acquired and the modelled spectrum. (b) The result of modelling the above spectrum with the additional resonances (dashed line). Improvement in the fit of the modelled spectrum is obtained.

reasonable fit of the spectrum was observed except for the spectral region at ≈ 2.1 and 2.9ppm (Figure III.7a). These two regions were consistently modelled inadequately for the *in vivo* spectra. The result of averaging the residuals from each of the modelled spectra were two relatively broader resonances with amplitudes above the baseline noise at 2.13 and 2.90ppm (not shown). These resonances are consistent with recent reports that have assigned these resonances to mobile cytosolic proteins and polypeptides (Kauppinen et al. 1992; Behar and Ogino 1993). It appears that with a TE of 20ms, the ^{1}H MR signal of macromolecules are observed and must be accounted for in the modelling. Therefore, these two resonances were included in the model for the *in vivo* spectra of the prefrontal cortex. An improvement in the model was observed and a typical example is shown in Figure III.7b.

III.3.5 8 vs 4cm^3 VOI.

The mean quantified relative metabolite levels from the 10 repeated measures of 8 and 4cm^3 VOI's are presented in Table III.2. The predominant resonances of NAA, PCr+Cr, and Cho$_t$ had coefficients of variation of <10%. The results of a two-tailed paired t-test showed significant increases in the glutamate and PCr+Cr levels and a significant decrease in Cho$_t$ levels in the spectra with 4cm^3 VOI compared to the spectra with 8cm^3 VOI (Table III.2). Regional differences in metabolic concentrations do exist in the brain. Recent *in vivo* ^{1}H MR studies on the human brain have reported higher PCr+Cr and glutamate concentrations and lower Cho$_t$ concentrations in grey matter than in

Table III.2. Mean Relative Metabolite Level from the Spectra with 8 and 4cm³ VOI.

	Relative Metabolite Level (arbitrary units)						Two-tail
	8cm³ VOI (N=10)			4cm³ VOI (N=10)			paired
	Mean±SD	SEM	%SD	Mean±SD	SEM	%SD	t-test[a]
NAA	15.1±1.1	0.35	7.3	15.7±1.3	0.41	8.3	
NAAG	1.1±1.1	0.35	98	1.2±0.5	0.16	43	
NAA+ NAAG	16.2±0.8	0.24	4.7	16.9±1.4	0.44	8.2	
Glu	9.8±2.1	0.68	22	12.0±2.1	0.67	18	**p=0.026**
Gln	5.2±1.8	0.58	35	6.2±2.4	0.75	38	
GABA	4.3±2.0	0.63	46	4.9±1.1	0.36	23	
Asp	3.1±1.6	0.49	50	3.6±1.8	0.58	51	
PCr+Cr	13.2±0.8	0.27	6.4	14.1±0.6	0.20	4.6	**p=0.005**
Cho_t	4.21±0.41	0.13	9.7	3.96±0.28	0.09	7.1	**p=0.046**
Glc	9.4±5.0	1.6	53	6.3±3.5	1.1	55	
scyllo-Ins	0.84±0.42	0.13	51	0.81±0.21	0.068	26	
Tau	1.8±1.2	0.36	64	2.6±1.3	0.41	50	
Macromolecule signal@2.13ppm	4.0±3.2	1.00	80	9.0±7.2	2.3	80	**p=0.039**

[a] Comparing the metabolite levels from the spectra with 8 and 4 cm³ VOI.

white matter (Hänicke et al. 1993; Kreis et al. 1993; Michaelis et al. 1993). Metabolite levels observed in this study indicate the mean % grey matter volume should be greater in the 4cm^3 VOI compared to the 8cm^3 VOI, which was in fact the case (Table III.1).

A trend for larger NAA levels was observed in the spectra with relatively more grey matter. This observation is consistent with several *in vivo* ^{1}H MR reports where larger NAA concentrations were estimated in grey matter (Frahm et al. 1989b; Narayana et al. 1989; Hennig et al. 1992; Kreis et al. 1993; Michaelis et al. 1993). The quantified NAAG levels did not differ significantly between the 8 and 4cm^3 VOI spectra. NAAG represented ≈ 7% of the total NAA + NAAG. Frahm et al. (1991) estimated NAAG in white matter contributed 10-20% of the total NAA + NAAG while Holowenko et al. (1992) estimated 11.5%. The lower levels of NAAG estimated with our model is consistent with the *in vitro* modelling results which showed that NAAG was underestimated by 30% to 40%.

III.3.6 Estimation of the mmol/kg wet weight Concentration.

The relative metabolite levels in Table III.2 have units of mM/L, however, the T_1 and T_2 relaxation effects on these metabolites and on the internal water reference have not been accounted for. By substituting the T_1 and T_2 values from (Frahm et al. 1989b) into Eqs. [B.4], the absolute concentration of NAA, PCr+Cr and Cho, with units of mmol per kg wet weight were estimated using Eq. [B.7] for the 8 and 4cm^3 VOI. To correct for the relaxation on the tissue

water signal, a T_2 value of 80ms was used in Eq. [B.6] and the saturation factor was estimated at 1.24 (derived by averaging the tissue water integral ratio between ^{1}H STEAM data collected with a TR of 10,000msec and 1,500ms from six controls). To approximate glutamate and glutamine concentrations a range of T_2 decay times (i.e., the minimum and maximum T_2 values from (Frahm et al. 1989b)) and the reported T_1 value from (Hänicke et al. 1993) were used. The estimated concentrations are presented in Table III.3.

The estimated NAA concentrations of 10.8 and 11.4mmol/kg (Table III.3) are higher than reported values of 7.5 up to 8.8mmol/kg in white matter from other *in vivo* ^{1}H MR studies (Hagberg et al. 1993; Kreis et al. 1993; Michaelis et al. 1993). Only those *in vivo* ^{1}H MRS studies which assumed a constant PCr+Cr concentration of approximately 10.4mmol/kg (Lowry et al. 1977) as an internal reference have estimated comparable values (Hanstock et al. 1988; Frahm et al. 1989b, Hagberg et al. 1993). The estimated PCr+Cr concentrations of 10.3 and 11.1mmol/kg (Table III.3) are consistent with the results of enzymatic analysis of human brain tissue where the PCr+Cr concentration ranged from 9.5 to 13.2mmol/kg (Lowry et al. 1977). However, previous *in vivo* ^{1}H MRS studies have estimated lower concentrations of PCr+Cr in white matter ranging from 5.3 to 8.9mmol/kg (Narayana et al. 1989; Kreis et al. 1993; Michaelis et al. 1993). Furthermore, larger Cho_t concentrations (by approximately a factor of two) have been observed relative to other *in vivo* ^{1}H MRS reports on the human brain (Narayana et al. 1991;

Table III.3. Mean Metabolite Concentration from the Spectra with 8 and 4cm³ VOI.

	Metabolite Concentration (mmol/kg wet weight)					
	8cm³ VOI (N=10)			4cm³ VOI (N=10)		
	Mean±SD	Min.[a]±SD	Max.[b]±SD	Mean±SD	Min.[a]±SD	Max.[b]±SD
NAA	10.8±0.8			11.4±1.0		
PCr+Cr	10.3±0.7			11.1±0.6		
Cho_t	2.72±0.26			2.60±0.19		
Glu		9.2±2.0	9.6±2.1		11.4±2.1	11.8±2.1
Gln		4.7±1.7	4.9±1.7		5.7±2.0	5.9±2.3

[a] The T_2 of the metabolite was assumed to be 450ms (i.e., the maximum T_2 value from Frahm et al. (1989b) to represent the lower boundary value.

[b] The T_2 of the metabolite was assumed to be 240ms (i.e., the minimum T_2 value from Frahm et al. (1989b) to represent the upper boundary value.

Kreis et al. 1993; Michaelis et al. 1993). The tendency of observing overestimated concentrations may be explained by the absolute quantification technique. The acquired unsuppressed tissue water signal with an echo time of 20ms, may not represent the total tissue water content due to water compartments in brain tissue that have shorter T_2's, and subsequently, are not or partially observed (Menon and Allen 1991).

The estimated glutamate concentrations ranged from 9.2 to 11.8mmol/kg and glutamine concentrations ranged from 4.7 to 5.9mmol/kg. From *in vitro* brain studies, Perry et al. (1971; 1975; 1981) have estimated the glutamate concentrations between 6.0 and 10.2mmol/kg and the glutamine concentrations between 5.4 and 5.9mmol/kg. From *in vivo* ^{1}H MRS data, Hänicke et al. (1993) reported glutamate concentrations of 8.3 and 5.5mmol/kg in grey matter and white matter, respectively, and glutamine concentrations of 3.5 and 2.2mmol/kg in grey and white matter respectively (Hänicke et al. 1993). Our glutamate and glutamine concentrations appear to be in better agreement with the *in vitro* studies rather than *in vivo.*

III.3.7 The Less Predominant Metabolites.

In Figure III.1, the resonances of GABA, aspartate, taurine and *scyllo*-inositol are much less pronounced than NAA, PCr+Cr or Cho_t. The main reason for this is not that these metabolites have relatively short T_2 decay times but their concentrations in human brain are of the order of 1-2mmol/kg (Perry et al. 1981; Petroff et al. 1989), the lower limit of *in vivo* ^{1}H MR signal detection.

The low cerebral concentration of these metabolites is reflected in the observed large coefficients of variation between 24% and 64%, Table III.2. As a result, without the use of spectroscopic editing techniques (Wilman and Allen 1993) or externally enhancing the concentration of these metabolites, the quantification of GABA, aspartate, taurine and *scyllo*-inositol is unreliable (i.e., where the coefficient of variation is greater than 10%). For the *in vitro* results the S_{NAA}/N_{rms} spectra with NAA:GABA:Aspartate of 6:3:1 would need to be >100 for reliable results. The coefficients of variation of these metabolites are consistent with the reported values of Provencher (1993).

The concentration of glucose in brain tissue was estimated to be 1.0mmol/L (Gruetter et al. 1992). Even with extreme correction values for relaxation, the observed levels of glucose in Table 2 tend to be larger than expected. The glucose concentration in CSF is much larger with a value of 3.3mmol/L (McGale et al. 1977). However, the observed CSF contribution in these VOI's can not account for this discrepancy. Since the glucose resonances are at the end of the selected quantification region and *myo*-inositol is not included in the model, the extension of the wing from the *myo*-inositol resonance would cause an overestimation of the glucose level.

III.3.8 Spectral Contribution of Macromolecules.

From the *in vivo* data, the resonance at 2.13ppm has previously been assigned to mobile macromolecules (Kauppinen et al. 1992; Behar and Ogino 1993). Its contribution was significantly greater in spectra with relatively more

grey matter volume (Table III.2). There were large variations in the level of this resonance (%SD ≈ 80). The variations in level may reflect the true heterogeneity of these macromolecules in the prefrontal region, or the poor precision in quantifying this overlapping resonance. Further investigation is needed to identify and characterize the contribution of mobile proteins and polypeptides observed in *in vivo* spectra of the human brain. From cytosolic macromolecule fractions of rat brain, Behar and Ogino (1993) have observed several relatively broad resonances within the spectral region of 2.0 and 3.45ppm (including a predominant resonance at ≈ 2.1ppm). In this study, only resonances at 2.13 and 2.9ppm were modelled. Consequently, quantifying the macromolecules tended to be underestimated due to an incomplete *a priori* knowledge of these resonances. This could explain why in general the concentrations of the quantified metabolites were overestimated. The contribution of macromolecules to *in vivo* ^{1}H MR spectra should not be ignored.

CHAPTER IV

A ^{1}H MRS Study of Schizophrenic Patients and Controls

IV.1 Introduction.

The neurotransmitter system in the human brain is composed of predominantly EAA and inhibitory GABAergic pathways (Curtis and Johnston 1974; Fagg and Foster 1983; Erecińska and Silver 1990). Glutamate, and to a lesser extent aspartate, are the main neurotransmitters that bind to the EAA receptors. EAA receptor functions are responsible for learning and memory, neural development, synaptic plasticity and any excitotoxicity action (Cotman and Monaghan 1988). Since the symptoms of schizophrenia include a range of cognitive impairments, the EAA system and in particular the corticostriatal and limbic glutamatergic pathways could be implicated in this illness.

Convincing evidence which implicates the EAA system comes from studies with PCP which is a specific, non-competitive antagonist of the glutamate subtype receptor, NMDA (Lodge and Johnson 1990). PCP has been shown to induce psychosis resembling schizophrenia in normals and exacerbate psychosis in schizophrenic patients (Javitt and Zukin 1991). In several postmortem brain studies, evidence of anatomical and functional alterations involving the EAA system in patients with schizophrenia have been reported. Differences in the binding density of glutamate subtype receptors in various brain regions have been observed in postmortem schizophrenic patients

compared to controls (Ulas and Cotman 1993). Increased density of pyramidal neurons (layer V) and decreased density of interneurons were observed in the prefrontal area of schizophrenic patients compared to a control group (Benes et al. 1991). Sherman et al. (1991) observed a decrease in the release of glutamate and GABA as well as a decrease in the activity of glutamate decarboxylase in synaptosomes prepared from frontal and temporal cortex tissue of schizophrenic patients compared to a control group. Furthermore, a reduction of messenger RNA that encodes non-NMDA glutamate receptors in hippocampal tissue has been observed in patients compared to a control group (Harrison et al. 1991). In postmortem studies, however, there are many factors (such as the postmortem interval) that can influence results. In most cases these observations reflect the chronic stage of the illness (Collinge and Curtis 1991, Ulas and Cotman 1993).

MRS, a non-invasive technique, has an advantage by studying the biochemistry of a localized region in the human brain *in vivo* as discussed in Chapter I. Unlike postmortem studies of schizophrenia where the patients are usually older, chronically ill, and medicated, *in vivo* MRS allows the acquisition of brain spectra from schizophrenic patients at any stage of illness.

This study investigated the possible differences in the level of neurotransmitters and/or other ^{1}H metabolites between schizophrenic patients at different stages of illness and appropriately matched controls, that may provide evidence implicating the EAA system in schizophrenia. *In vivo* ^{1}H MR spectra

from the left dorsolateral prefrontal region of *(i)* first episode DN, *(ii)* NDM and *(iii)* CM schizophrenic patients were acquired and compared to controls. In addition, a blind data analysis was conducted and a spectral quantification method used to obtain the metabolite levels, incorporated *a priori* knowledge on the spectral peak arrangement for each metabolite (Chapter III).

IV.2 Method.

IV.2.1 Subjects.

Twenty-nine patients with schizophrenia ranging in age from 16 to 49 years participated in this study. There were thirteen first episode DN schizophrenic patients, of which eleven were classified as paranoid and two as undifferentiated. The length of illness (LOI) for the DN patients ranged from one month to six years. None had been exposed to any antipsychotic medication prior to the MRS examination. However, seven patients had received 1 to 3mg of lorazepam in the 24 hours before assessment. The remaining patients included twelve NDM schizophrenic patients (of which eight had been examined previously as first episode DN patients) and twelve CM schizophrenic patients. The NDM patients with a mean LOI of 2±2 years included ten classified as paranoid and two as undifferentiated. The CM patients group with a mean LOI of 17±6 years had six diagnosed as paranoid, two as undifferentiated and four as residuals. All medicated patients were receiving antipsychotic medication. Eighteen of them were also on

anticholinergic medication for side effects. The mean length of time on medication for the NDM patients was 14±10 weeks. Clinical information is shown in Table IV.1.

Twenty-four non-schizophrenic controls, ranging in age from 16 to 53 years, formed three control groups. Each patient, within the three patient groups, was matched in gender and age (mean difference was <½ a year) and comparably matched in education, parental education and handedness with a control subject. Subject characteristics of the "matched" control groups are shown in Table IV.1.

IV.2.2 Screening of the Subjects.

The schizophrenic patients and control subjects were recruited by Dr. Williamson, Dr. Malla and by psychiatrists from the local area. The diagnoses of the patients and evaluation of the control subjects were established with the SCID (structured clinical interview for DSM-II-R, Spitzer and Williams 1985) administered by a psychiatrist (Dr. Williamson). The diagnoses of the DN patients were re-confirmed with the treating psychiatrist six months after the MR experiments were done. Both, the SANS (scale for the assessment of negative symptoms, Andreasen 1984a) and SAPS (scale for the assessment of positive symptoms, Andreasen 1984b) were also administered to the patients by a psychiatrist (Dr. Williamson) without any knowledge of the MRS results. The LOI was based on the time between the onset of positive symptoms and the MRS examination. Education level was rated on a four-point scale (1, ≤ grade

Table IV.1 Subject Characteristics.[a]

	Gender	Age (yrs)	Length of Illness (yrs)	Handedness	Education Level[b]	Parental Education Level[b]	SANS score	SAPS score
Control Groups								
Controls (DN)	11M + 2F	26±7	---	11 right	2.5±1.0	2.6±0.9	---	---
Controls (NDM)	10M + 2F	26±7	---	11 right	2.5±0.9	2.7±0.9	---	---
Controls (CM)	11M + 1F	41±5	---	12 right	3.6±0.5	2.2±0.9	----	----
Schizophrenic Patient Groups								
First Episode DN	11M + 2F	26±7	2±2	13 right	2.3±0.9	2.3±0.8	37±13	30±11
NDM	10M + 2F	26±7	2±2	12 right	2.4±0.7	2.2±0.8	28±14	9±16
CM	11M + 1F	41±5	17±6	12 right	2.6±0.8	2.0±0.3	24±12	8±11

[a]Values are mean±1 standard deviation.

[b]Levels were rated with a four-point scale as described in section IV.2.2.

10; 2, grade 11-13; 3, 1-3 years college or university; 4, 3+ years college/university). Parental education ratings were also evaluated for the most educated parent or in certain cases for the most educated adoptive parent. The handedness of each subject was defined by the hand used to write and throw a ball.

Patients and controls were free of any history of head injury, drug or alcohol abuse, or serious medical illness based on the information provided during the SCID interview. No gross abnormalities were detected on routine clinical MR images that were also collected as part of the study on each subject.

IV.2.3 ^{1}H MR Spectroscopy.

The *in vivo* ^{1}H MRS experiments were conducted at 1.5 Tesla using a circularly polarized head coil on a whole body MR spectrometer. The STEAM sequence with an echo time of TE=20ms, provided the single voxel localization technique (Chapter I). The ^{1}H MR signal was obtained from a 2x2x2cm^3 VOI located in the left dorsolateral prefrontal region of the subjects. The positioning of the VOI was determined from a set of sagittal and coronal scout ^{1}H MR images as shown in Figure IV.1. The dashed lines in Figure IV.1 represent the anterior (a), posterior (b), lateral (c) and medial (d) surfaces of the three dimensional VOI (white box). Maximization of the magnetic field homogeneity was done by a global head shim followed by a localized shim on the VOI. A total of 4,096 complex data points were used to digitize 1 second of the time

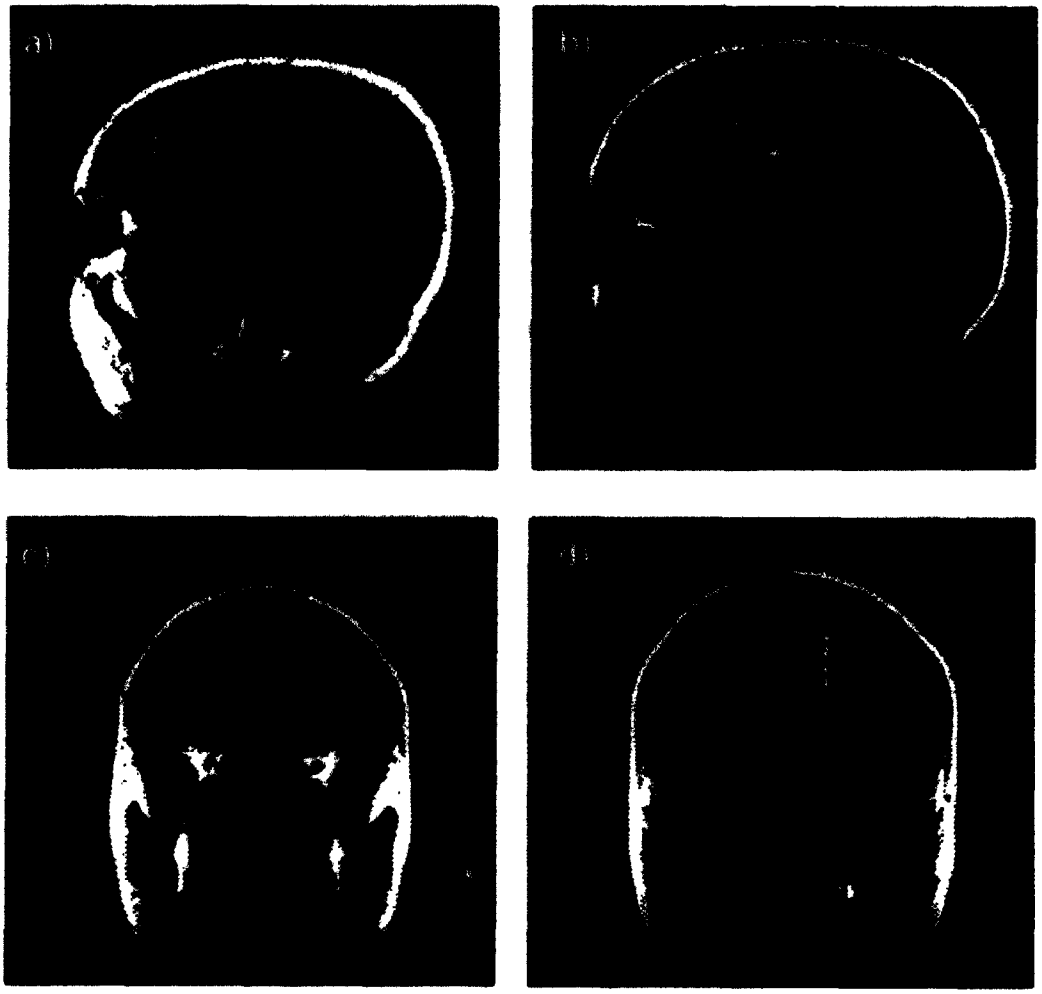

Figure IV.1 Sagittal and coronal ^{1}H MR images with the $2x2x2cm^{3}$ volume of interest (VOI, the white box) positioned in the left dorsolateral prefrontal region. The dotted lines represent the anterior (a), posterior (b), lateral (c) and medial (d) surfaces of the VOI.

domain signal (i.e., spectral bandwidth ±2.0kHz). The TR was 1,500ms and 450 acquisitions were averaged. For each water suppressed ^{1}H spectrum acquired, a water unsuppressed ^{1}H spectrum was also collected (55 acquisitions) by setting the amplitudes of the CHESS pulses to zero voltage.

IV.2.4 Post-Spectral Processing.

The data files were coded such that the operator was blind to the status of the subjects. A time domain deconvolution technique, QUALITY (de Graaf et al. 1990) was first applied to the MR signal to restore the spectral lineshapes to pure Lorentzian. The time domain signal was then multiplied by h(t), a Lorentzian-to-Gaussian transformation ($h(t)=\exp(-\pi \cdot a \cdot t+\pi \cdot a \cdot t^2/(4 \cdot b))$ where a=-0.6 and b=42/4,096), to enhance the apparent spectral resolution (Ferrige and Lindon 1978). The MR signal was then zero filled from 4,096 to 8,192 complex data points, Fourier transformed and phased with 0th order and 1st order within ±½ a dwell period. No spline function was applied to the baseline.

The levels of the ^{1}H metabolites from the *in vivo* ^{1}H spectra were obtained by fitting the spectral peaks between 1.88 and 3.45ppm with Gaussian lineshapes. To resolve the issue of quantifying complex ^{1}H spectra with multiple peaks that overlap each other, the technique described in Chapter III, which incorporated *a priori* knowledge into a frequency domain nonlinear least squares fitting algorithm (Marquardt 1963), was used. The quantified ^{1}H metabolites included NAA, glutamate, glutamine, GABA, aspartate, NAAG, PCr+Cr, Cho_t, glucose, taurine, *scyllo*-inositol and two macromolecule

resonances at 2.12 and 2.9ppm (Chapter III). The integral value of the phased water peak from unsuppressed water ^1H spectrum, which represents the total MR visible water content in the VOI, was used as an internal standard to normalize the spectral peak areas such that relative metabolite levels could be obtained (Eq. [B.9]). Since, f_{grey} and f_{white} were not estimated within the VOI, the tissue water concentration in Eq. [B.8] was estimated to be $0.73 \cdot 55.6 \times 10^3$mM (=$[H_2O_{tissue}]$). Fitting the peaks within a certain spectral region ensured that the residual from the "wings" of the water resonance would not interfere in the quantification.

IV.2.5 Statistical Analysis.

Each patient was matched in age and sex with a control subject, therefore, a two-tailed, paired t-test was used to determine any significant differences in age, education level, parental education level and the quantified metabolite levels between the three patient groups and the appropriately matched control groups. Probability values less than 0.05 were considered statistically significant. Of the eight patients that were examined twice, first as a DN then as a NDM patient, a two-tailed, paired t-test was also used to compare the SANS and SAPS scores and metabolite levels between pre- and post-medication measures. Pearson product moment correlations of age, LOI, SAPS and SANS scores with levels of NAA, glutamate, glutamine, GABA, PCr+Cr and Cho_t were evaluated for both the combined control and patient groups.

IV.3 Results.

Age, education and parental education levels of the three patient groups were not significantly different from the controls, except that the education levels of the CM patients were lower compared to the control group ($p=0.002$).

A typical processed and quantified *in vivo* ^1H spectrum acquired from the left dorsolateral prefrontal region of a control is shown in Figure IV.2. The spectrum contains no dominating broad spectral resonances that underlie the baseline noise over the 1.88 to 3.45ppm spectral region. Resonances of NAA, glutamate, glutamine, GABA, aspartate, PCr+Cr, Cho_t, *myo*-inositol, glucose, taurine and *scyllo*-inositol are all resolved. The signal to noise ratio (i.e. the signal of the NAA_{CH3} peak over the root mean square of the noise) is ≈ 80 (Figure IV.2) which is adequate to reliably quantify the spectrum (Chapter III). The result of quantifying this spectrum is displayed in Figure IV.2b as a sum of all spectral peaks of the metabolites superimposed on the acquired spectrum. The difference between the two is also shown in Figure IV.2b.

The mean quantified metabolite levels of NAA, NAAG, glutamate, glutamine, GABA, aspartate, PCr+Cr, Cho_t, taurine, *scyllo*-inositol and glucose for the three patient and control groups are shown in Table IV.2. In the controls, the standard deviations of the quantified levels for the dominating spectral peaks of NAA, PCr+Cr and Cho_t, were $\approx 10\%$. The standard deviation in the controls was $\approx 20\%$ for glutamate, $\approx 30\%$ for glutamine and $\approx 40\%$ for GABA while the standard deviations of aspartate, NAAG, taurine, *scyllo*-inositol

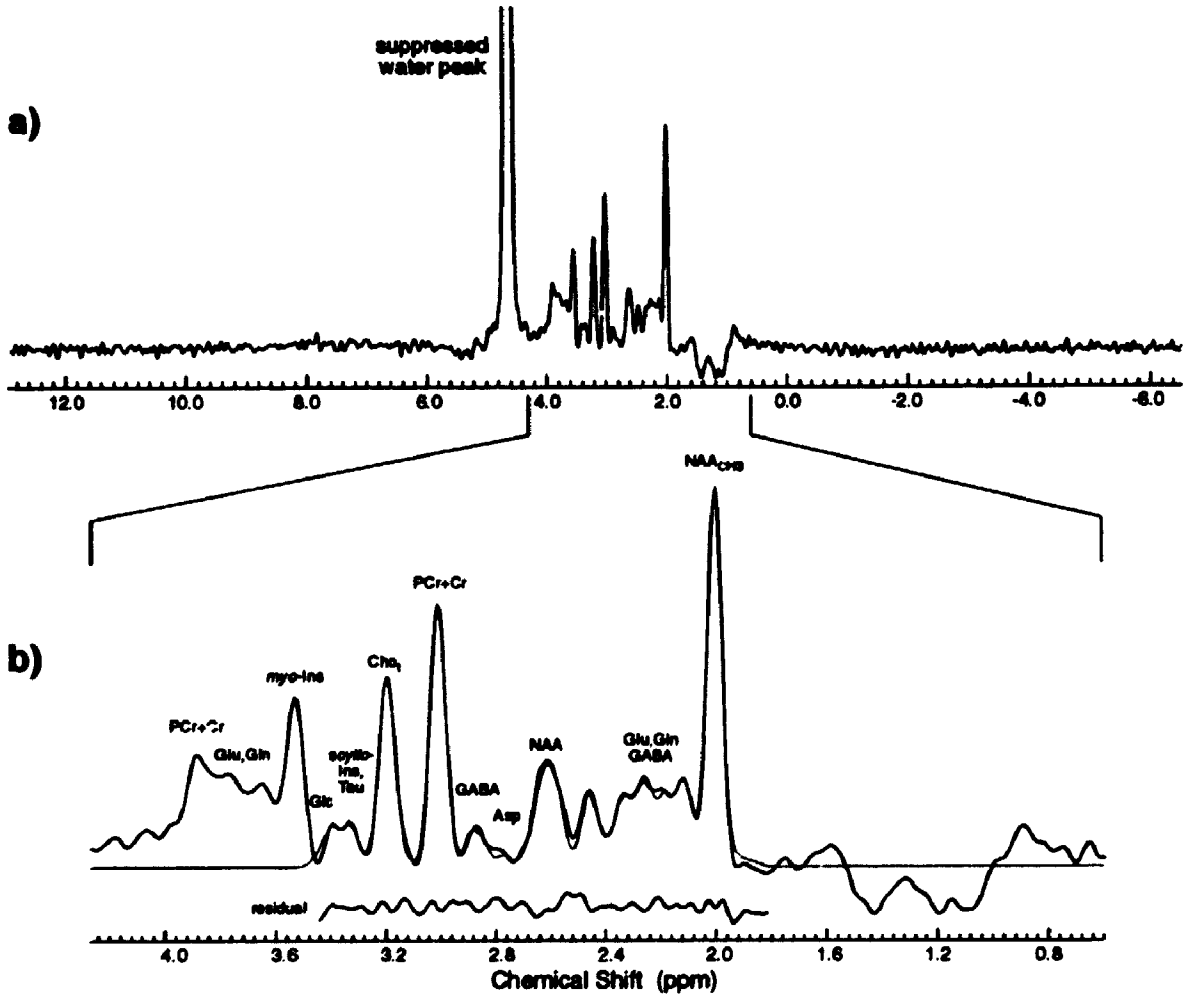

Figure IV.2 An *in vivo* ^{1}H MR spectrum acquired at 1.5Tesla. (a) Contains a typical processed *in vivo* ^{1}H MR spectrum from the left dorsolateral prefrontal region acquired with the STEAM sequence (TE=20ms) and (b) shows the same spectrum with the frequency region expanded. The result of modelling the spectrum with *a priori* knowledge is superimposed (thinner line) on spectrum in (b) and the difference between the acquired spectrum and the modelled spectrum is shown below.

Table IV.2 Pairwise Comparison of the Metabolite Levels between the Schizophrenic Patients and the Controls.

	Relative Metabolite Level (mean±1SD, arbitrary units)					
	Controls (DN)	DN Patients	Controls (NDN)	NDM Patients	Controls (CM)	CM Patients
NAA	15.0±1.5	15.0±1.7	14.9±1.6	15.9±2.4	13.7±1.1	13.9±1.6
NAAG	0.825±0.678	1.31±0.68	0.798±0.713	1.14±0.90	1.16±0.64	1.18±0.80
Glu	8.83±2.13	9.68±2.28	8.43±1.82	10.4±2.1[a]	8.12±1.50	7.94±1.48
Gln	5.43±1.76	4.40±1.96	5.80±1.75	4.45±2.56	4.80±1.41	6.55±1.86[b]
GABA	3.63±1.42	2.95±1.63	3.61±1.49	3.73±1.47	3.22±0.94	3.78±1.14
Asp	2.41±1.19	2.31±0.92	2.63±1.27	2.45±1.17	1.94±0.95	2.78±1.05
PCr+Cr	12.7±1.1	13.1±1.4	12.5±1.0	13.4±1.8	12.6±1.5	13.1±1.0
Cho_t	3.84±0.42	3.68±0.39	3.81±0.42	3.91±0.52	3.76±0.53	4.08±0.54
Tau	2.42±1.50	1.62±1.50	2.27±1.44	1.63±2.22	1.80±1.55	3.02±1.61[c]
Scyllo-Ins	0.546±0.460	0.535±0.408	0.601±0.451	0.710±0.397	0.754±0.295	0.618±0.490
Glc	5.63±4.05	7.56±4.78	5.37±4.50	8.93±4.59	4.29±3.41	6.37±4.46

[a]Significantly different from the control (NDM) group (p=0.019).

[b]Significantly different from the control (CM) group (p=0.015).

[c]Significantly different from the control (CM) group (p=0.027).

and glucose were all >50%.

There were no significant differences when comparing the ^{1}H metabolite levels of the first episode DN and NDM patients with the control group, except for a significant increase in the glutamate level of the NDM patients. The PCr+Cr to glutamate ratio tended to be lower in the NDM patients compared to the control (NDM) group, but was not significant. When comparing the metabolite levels between the CM patients and the control group, the only significant differences noted were increases in glutamine and taurine levels of the patients. The PCr+Cr to glutamine and NAA to glutamine ratios were lower in these patients, but not significantly different compared to the control group. However, the glutamate to glutamine ratio was significantly different in the CM patients compared to the controls. The NAA to taurine and PCr+Cr to taurine ratios were not significantly different between the CM patients and the controls. In a two-tailed t-test, there was a significant decrease in the SAPS scores of the NDM patients compared to the DN patients ($p=0.001$), while there were no differences in the SANS score. In the paired t-test of the eight patients that were examined as a DN and NDM patient, SAPS scores ($p=0.006$) and glutamine levels ($p=.02$) were both significantly reduced in the post-medication measures compared to the pre-medication measures. There were no significant differences in the two macromolecule resonances between any patient group and the control group. These results are summarized in Tables IV.2 and IV.3.

Table IV.3 Pairwise Comparison of the Metabolite Ratios between the Medicated Schizophrenic Patients and the Controls.

	Metabolite Ratio			Metabolite Ratio		
	Controls (NDN)	NDM Patients		Controls (CM)	CM Patients	
NAA / Glu	1.84±0.39	1.57±0.27	(p=0.135)	---	---	
NAA / Gln	---	---		3.08±0.93	2.33±0.89	(p=0.058)
NAA / Tau	---	---		10.6±13.0	7.76±8.71	(p=0.580)
(PCr+Cr) / Glu	1.56±0.40	1.32±0.20	(p=0.065)	---	---	
(PCr+Cr) / Gln	---	---		2.83±0.81	2.21±0.86	(p=0.063)
(PCr+Cr) / Tau	---	---		10.1±13.4	7.48±7.60	(p=0.616)
Glu / Gln	1.68±0.91	4.56±6.51	(p=0.174)	1.87±0.79	1.32±0.51	(p=0.015)

Combining the schizophrenic patients together, the LOI, SANS and SAPS scores were not significantly correlated with either the levels of NAA, glutamate, glutamine, GABA, PCr+Cr or Cho_t, except for a significant positive correlation between the glutamine level and the LOI ($r=0.48$, $p=0.003$). The glutamine level and age correlation was not significant in the combined controls. The glutamine level of each patient is plotted as a function of LOI in Figure IV.3. Furthermore, there was no significant correlation between the ^1H metabolite levels and the number of weeks that the NDM patients had been on medication.

IV.4 Discussion.

IV.4.1 First Episode Drug Naive Patients.

The two EAA's, glutamate and aspartate, observed in the first episode DN schizophrenic patients had levels comparable to controls. There were also no significant differences in the glutamine and GABA levels between the DN patient and control groups. Glutamine is a metabolite that plays an important role in recycling neurotransmitter glutamate (Nicholls 1989) and GABA, the most abundant inhibitory neurotransmitter in the central nervous system, is synthesized principally from glutamate by glutamate decarboxylase (Curtis and Johnston 1974; Martin and Rimvall 1993). Therefore, these *in vivo* measures in the left dorsolateral prefrontal region suggest resting levels of EAA's, GABA and glutamine do not differ between controls and patients at this stage of illness.

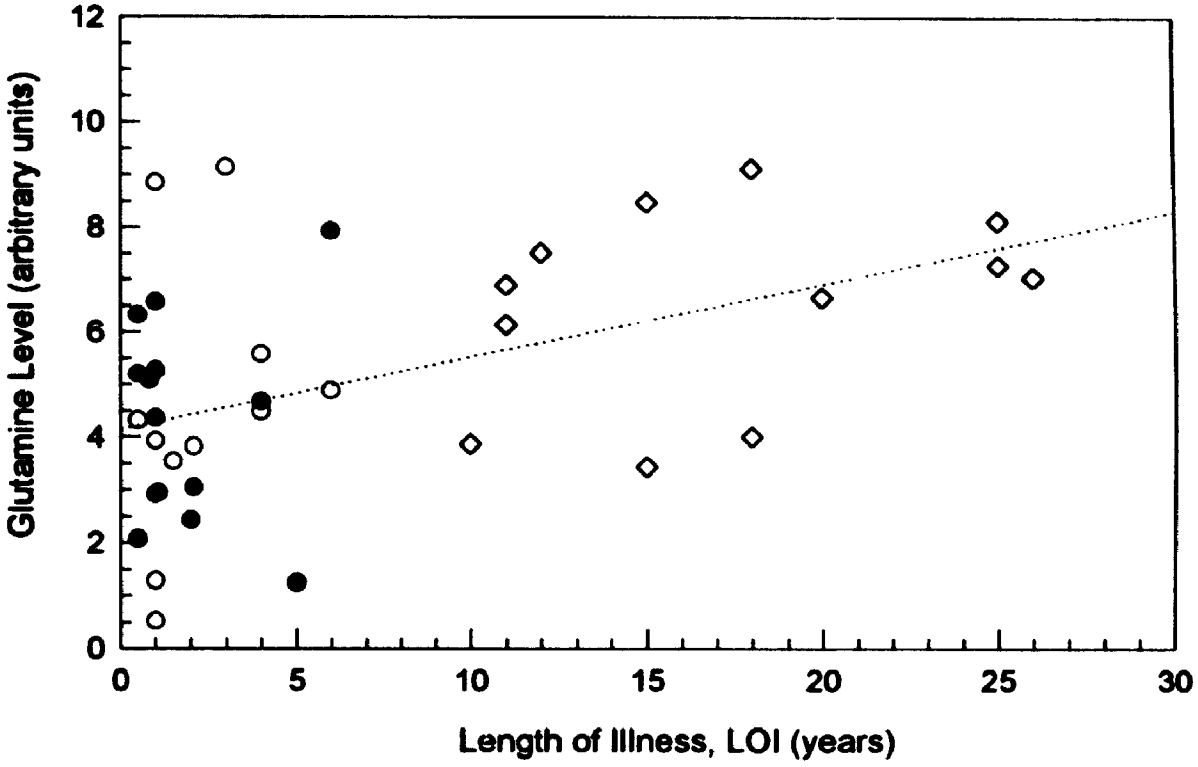

Figure IV.3 Scatter plot of the glutamine levels versus LOI of the DN (●), NDM (○) and CM (◊) patients. The dotted line represents the regression line (r=0.48).

The NAA, PCr+Cr and Cho_t levels of the DN patients were not significantly different compared to the levels in the control group. These three metabolites have spectral peaks that dominate the spectrum and consequently the standard deviation of these levels were ≈10% in the control group. The function of NAA in the brain has not been firmly established (Birken and Oldendorf 1989). In terms of the total concentration of free amino acids in mammals, NAA is second only to glutamate and NAA is localized predominantly within neurons (Tallan 1957; Matalon et al. 1988; Birken and Oldendorf 1989; Urenjak et al. 1993). Therefore, quantifying the NAA level provides information on neuronal cell viability. The observed Cho_t level includes the contribution of GPCho, PCho and to a lesser extent choline. Recent *in vivo* ^1H MRS studies on normal human brains have reported lower Cho_t and higher PCr+Cr concentrations in grey matter than in white matter (Kreis et al. 1993; Michaelis et al. 1993; Chapter III). Our observations on the NAA, PCr+Cr and Cho_t levels of DN patients suggest there is no major neuronal cell loss, and the grey matter and white matter volumes are comparable to controls.

Parallel to this study, *in vivo* ^{31}P MR spectra of the left dorsolateral prefrontal cortex were also collected on these subjects (Chapter V). It is of interest that levels of NAA, PCr+Cr and especially Cho_t which includes contributions of intermediate products of the membrane phospholipid metabolism, were not significantly different in DN patients, while alterations in the membrane phospholipid metabolism have been observed in ^{31}P MRS data

of DN patients compared to controls (Pettegrew et al.1991; Pettegrew et al. 1993; Chapter V). This may suggest that the alterations in the metabolism of cell membranes observed in ^{31}P MRS may be associated with another synaptic function rather than a loss of synapses.

No significant differences in the glucose level were observed in the DN patients compared to the control group. The estimated concentration of glucose in brain tissue is approximately 1.0 mmol/L (Gruetter et al. 1992) while in CSF its concentration of 3.3 mmol/L (McGale et al. 1977) is significantly greater. *In vivo* ^{1}H MRS studies of the human visual cortex, have observed decreases in glucose level during photic stimulation (Merboldt et al. 1992, Chen et al. 1993), which suggests that glucose acts as a state dependent variable. The absence of a difference in the glucose level in these patients suggests that the observed CSF volume within the VOI are comparable to the controls and that there is no difference in the metabolic rate of glucose consumption in the dorsolateral prefrontal region of first episode DN patients.

Levels of taurine, *scyllo*-inositol and NAAG were comparable in the DN patients and the controls. Therefore, the following physiological roles of these metabolites are not implicated in the DN patients. Taurine has characteristics of an inhibitory neurotransmitter, neuromodulator and brain tissue osmoregulator (Cooper et al. 1982; van Gelder 1983; Holopainen et al. 1985; Ottersen et al. 1988). *Scyllo*-inositol is one of five different naturally occurring isomers of inositol and due to its close metabolic coupling to *myo*-inositol

(Sherman et al. 1968; Michaelis et al. 1993), *scyllo*-inositol may be interpreted as a storage form for the IP_3 second messenger system (Fisher et al. 1992). The dipeptide NAAG has been identified to have many different roles in the central nervous system, including a neurotransmitter (Blakely and Coyle 1988; Birken and Oldendorf 1989).

IV.4.2 Newly Diagnosed Medicated Patients.

The increased glutamate level was the only significant difference observed when comparing ^1H metabolite levels of the NDM patients with that of the control group and this difference was not observed in either the DN or CM patients. This would suggest the neuroleptic medication, which had been administered to these patients for a mean length of time of 14±10 weeks and whose function is to block dopamine receptors, gave rise to an increase in availability of glutamate in the neurotransmitter pool and/or metabolic pool. Glutamatergic neurons have high glutamate concentrations throughout the entire cell and particularly in the presynaptic region (Erecińska and Silver 1990). Within the neurotransmitter pool, under resting conditions, the glutamate concentration is ≈100mM in synaptic vesicles, 10mM in the presynaptic cytoplasm and 1μM in the extracellular space (Nicholls and Attwell 1990). Approximately 15% of the glutamate stored in synaptic vesicles participates in calcium-dependent exocytosis as a neurotransmitter (Nicholls 1989). There is additional evidence that may resolve which aspect of the glutamate system is affected. The glutamine level of the post-medication measures were

significantly lower compared to the pre-medication measures of the eight schizophrenic patients. Glutamine is involved in the recycling of the neurotransmitter glutamate (Nicholls and Attwell 1990). Following the release of glutamate by calcium-dependent exocytosis, excess glutamate is transported into glia and is subsequently converted to glutamine by glutamine synthetase. Glutamine may then enter the presynaptic neuron and serve as a precursor for glutamate by mitochondrial glutaminase. Therefore, the increase in the glutamate level may reflect a reduction in the release of glutamate into the synaptic cleft (Deutsch et al. 1989). Subsequently the glutamine level would decrease due to a decrease in glutamate availability as substrate for the glutamine synthetase activity in glia. This would be consistent with the reported decrease of glutamate release in prepared synaptosomes from the prefrontal cortex by Sherman et al. (1991). However, it must be noted that these differences seem to occur only early in the illness after the patients have been on medication. In the presynaptic neuron, an increased conversion of glutamine to glutamate by mitochondrial glutaminase may also account for the observed measurement of glutamate and glutamine.

This evidence of neuroleptic drugs affecting the glutamate system in the prefrontal region would not be consistent with *in vitro* studies of rats. Under chronic administration of neuroleptic medication (whose role is to block dopamine receptors) in these rats, there were no differences observed in the glutamate level in the prefrontal region (Perry et al. 1979; Kim et al.1983; Petty

et al. 1984; Sherman and Mott 1984). Berger et al. (1991) have demonstrated unexpected differences in the regional and laminar distribution of cortical dopamine projections between rodents and primates that may account for the inconsistency.

IV.4.3 Chronic Medicated Patients.

No abnormalities in the EAA system were evident as the glutamate, aspartate and GABA levels of CM patients were comparable to controls. No observed difference in the NAA level suggests the neuronal population (or volume) of these patients is also similar to controls. Additionally, the normal PCr+Cr and Cho_t levels in the CM patients indicate no abnormal alterations in the observed grey/white matter ratio of these VOI's. However, significant increases in glutamine and taurine levels were observed in these CM patients compared to controls. The glutamine difference is supported by the significant difference observed in the glutamate to glutamine ratio of these patients compared to controls. In addition, the glutamine level correlated positively with the LOI in the combined patients. Both, glutamine and taurine are metabolites that predominantly reside in glia (Erecińska and Silver 1990; Urenjak et al. 1993) and consequently their *in vivo* levels are greater in grey matter than in white matter (Hänicke et al. 1993; Provencher 1993). The increased glutamine and taurine levels would suggest there is an increase in glia volume while a normal volume of neurons and grey matter is maintained. This increase in glutamine and taurine levels could also indicate an abnormally high glutamine

and taurine concentration in glia. However, observing normal levels of the EAA's suggest the metabolic pool and/or the neurotransmitter pool of glutamate is not implicated and, hence, the metabolic activity of glutamine would also not be implicated. Recent volumetric MRI studies on the prefrontal region of schizophrenic patients have reported conflicting results of either a decrease in grey matter volume and no change in the white matter volume (Zipursky et al. 1992) or no change in grey matter volume but a decrease in white matter volume (Breier et al. 1992; Buchanan et al. 1993). Furthermore, increased packing of pyramidal cells and decreased density of interneurons in the prefrontal area of schizophrenic patients have been observed (Benes et al. 1991). In a preliminary study, Selemon et al. (1992) observed increased neuronal density in Brodmann's areas 9 and 46 and increased glial density in only area 46. To compare, the positioning of the VOI in this study would include part of area 9 and to a lesser extent part of area 46 (Figure IV.1). Therefore, the above studies lend support to an increase in glia volume assuming there is no major change in grey matter volume and neuronal volume but there is increased packing of pyramidal cells.

IV.4.4 Limitations.

Instructions to perform specific physical or psychological tasks were not given to the subjects during the collection of the data. Therefore, in general the observed metabolite levels reflect steady-state values at rest. It is of interest to note, that two preliminary studies have shown differences in ^{1}H metabolite

levels in the motor cortex during finger tapping tasks compared to rest conditions (Meyerand et al. 1993; Xue et al. 1993). This may indicate that differences in metabolite levels may also occur during frontal lobe activation. Since this aspect was not controlled for in this study, subject variation due to their degree of frontal lobe activity during data collection, may account for part of the variation observed on the measurements. The effect of frontal lobe activity on the ^{1}H metabolites needs further investigation. The *in vivo* cerebral concentration of aspartate, NAAG, taurine, *scyllo*-inositol and glucose is of the order of 1-2mmol/kg wet weight (Perry et al. 1981. Petroff et al. 1989) compared to NAA which has a concentration of ≈ 8-9mmol/kg wet weight in white matter (Michaelis et al. 1993; Kreis et al. 1993). Consequently, the spectral signal-to-noise ratio of these metabolites is relatively poor compared to NAA (Figure IV.2). Therefore, quantifying these metabolites, which resulted in standard deviation of >50%, would tend to provide less reliable values. The sagittal and coronal images in Figure IV.1 suggest that within the dimension of the VOI, the observed ^{1}H MR signal is dominated by white matter compared to grey matter. The identical spectroscopy protocol was used in the repeated measure study, and the volume of grey matter for the 8cm^3 VOI was estimated at ≈ 30% (Chapter III). If metabolite differences are only present in grey matter of schizophrenic patients, then the observed intensity of the difference is reduced due to sampling relatively less grey matter volume. However, acquiring ^{1}H spectra with a smaller VOI to reduce the partial white matter

volume, results in a decrease in the observed MR signal which reduces the reliability of the quantification. In the statistical analysis, eleven metabolites were tested for significant differences between each patient and control group. With a significance level of 0.05, by chance there is a 5% probability of detecting a false significant difference (i.e., a "type I" error). The number of significant differences observed in the patient groups compared to the controls accounts for 9% of comparisons which just exceeds the probability of making a "type I" error. However, there are reasons to believe that the observed differences are not random. The observed increase in glutamine levels of the CM patients seemed to be consistent with the increase in taurine since both glutamine and taurine reside predominantly in glia. Furthermore, the significant correlation between glutamine and LOI suggests that there was a true difference in the levels of these metabolites in the CM patients compared to controls. The *in vivo* T_1 of glutamine is $\approx$ 2,100msec (Hänicke et al. 1993) which is greater than the inter-pulse repetition time used and implies that the observed glutamine signal is partially saturated. A decrease in T_1 of glutamine could account for the observed increase, however, the T_1 would have to decrease by $\approx$ 34% to observe the 30% increase in glutamine level. Differences in linewidths (or T_2's) between the metabolites were unmeasurable due to the method in which the *a priori* knowledge was incorporated in the fitting routine (Chapter III). Therefore, the T_2's were assumed not to differ between the values of the patients and the values of the controls.

CHAPTER V

A ^{31}P MRS Study of Schizophrenic Patients and Controls

V.1 Introduction.

One of the most consistent findings in schizophrenia has been a functional abnormality in the frontal lobes. Activation deficits have been demonstrated with quantitative EEG measures (Hoffman et al. 1991; Morrison-Stewart et al. 1991), cerebral blood flow (Berman et al. 1986; Weinberger et al. 1986; Berman et al. 1988; Weinberger et al. 1988), and PET (Cohen et al. 1987; Volkow et al. 1987; Buchsbaum 1990; Buchsbaum et al. 1990; Andreasen et al. 1992; Buchsbaum et al. 1992). There is some evidence that this lack of activation is specific to schizophrenia (Berman et al. 1993).

Reports of structural changes in the frontal lobes have been inconsistent. Most MRI studies have failed to find volumetric differences from controls (Kelsoe et al. 1988; Suddath et al. 1989; Andreasen et al. 1990; Suddath et al. 1990). However, more recent studies using thinner imaging slices to calculate volumes have suggested that there may be prefrontal volume deficits in at least some schizophrenic patients (Breier et al. 1992; Buchanan et al. 1993). Both reduced grey matter (Zipursky et al. 1992) and white matter volumes (Breier et al 1992; Buchanan et al. 1993) have been found in prefrontal regions in schizophrenic patients compared to controls. The T_2 relaxation decay constant, an *in vivo* MRI measure reflecting the water environment in tissue, has also

been reported to be longer in left prefrontal white matter of patients with schizophrenia compared to controls (Williamson et al. 1992).

While many schizophrenia studies have shown functional and/or structural deficits in prefrontal regions, the nature of these deficits has remained elusive. One technique which offers some potential to understand these differences is ^{31}P MRS (Bottomley 1989; Keshavan et al. 1991). This non-invasive technique provides quantitative information on the metabolism of high-energy phosphates: ATP, PCr and Pi; and membrane phospholipid metabolism through PME's and PDE's. The intracellular pH and the $[Mg^{2+}]_{intra}$ can also be calculated from the positions of spectral peaks.

Pettegrew and co-workers (1991) observed decreased levels of PME, which are precursors to the synthesis of membrane phospholipids, and higher levels of PDE which are the breakdown products of membrane phospholipids in the prefrontal region of first episode DN schizophrenic patients compared to controls. Increased levels of ATP and decreased levels of Pi were also observed. This suggests that these alterations in the metabolism of membrane phospholipids may be involved in the prefrontal functional and/or structural deficits seen in schizophrenia. However, these alterations are observed in schizophrenic patients that are at the early stage of illness and it is unclear if these differences are maintained or not at later stages of illness.

Our objectives were to examine the effects of stage of illness on the ^{31}P MR metabolites with blindly analyzed data and to test the reproducibility of

Pettegrew's pilot study on first episode DN schizophrenics (Pettegrew et al. 1991). Additionally, we wished to examine correlations between membrane phospholipid and high-energy phosphate metabolism as well as correlations between clinical symptom measures and ^{31}P MRS parameters. Therefore, ^{31}P MR spectra from the left dorsolateral prefrontal cortex of: (*i*) first episode DN, (*ii*) NDM and (*iii*) CM schizophrenic patients were acquired and compared with appropriately matched controls.

V.2 Method.

V.2.1 Subjects.

Schizophrenic patients participating in this study included eleven first episode DN patients, eight NDM patients and ten CM patients. Two NDM patients were also examined prior to medication, and therefore, their previous measures were included in the DN group. The screening procedure used was identical to that described in Chapter IV. Patient characteristics are shown in Table V.1. Of the eleven DN patients, (aged 18 to 39 years), nine were classified as paranoid and two as undifferentiated. The LOI ranged from 1 month to 6 years. None had been exposed to anti-psychotic medication, however, six had received 1 to 3mg of lorazepam in the 24 hours before assessment. Within the eighteen medicated patients, (aged 17 to 59 years), eight were considered NDM with a mean LOI of 4±2 years and ten were considered CM with a mean LOI of 18±6 years (Table V.1). Ten patients were

Table V.1 Subject Characteristics.

	Gender	Age (yrs)	Length of Illness (yrs)	Handed-ness	Education Level[a]	Parental Education Level[a]	SANS score	SAPS score
Control Group								
	17M + 4F	31±9	---	17 right	2.7±1.0	2.4±0.7	----	----
Schizophrenic Patients								
First Episode DN	8M + 3F	26±7	2±2	11 right	2.4±0.8	2.4±0.7	41±11	31±10
NDM	8M + 0F	23±6	4±2	8 right	2.3±0.7	2.4±0.8	35±14	9±10
CM	9M + 1F	43±7	18±6	9 right	2.8±0.6	1.9±0.9	19±10	5±7

[a]Levels were rated based on a four-point scale as described in Chapter IV section IV.2.2.

diagnosed as paranoid, two as undifferentiated and six as residual. All medicated patients were receiving antipsychotic medication (mean equivalent dose of chlorpromazine ± SD, 560±410mg). Fourteen reported that they were also taking anticholinergic medication for side effects.

Twenty-one controls ranging in age from 18 to 53 years, participated in this study. The controls were comparably matched in gender, education level, parental education level and handedness. Subject characteristics of the control group are shown in Table V.1.

V.2.2 ^{31}P MR Spectroscopy.

All experiments were conducted using a whole body MR spectrometer operating at 2 Tesla with a 5cm diameter transmit/receive surface coil. The use of the FROGS sequence along with the surface coil provided the localization of approximately 15 to 20cm^3 of brain tissue in the left dorsolateral prefrontal cortex (Chapter I). Correct positioning of the surface coil over the area of the left dorsolateral prefrontal cortex and the saturation slice was confirmed by ^{1}H MR sagittal images acquired with the surface coil. Depending on the skull thickness of the subjects, the thickness of the saturation slice ranged from 2.0 to 3.0cm. With a TR of 2,000ms, the amplitude of the excitation pulse was adjusted to maximize the ^{31}P MR signal. The FID signal, 300ms in length, was digitized with 4,096 complex data points (i.e., spectral bandwidth of ±6,666Hz) and 600 acquisitions were averaged. The pre-acquisition delay time was 1ms. Furthermore, the static magnetic field homogeneity was maximized before data

acquisition by shimming over the region such that the FWHM of the H_2O resonance was ≈ 12Hz.

V.2.3 Post-Spectral Processing.

All data files were coded to completely blind the operator to the status of the subjects. A non-interactive modelling technique based on linear prediction and singular value decomposition (LPSVD, Barkhuijsen et al. 1985), was then applied to reconstruct the missing data points in the pre-acquisition delay time. The use of a 1ms delay time, minimized the contribution of any short T_2 species (i.e. bone and membrane phospholipids) in the reconstruction. The FID was exponentially filtered with 6Hz linebroadening, zero-filled from 4,096 to 8,192 data points and then Fourier transformed. Reconstructing the initial data points on the FID guaranteed a pre-acquisition delay time of zero, therefore, the adjustment of 1st order phasing was within ± ½ a dwell period. The operator then only adjusted the 0th order phase.

Peak areas were obtained by modelling spectral peaks with Lorentzian lineshapes. By varying the amplitude, linewidth and position of each peak, the "best fit" between the sum of the modelled lineshapes and the acquired spectrum was achieved with a non-linear least squares fitting algorithm (Marquardt 1963). β-ATP was fitted with three Lorentzian lineshapes of equal linewidths and γ- and α-ATP were fitted with two Lorentzian lineshapes of equal linewidths. The result of modelling a typical *in vivo* ^{31}P MR spectrum is shown in Figure V.1. All metabolite levels were expressed as a % of the total area of

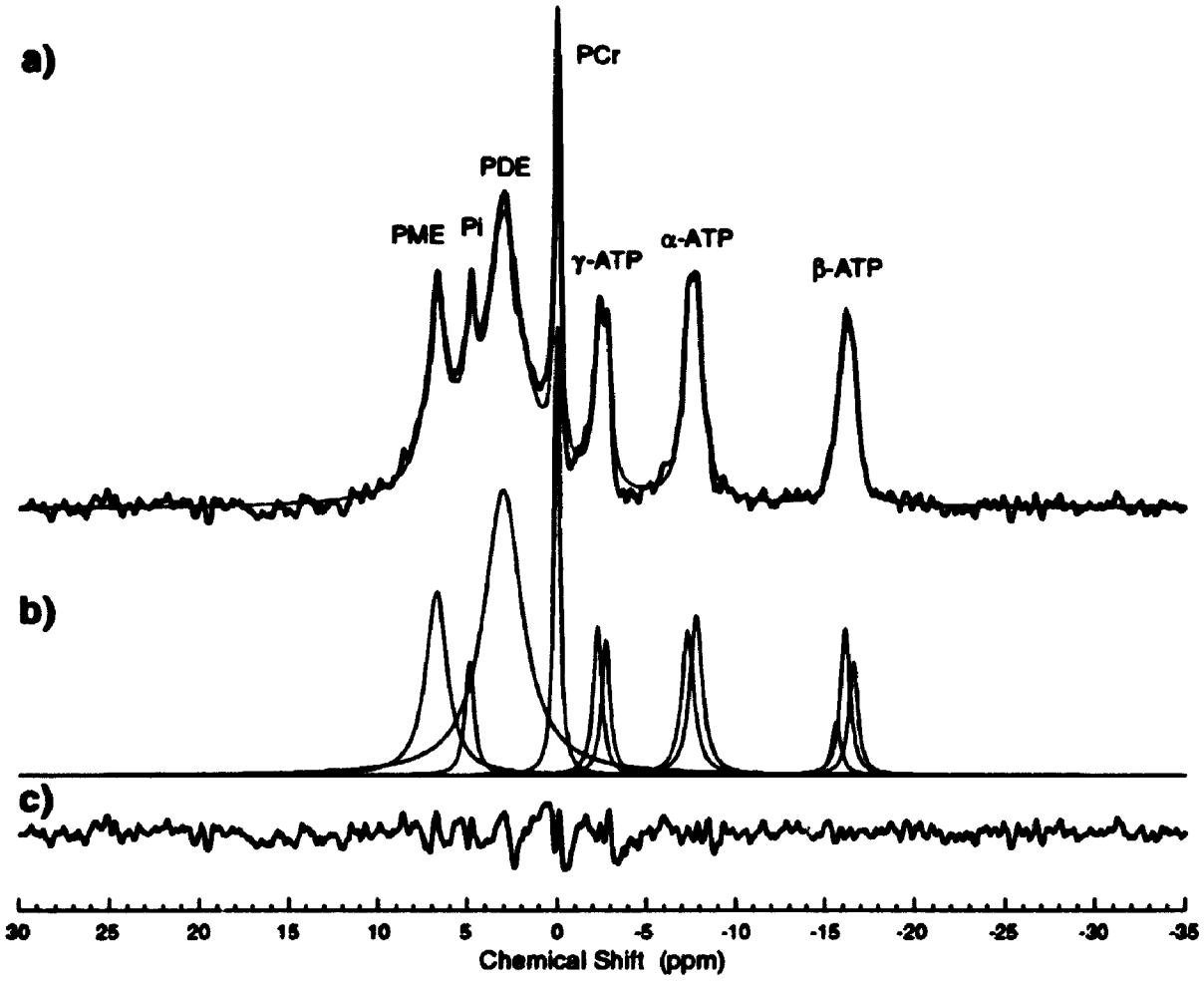

Figure V.1 Modelling an *in vivo* ^{31}P MR spectrum with Lorentzian lineshapes. a) A typical *in vivo* ^{31}P MR spectrum (thick line) from the left dorsolateral prefrontal cortex of a control, superimposed on the modelled spectrum (thin line). b) The individual Lorentzian lineshapes of the modelled spectrum. c) The difference between the acquired spectrum and the modelled spectrum.

the observed ^{31}P MR signal. Quoted values of the peak's FWHM and the peak's chemical shift were taken from the modelled spectra. The intracellular pH was calculated from the chemical shift difference between Pi and PCr (Chapter I). Each spectrum was modelled a second time using single Lorentzian lineshapes for the fitting of the γ-, α- and β-ATP peaks in order to calculate the $[Mg^{2+}]_{intra}$ from the chemical shift difference between α-ATP and β-ATP (Chapter I).

V.2.4 Reliability Study on the Method.

In a serial *in vivo* study, there are many factors that can contribute to the observed variation in the MRS measures such as instrumentation and acquisition parameters positioning of the VOI, post-spectral processing and biological variations. Consequently, these are the factors that will influence the reliability and the degree of robustness of these *in vivo* ^{31}P MRS measures. To investigate this reliability issue, ^{31}P MRS measures were repeated on five CM schizophrenic patients and five controls. This enabled us to compare repeated measures with the original measures of both schizophrenic patients and controls. All the experiments, except for one subject, took place during the same time of the day (±2hours). The time interval between test/retest varied from the same day up to 12 months.

The mean ^{31}P metabolite levels (expressed as a % of the total observed signal) of the first and second measures for the patients and controls are shown in Figure V.2. From the ANOVA results, a significant decrease in PME,

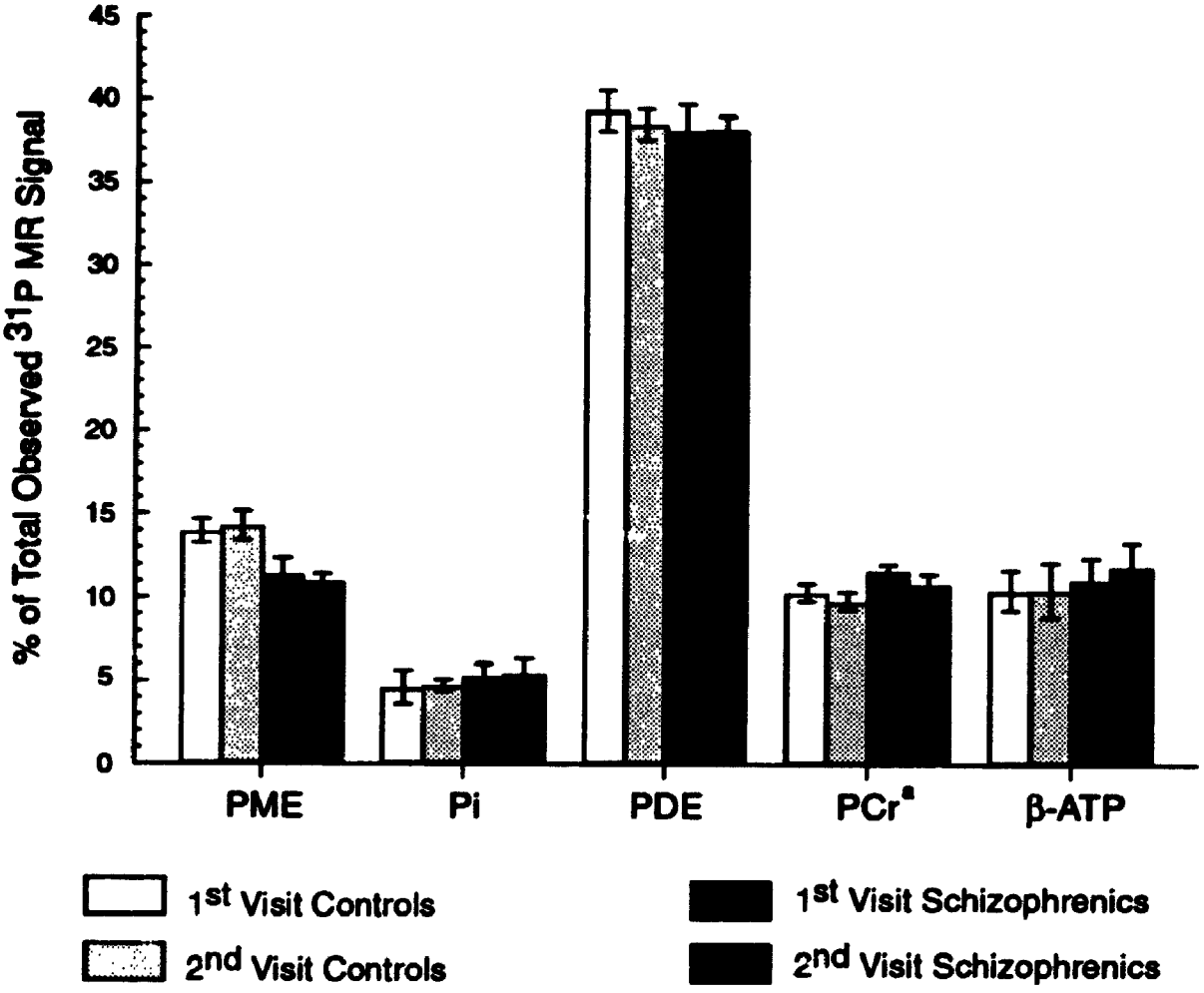

Figure V.2 ^{31}P metabolite levels of first and second visit. Error bars are ± 1 standard deviation.

*The PCr level is significantly lower on the second measure relative to the first measure of the schizophrenic patients (p=0.03).

($p=0.01$), and significant increases in PCr, ($p=0.002$), the calculated $[Mg^{2+}]_{intra}$ ($p<0.001$) and β-ATP ($p<0.02$) were observed in the CM schizophrenic patients compared to the controls. Except for PCr, no significant differences between the first and second *in vivo* ^{31}P MRS readings were observed (Figure V.2). An interaction between the two readings and the type of subject was observed for pH ($p<0.03$). For both subject groups combined, the correlation between the first and second readings were significantly different from zero for PME ($r=0.82$), PCr ($r=0.70$), and the $[Mg^{2+}]_{intra}$ ($r=0.86$), as indicated in Figure V.3. Normal and abnormal ranges were considered. Using a PME cut off of 12.8% (of the total signal) and a $[Mg^{2+}]_{intra}$ cut off of 400μM, the Kappa-coefficients were significantly different from zero for PME ($K=0.8$, $p<0.01$) and for $[Mg^{2+}]_{intra}$ ($K=1.0$, $p<0.001$). A scatter plot of the first and second readings with the cut-off levels are shown in Figure V.4. In summary, these test/retest results suggest that ^{31}P MRS measures are sufficiently reliable that CM schizophrenic patients can be distinguished from controls.

V.2.5 Statistical Analysis.

A two tailed t-test was used to determine any significant differences in age, education level and parental education level when comparing the DN and the combined medicated patients with the control group. If normality of the data failed (i.e., $p<0.05$), a Mann-Whitney Rank sum test was performed. Quantified ^{31}P MR parameters were modelled in a step-wise multiple regression analysis with subject group (i.e. patient and control), age, gender, education level and

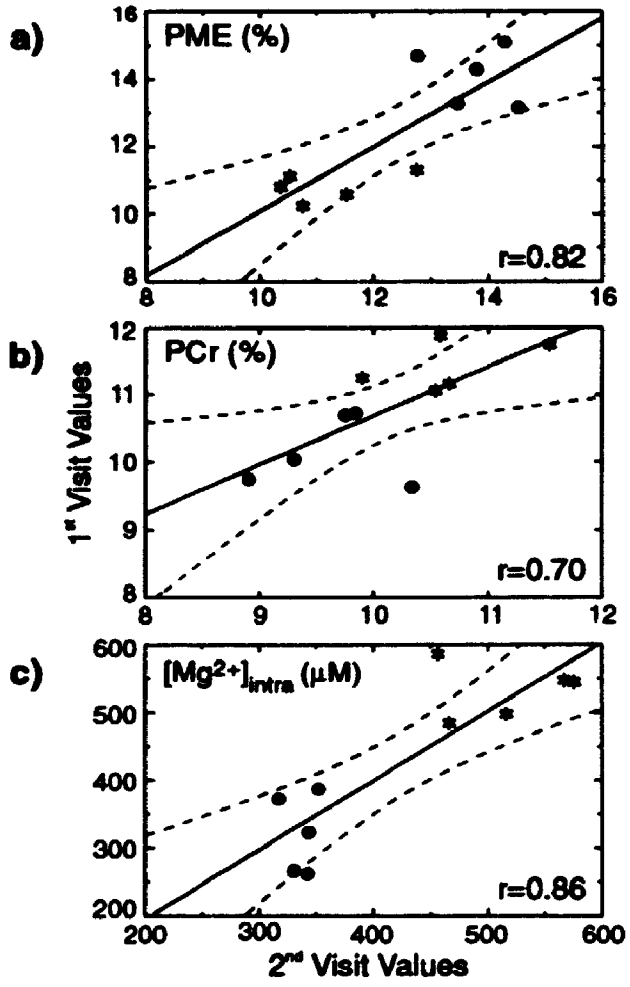

Figure V.3 Scatter plots (first measures vs the second measures) of the (a) PME, (b) PCr and (c) $[Mg^{2+}]_{intra}$ values. The ●'s are values from the controls and the ✱'s are values from the schizophrenic patients. The correlations (solid lines) are r=0.82, r=0.70 and r=0.86 for (a), (b) and (c), respectively. The dashed lines represent the 95% confidence interval.

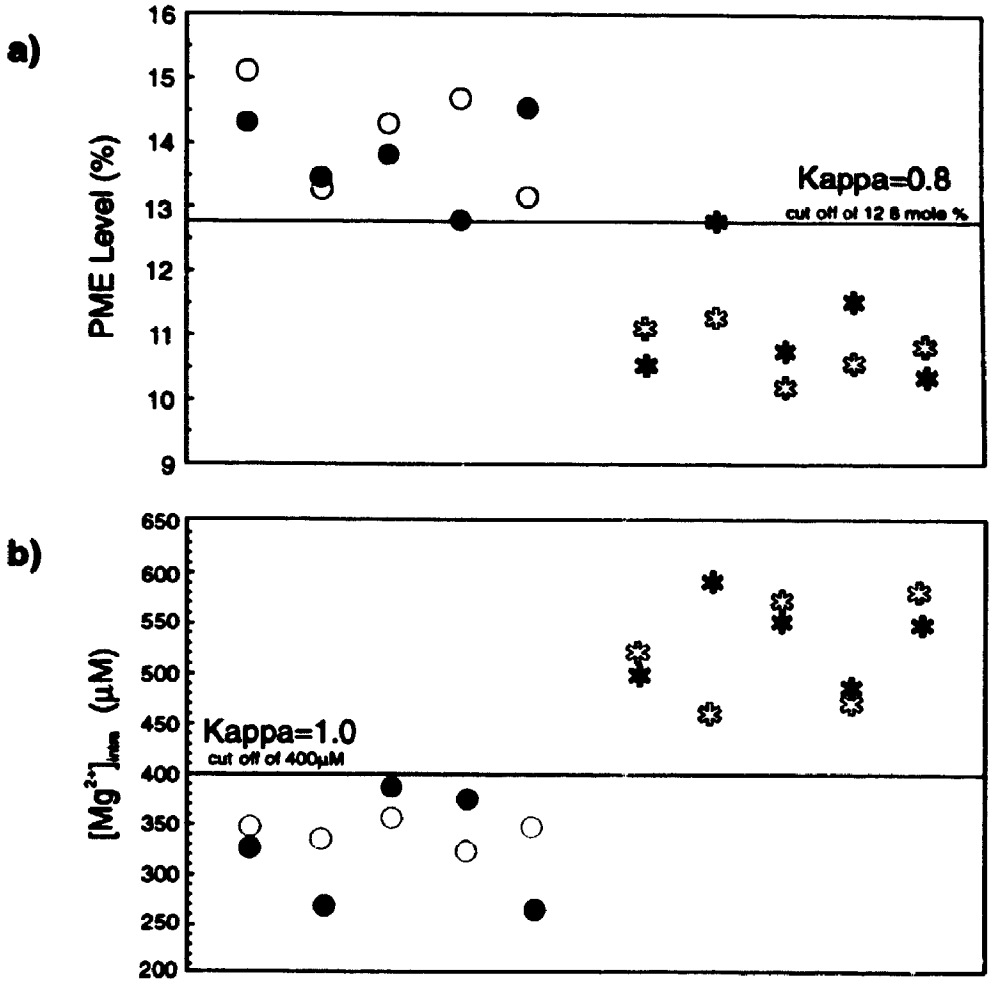

Figure V.4 Scatter plot of the (a) PME and (b) $[Mg^{2+}]_{intra}$ values for the first (solid symbols) and second (open symbols) measures of the controls (circles) and schizophrenic patients (stars). The solid lines represent the cut off values as indicated.

parental education level as independent parameters. This method enabled us to compare differences in the ^{31}P MR parameters between patient and control groups while adjusting for the co-variables of age, gender, education level and parental education level. Probability values of less than 0.05 were considered statistically significant and a threshold value of p=0.15 was used to enter or remove independent variables from the multiple regression analysis. Pearson product moment correlations between the observed ^{31}P metabolic levels and $[Mg^{2+}]_{intra}$ were evaluated for the control group and combined patient groups. The correlations also included such variables as SANS and SAPS scores as well as LOI.

V.3 Results.

There were no significant differences in age, education level and parental education level when comparing the DN and the combined medicated patients with the control group.

A typical *in vivo* ^{31}P MR spectrum from the left dorsolateral prefrontal cortex of a control is shown in Figure V.5c. In the spectrum PME, Pi, PDE, PCr and the three phosphate peaks from the ATP molecule are resolved (Figure V.5c). The S/N_{rms} ratio of 100 for the PCr peak and 40 for the β-ATP peak is sufficient to reliably quantify the ^{31}P MR spectra. The result of acquiring a spectrum without and with the saturation slice is shown in Figures V.5a and V.5b, respectively. Spectrum (a) in Figure V.5 has a broad, symmetrical lineshape (which has characteristics of bone signal, Murphy et al. 1989)

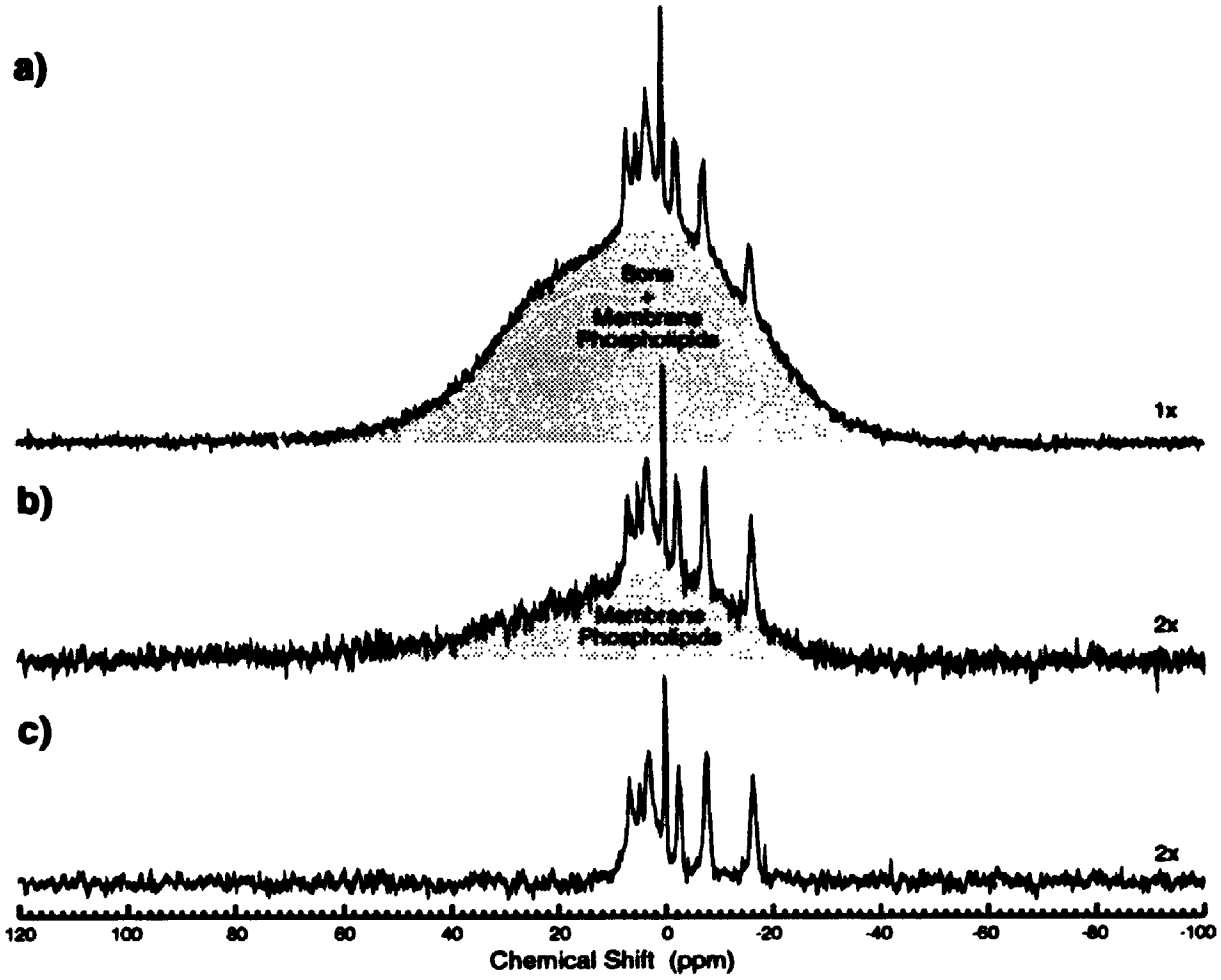

Figure V.5 *In vivo* ^{31}P MR spectra collected without and with the saturation slice at 2.0Tesla. a) A typical *in vivo* ^{31}P spectrum from the left dorsolateral prefrontal cortex acquired without the saturation slice. The spectrum consists of a large broad lineshape due to the ^{31}P MR signal from immobile membrane phospholipids and bone. b) A spectrum acquired identical to (a), however, the saturation slice is present. The spectrum still has a broad lineshape primarily due to the ^{31}P MR signal from immobile membrane phospholipids. c) The spectrum was processed from the FID of spectrum (b), but with a pre-acquisition delay time of 1,000μs to minimize the contribution of broad lineshapes due to immobile molecules.

underlying the ^{31}P metabolites (PME, Pi, PDE, PCr and ATP) while spectrum (b) has a broad, non-symmetrical lineshape (which has characteristics of membrane phospholipid signal, Murphy et al. 1989). The latter spectrum which has minimal contribution of bone demonstrates the effectiveness of the FROGS technique to eliminate the signal at the surface due to scalp and skull. Furthermore, the broad contribution of the ^{31}P MR signal in Figure V.5b is minimized by post-processing the FID with 1,000μs pre-acquisition delay time as shown in Figure V.5c.

The mean ^{31}P metabolite levels of the patient groups and the control group are shown in Table V.2 and Figure V.6. Significantly decreased levels of PME's were observed in the first episode DN group ($p<0.001$), the NDM group ($p<0.001$) and in the CM group ($p<0.001$) compared to the control group. All 29 PME values from the patients failed to overlap within one standard deviation of the PME values from the controls. Combining the three patient groups together there was a significant decrease in the FWHM of the PME peak ($p<0.001$) compared to the control group (Table V.3). A significant increase in the PDE level of first episode DN schizophrenic patients was observed compared to the control group (Figure V.6). However, no significant differences in PDE levels were observed between the NDM and CM schizophrenic patients and the control group. In the combined patient group, the correlation between the PDE level and LOI was -0.432 ($p = 0.02$, which is not significant with a Bonferroni correction for multiple comparisons) while in the control group, the PDE and

Table V.2 The Mean ^{31}P MR Metabolite Levels of the Schizophrenic Patients and the Controls.

	Mean % Level of the Total Obeerved ^{31}P MR Signal (±SD)				
	PME	PI	PDE	PCr	β-ATP
Control Group					
	14.6±1.1	4.0±0.7	38.9±2.0	9.7±0.6	9.9±1.4
Schizophrenic Patients					
First Episode DN	11.8±1.1[a]	3.7±0.9	40.2±2.0[b]	9.2±1.4	9.9±1.4
NDM	11.9±0.6[c]	3.42±0.5[d]	39.7±1.5	8.8±0.5	10.3±1.0
CM	11.6±1.0[e]	4.1±0.9	38.3±1.9	9.8±0.8	10.4±1.2

[a]Significantly different from the control group ($p < 0.001$).

[b]Significantly different from the control group ($p = 0.048$).

[c]Significantly different from the control group ($p < 0.001$).

[d]Significantly different from the control group ($p = 0.05$).

[e]Significantly different from the control group ($p < 0.001$).

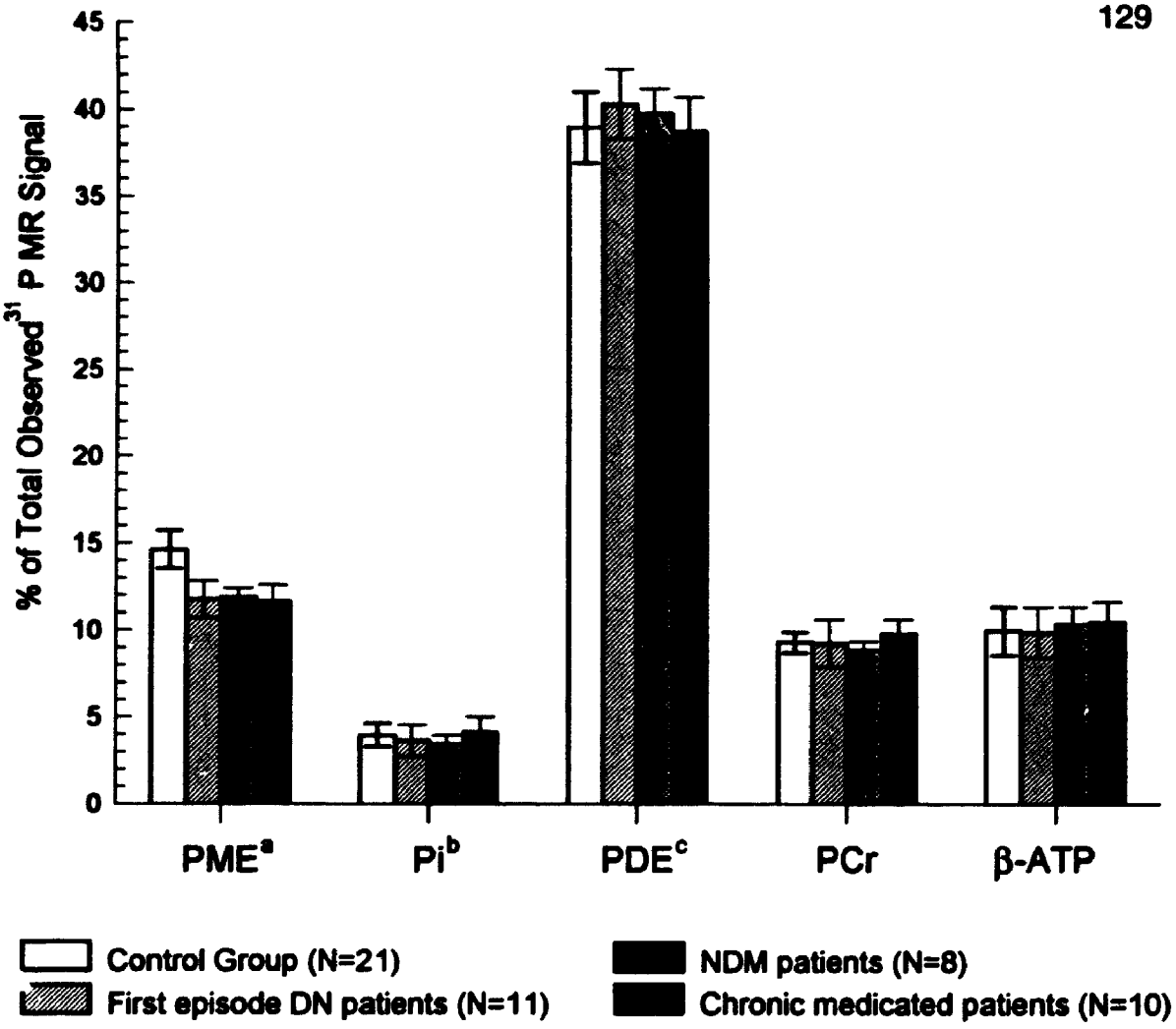

Figure V.6 The mean ^{31}P metabolite levels, expressed as a % of total observed ^{31}P MR signal, of the control group, DN, NDM and CM schizophrenic patients. The error bars represent 1 standard deviation.

[a]Significantly different between DN and controls ($p<0.001$).

Significantly different between NDM and controls ($p<0.001$).

Significantly different between CM and controls ($p<0.001$).

[b]Significantly different between NDM and controls ($p=0.05$).

[c]Significantly different between DN and controls ($p=0.048$).

Table V.3 Additional Quantifiable Parameters of Schizophrenic Patients and Controls.[a]

			PME peak		PDE peak	
	Intracellular pH	$[Mg^{2+}]_{free}$ (μM)	FWHM (Hz)	Chemical Shift (ppm)	FWHM (Hz)	Chemical Shift (ppm)
Control Group						
	7.057±0.020	321±27	51±6	6.71±0.04	86±6	2.96±0.04
Schizophrenic Patients						
First Episode DN	7.053±0.021	418±89[b]			92±7[e]	2.91±0.04[f]
NDM	7.068±0.017	352±36[g]	44±4[c]	6.69±0.03[d]	88±6	2.95±0.04
CM	7.068±0.021	375±32[h]				

[a]Values are expressed as mean± 1 standard deviation.

[b]Significantly different from the control group ($p< 0.001$).

[c]Significantly different from the control group $p< 0.001$).

[d]($p= 0.07$) when comparing the combined patients with the control group.

[e]Significantly different from the control group ($p= 0.009$).

[f]Significantly different from the control group ($p=0.004$).

[g]Significantly different from the control group ($p= 0.014$).

[h]Significantly different from the control group ($p< 0.001$).

age correlation was 0.370 (p =0.1). When comparing FWHM values and chemical shift of the PDE peak between the DN patient group and the control group, a significant increase and a significant shift in resonance was observed, respectively (Table V.3). Except for a significant decrease in the Pi level in the NDM group, no other significant differences in the high-energy phosphate metabolites were observed between any of the patient groups compared to the control group (Figure V.6). The Mg^{2+}_{intra} concentration was significantly increased in first episode DN, NDM, and CM patients ($p<0.001$) compared to the control group (Table V.3). No significant differences in the intracellular pH were observed.

In the combined patient group, ^{31}P metabolite levels and $[Mg^{2+}]_{intra}$ were not significantly correlated with the SANS or SAPS scores. However, the correlation between PCr and Pi levels was significantly different from zero (r= 0.604, p=0.001) while in the control group, this correlation was not significantly different from zero. The PDE and β-ATP level significantly correlated in both the combined patient groups (r=-0.589, p=0.001) and in the control group (r=-0.668, p=0.001). The above correlations remained significant after applying the Bonferroni correction for multiple comparisons.

V.4 Discussion.

V.4.1 Membrane Phospholipid Metabolism.

A significant reduction in PME level in the left dorsolateral prefrontal

cortex was observed in first episode DN, NDM and C.M schizophrenic patients compared to the control group. The PME reduction of approximately 20% was striking as none of the 29 patients had PME values within one standard deviation of the control group. In addition, the PME linewidth was significantly narrower and the PME chemical shift tended to be less than the chemical shift of the controls (Table V.3). PCho, PE and PS are the predominant metabolites contributing to the observed PME signal with their own distinct resonant frequencies (Pettegrew et al. 1987). Therefore, evidence of a reduction in area and linewidth and a trend in chemical shift away from the PE resonant frequency of 6.78ppm (Merboldt et al. 1990), suggests that the reduced PME observed throughout the illness of schizophrenia could be due to a reduction in the PE level. There are many processes that could result in a reduction in the PME level: decreased kinase activity, decreased phospholipase C (PLC) activity, decreased phosphodiesterase activity or increased phosphatase activity (Dawson 1985).

Significantly increased levels of PDE were observed only in first episode DN patients compared to the control group. From the correlation, the PDE level seems to be dependent on the length of illness of these patients. Metabolites dominating the observed PDE signal include GPE at 3.51ppm (Merboldt et al. 1990) and GPC at 2.99ppm (Merboldt et al. 1990). For these patients in the early stage of illness, the PDE linewidth was significantly broader and there was a significant shift in the PDE resonant frequency closer to the

GPC resonant frequency. Therefore, GPC could be implicated for the significant increase in PDE in patients early in their illness. Processes that can increase the PDE level include a reduction of phosphodiesterase activity or increased phospholipase A_1 (PLA_1) and phospholipase A_2 (PLA_2) activity (Dawson 1985). Gattaz et al. (1987; 1990) have observed increased platelet PLA_2 activity in schizophrenia. However, Bennett et al. (1991) reported no differences in the PLA_2 activity in lymphoblast cell lines of schizophrenic patients compared to controls.

The observed differences in the PME and PDE levels are consistent with the previous ^{31}P MRS study by Pettegrew et al. (1991). However, the observed increase in PDE level of NDM patients (Appendix C) was not reproduced in this blind study. Phosphomonoesters are involved predominantly in the phospholipid synthesis of cell membranes while phosphodiesters are found predominantly in the catabolic pathway of membrane phospholipids (Dawson 1985). These observations suggest that initially in the illness of schizophrenia, membrane phospholipid breakdown products from phosphatidylcholine (PtdCho) are increased and precursors to the synthesis of PtdE, (phosphatidylethanolamine, a phospholipid that is localized mainly on the cytoplasmic side of the membrane bilayer) are decreased. As the illness progresses, the levels of breakdown products are normalized but precursors of membrane phospholipids are still reduced. It is of interest that abnormalities in the membrane phospholipid composition in erythrocytes and platelets of

schizophrenic patients have been observed (Ryer et al. 1991). Several authors have reported conflicting results, observing either a decrease in the PtdE concentration (Stevens 1972; Sengupta et al. 1981; Tolbert et al. 1983; Keshavan et al. 1993a) or no difference (Lautin et al. 1982; Hitzemann et al. 1984; Pangerl et al. 1991) compared to controls. Significantly decreased concentrations of PtdC in patients compared to controls have been observed in several studies (Stevens 1972; Tolbert et al. 1983; Hitzemann et al. 1984; Hitzemann et al. 1985) while no differences (Lautin et al. 1982; Pangerl et al. 1991; Keshavan et al. 1993a) and an increase (Sengupta et al. 1981) in concentrations have also been observed. Furthermore, the reduction in synthesis of PtdE has the potential to reduce the synthesis of PtdCho via the phospholipid methylation pathway or the base-exchange process (Farooqui and Horrocks 1985). Several studies have observed a reduction in methylation activity in erythrocytes of schizophrenic patients relative to controls (Andreoli and Maffei 1979; Kelsoe et al. 1982; Hitzemann et al. 1984; Hitzemann et al; 1985).

Under normal conditions, membrane phospholipids are constantly turning over at different metabolic rates with different metabolizing enzymes. Maintaining the proper structural integrity and functional activity of neuronal membrane phospholipids are crucial for neurotransmitter release, ion transport, calcium homeostasis, receptor binding and membrane fusion (Farooqui and Horrocks 1985). Hudson et al. (1993) have suggested that decreased PME

levels and increased PDE levels may reflect disturbances in transmembrane signal transduction and second messenger function at the point of G protein-effecter enzyme interaction. The consequences of such alteration in the metabolism of phospholipids in cell membranes may further impair the normal synaptic plasticity and neural development. This would be consistent with the observed structural abnormalities in the prefrontal regions, specifically reduced grey matter (Zipursky et al. 1992) and white matter (Breier et al. 1992; Buchanan et al. 1993) volume and abnormal migration of neurons toward the cortical plate (Akbarian et al. 1993). A positive correlation between PDE levels and corpus collosal area has also been reported (Keshavan et al. 1993b), however, additional volumetric measures are required to determine if PDE or PME correlate with prefrontal white and/or grey matter deficits. Pettegrew et al. (1991; 1993) have suggested that the enhanced decrease in membrane phospholipid synthesis and increase in membrane phospholipid breakdown, relative to the ^{31}P MRS observations of normals in late adolescence and young adulthood, is the result of an exaggeration of normal synaptic pruning of prefrontal axonal terminals.

V.4.2 High-Energy Phosphate Metabolism.

Pettegrew et al. (1991) have also observed increased ATP levels and decreased Pi levels in DN patients compared to controls which suggests hypofrontality. In our study, no differences in high-energy phosphate metabolism was observed between any of the patient groups and the control

group except for the decreased Pi levels in the NDM patients. The observed change in Pi may be due to the initial administration of the medication. Therefore, our observations do not provide evidence to support a reduction in the utilization of ATP (Pettegrew et al. 1991) in the left dorsolateral prefrontal cortex of schizophrenic patients.

V.4.3 The Intracellular Concentration of Mg^{2+}.

Within the combined patient group, the $[Mg^{2+}]_{intra}$ did not correlate statistically with either the PME or PDE levels. Mg^{2+} is an abundant intra- and extracellular cation which is a necessary co-factor for many enzymes including those involved in the transfer of phosphate groups (Stanfield 1988; Flatman 1991). In addition, abnormal regulation of the $[Mg^{2+}]_{intra}$ has the potential to block the signal transduction of glutamate subtype receptor channels (N-methyl-D-aspartate, NMDA) and ion receptor channels in a voltage-dependent manner (Johnson and Ascher 1990). As a result, a reciprocal relationship exists between the $[Mg^{2+}]_{intra}$ and the binding of inositol-(1,4,5)-triphosphate (IP_3) to its receptor and subsequent release of calcium from intracellular stores (White et al. 1991). Therefore, abnormal levels of Mg^{2+}_{intra} could suggest that cellular metabolic activity is reduced which could lead to further suppression of neuronal function(s). This observation would be consistent with the potential alteration of transmembrane signal transduction due to abnormal levels of PME and PDE, and furthermore, would concur with results of functional abnormalities in schizophrenic patients by other techniques as noted above.

V.4.4 Limitations.

A number of limitations must be acknowledged. Tissue volumes sampled varies between subjects and grey matter volume contribution varies within those tissue volumes. Normalizing the peak areas of the metabolites to the total observed peak areas corrects for the variation in volume of excitation from subject to subject but assumes a constant proportion of grey to white matter. Cerebral spinal fluid has no contribution to the observed ^{31}P MR signal (Hugg et al. 1992). Our assumption of a similar grey/white matter in patients and controls is based on the following argument: the proportion of PtdE relative to the total phospholipid composition is greater in white matter than in grey matter while the proportion of PtdC is significantly lower in white matter than in grey matter (Soderberg et al. 1990; Kwee and Nakada 1988). Therefore, the reduction of PME observed in patients throughout the illness seems to implicate the precursor of PtdE and not the precursor of PtdC, and does not support observed differences in proportion of grey to white matter between the patients and controls to account for the decrease in PME.

It is possible that MR relaxation effects cause the observed differences in the PME area. The ^{31}P MR signal, which constitutes long T_1-species, does not fully recover its equilibrium magnetization because of the short repetition time used between acquisitions (i.e., the observed ^{31}P MR signal < ^{31}P MR signal at equilibrium). Consequently an increase in the T_1 of the PME's could also account for the decrease in the PME level in the patients. However, an

alteration in the physical and/or chemical environment of the PME's sufficient to cause a change in T_1 could also affect the synthesis of the membrane phospholipids. Second, the ^{31}P MR signal was acquired immediately following the excitation pulse. Therefore, a change in T_2 of a metabolite does not reflect a change in spectral peak area (assuming that there was no attenuation in the ^{31}P MR signal by our post-spectral processing method since the T_2 of the observed metabolites are greater than 1ms (Merboldt et al. 1990).

Even though Mg^{2+} is an important co-factor in many enzymatic reactions in which ATP is a substrate, it must be noted that the observed differences in chemical shift from which $[Mg^{2+}]_{intra}$ is calculated could also be explained by an abnormal level of another cation binding to the β- and γ-phosphate sites of ATP rather than Mg^{2+}.

CHAPTER VI

General Discussion, Summary and Future Work

VI.1 Evaluation of the Quantification Technique.

A goal of this thesis was to obtain the *in vivo* metabolite levels of glutamate from schizophrenic patients and compare those levels to that of normal controls. Therefore, a short echo localization pulse sequence was required to obtain this data. As a result, complex overlapping resonances had to be quantified. To circumvent the complexity, a technique was developed to quantify these overlapping resonances which incorporated *a priori* knowledge. This *a priori* knowledge, which included information about the spectral peak arrangement of each metabolite, was obtained by modelling *in vitro* ^{1}H spectra of the individual metabolites in aqueous solution. The accuracy and precision of this quantification technique was evaluated in two parts. The first was the fitting of simulated *in vitro* spectra of varying S/N's containing NAA, glutamate, glutamine, GABA, and aspartate. The second part was the quantification of repeated *in vivo* measurements on a subject.

The quantified NAA levels deviated by no greater than 3.4% from the expected values while the deviation of glutamate and glutamine were < 10% from their expected values for the *in vitro* studies (which used simulated data of comparable metabolite levels and S/N's to that of *in vivo* data). The quantified levels of GABA and aspartate were less precise, with deviations as large as

19% from their expected values. From the repeated *in vivo* measurements, the accuracy of quantifying the *in vivo* metabolite levels was investigated by obtaining absolute concentration levels of glutamate, glutamine, NAA, PCr+Cr and Cho_t. The estimated concentration levels were within the range of previously published *in vivo* and *in vitro* concentration levels of cerebral metabolites. The coefficient of variation of NAA, PCr+Cr and Cho_t (i.e., the metabolites with dominating spectral peaks) ranged from 5 to 10%. The coefficient of variation of the *in vivo* quantified glutamate and glutamine levels were ≈ 20% and 30%, respectively. The cerebral concentration of GABA, aspartate, taurine and *scyllo*-inositol are ≈ 1-2mmol/kg compared to ≈ 9mmol/kg for NAA and consequently, the quantified levels of these metabolites were less reliable with coefficients of variation ranging from 46 to 64%.

From the above measurements, the uncertainty due to the quantification technique cannot account wholly for the uncertainty observed in the *in vivo* measurements. Additional sources that can contribute to the uncertainty include position of the VOI (since regional distribution of metabolite levels does exist), spectral processing (i.e., manual phasing), S/N of the metabolites, and biological variation. These factors including biological variation were not characterized in terms of their contribution to the uncertainty of the *in vivo* metabolite levels. In comparison, the uncertainties of the metabolite levels using this quantification technique are consistent with that of a recent study by Provencher (1993).

In summary, a major contribution of this thesis has been to develop a technique to quantify short echo ^{1}H MRS data. I established a novel method to critically evaluate this quantification technique. As a result, quantifying the *in vivo* levels of NAA, PCr+Cr and Cho_t were reliable with coefficients of variations of ≈ 10%. The less predominant metabolites including GABA, aspartate, taurine and *scyllo*-inositol, are less reliable with coefficients of variations ≥ 46%. To detect a significant difference between patients and normal controls, the *in vivo* level of glutamate would have to increase or decrease by ≈ 20% or greater with these small samples (i.e., N of ≈ 12 for a two-tailed t-test).

VI.1.1 Caveats.

The following includes a discussion acknowledging the imperfections of quantifying short echo *in vivo* ^{1}H MR spectra and of the technique used to quantify these spectra: *i)* It can be argued that if NAA, PCr+Cr and Cho_t are the only metabolites with uncertainties of 10% or less, then a longer echo time pulse sequence would provide the information on these metabolites without the complexity of quantifying overlapping resonances. Glutamate, glutamine and GABA are still resolved in *In vivo* ^{1}H MR spectra collected with longer echo time (i.e., 20ms < TE < 272ms), however, these resonances are less intense because of greater J-modulation effects. In either situation, incorporating *a priori* knowledge to quantify the data would be preferable in order to achieve accurate and precise quantification results (de Beer and van Ormondt 1992). *ii)* A proper balance was chosen between adequate S/N and the size of the

VOI. It was important in this schizophrenia study to have the VOI encompass as much grey matter as possible, therefore, the VOI was not made larger knowing that the S/N would increase and hence the reliability of these *in vivo* measurements would also increase. *iii)* The *a priori* knowledge in terms of what cerebral metabolites (i.e., amino acids and peptides) are observed in *in vivo* ^{1}H MR spectra has been well documented (see Chapter III). There are, however, resonances from mobile proteins and macromolecules that may be observed in short echo ^{1}H MR spectra which are not well understood. These resonances were not accounted for in the *a priori* knowledge except for two resonances at 2.13 and 2.90ppm. In general, it would seem that the quantified levels of mobile proteins and macromolecules are underestimated (which would lead to over estimating the cerebral metabolites such as glutamate and GABA). This approach was a "first order" approximation and future investigation is required to characterize these resonances due to mobile proteins and macromolecules. In the study by Provencher (1993), it was claimed that the *a priori* knowledge of the protein and macromolecule resonances was not required, as the residual of the fit (which includes these resonances) was modelled with a cubic-spline. *iv)* One aspect of the *a priori* knowledge was to maintain the relative linewidth differences between the metabolites. This criteria was required to prevent the linewidths of the less intense metabolites from having infinite values after a fit. As a result, this quantification technique is insensitive to any T_2 changes in the metabolites. It is possible that a different

T_2 value for a metabolite or metabolites does exist for the patients compared to the normal controls, which would not be detected with this technique (except for PCr+Cr and Cho_t). In the case of a decrease in T_2 of a metabolite (assuming no change in metabolite level), without *a priori* knowledge, the intensity of the peak(s) would be relatively less and the linewidth(s) would be relatively broader. However, with *a priori* knowledge, the quantified level of this metabolite would appear to decrease as the intensity would decrease but the linewidth would not be broader since the relative linewidth differences between the metabolites are maintained. It is assumed that the T_2 values of the ^1H metabolites are similar between the normal controls and patients.

VI.2 ^1H and ^{31}P Metabolite Differences in Schizophrenia Compared to Controls.

Both ^1H and ^{31}P MR spectra from the left dorsolateral prefrontal region of patients with schizophrenia at different stages of illness were acquired and compared to controls. A summary of the results is shown in Table VI.1. Three patient groups were established to represent three different stages of illness in schizophrenia. These stages were *i)* first episode patients that are neuroleptic naive (DN), *ii)* patients who have just been diagnosed and are now on neuroleptic medication (NDM), and *iii)* chronic patients that have been ill for at least 10 years and are on neuroleptic medication (CM). From Table VI.1, there are differences in metabolites that are observed in all three stages (a decrease

Table VI.1 Summary of the Results from the ^{1}H and ^{31}P MRS Study on Schizophrenia.[a]

Patients			
DN	**NDM**	**CM**	Comments
↓ PME[b]	↓ PME	↓ PME	-suggests a reduction in precursors of membrane phospholipid.
↑ PDE[b]			-suggests an increase in breakdown products of membrane phospholipid; PDE levels correlated negatively with the LOI.
	↓ Pi		-suggests there's an alteration in the high-energy phosphate metabolism.
↑ $[Mg^{2+}]_{intra}$	↑ $[Mg^{2+}]_{intra}$	↑ $[Mg^{2+}]_{intra}$	-suggests the signal transduction via NMDA receptors have altered.
	↑ Glu		-the initial administration of medication has altered the glutamate system.
	↓ Gln[c]	↑ Gln	-glutamine levels correlated positively with the LOI; glutamine predominantly resides in glia.
		↑ Tau	-taurine predominantly resides in glia.

[a]These results are the differences observed between patient and control groups, unless otherwise stated.

[b]This observation replicates the finding of Pettegrew et al. (1991).

[c]This decrease was observed when comparing the DN measurements with the NDM measurements of the same patients.

in the PME's and an increase in the $[Mg^{2+}]_{intra}$), and unique differences that are observed at each stage (including an increase in the PDE's at the DN stage, a decrease in Pi and glutamine, and an increase in glutamate at the NDM stage, and an increase in glutamine and taurine at the CM stage). In addition, combining the patients that have both ^{1}H and ^{31}P measurements, there were no significant correlations between the ^{1}H and ^{31}P metabolites (not shown in Chapter IV or V).

Of all the metabolites observed in the patients and controls, the most convincing finding is the significant decrease in the PME's which was lower at all stages of illness. This observation is striking as none of the twenty-nine patients had PME values within one standard deviation of the controls. The observed PME's are predominantly precursors of membrane phospholipid but the physiological implication of observing decreased levels of precursors of membrane phospholipids is still unknown. There is no ^{31}P MRS data to show that the concentration of PME's is greater in grey matter than in white matter. If grey matter is reduced then you could argue that the PME levels could alter. However, evidence from the ^{1}H MRS study suggests that there is no alteration in grey matter. In addition, recent volumetric MRI studies on the prefrontal region of schizophrenic patients have reported conflicting results about differences in grey matter and white matter as discussed in Chapter IV. An increase in the T_1 of the PME's and not a decrease in concentration would also result in quantifying a decrease in the PME's of the patients. If the

physical/chemical environment of the PME's have altered to cause a change in T_1 then the PME's would still be implicated in the illness of schizophrenia.

The other difference observed at all stages of illness, was a significant increase in the calculated $[Mg^{2+}]_{intra}$. Mg^{2+}, a cation, exists in both intra- and extracellular space and is known to act as a co-factor and regulator in the function of certain enzymes. Observing altered levels of Mg^{2+}_{intra} in these patients may suggest there is an alteration in cellular metabolic activity, which could lead to further abnormal neuronal function(s). In calculating this concentration, Mg^{2+} is the cation assumed to bind to the β-phosphate site of ATP to cause this statistically significant shift in the β-ATP resonance. A change in the intracellular pH can also cause the β-ATP resonance to shift but a significant difference in the pH was not observed in the patients. Quantifying the PME level and calculating the $[Mg^{2+}]_{intra}$ were also shown to be reliable from the repeated measurements on patients and controls. These two abnormalities in the PME level and the $[Mg^{2+}]_{intra}$ appear to be insensitive to neuroleptic medication (which excludes any effect(s) observed immediately after medication, i.e., the same day or a couple days later) and the length of illness.

VI.2.1 Implication of Glutamate.

There were no significant differences between the ^1H metabolite levels observed in the DN patients compared to controls (including glutamate). We did hypothesize that the glutamate level would be altered based on previous functional and anatomical studies where glutamate was implicated. According

to the results from Chapter III, the uncertainty of the quantified *in vivo* glutamate level is ≈ 20%. It is possible that glutamate levels are altered and the true differences are overlooked by the lack of precision with this experimental protocol and quantification technique. If the glutamate level is altered in the DN patients then the % difference compared to the controls would be approximately < 20% with this small sample size. Furthermore, it is unclear how much of a change in the glutamate level is required until abnormal physiological functions occur. With the limitations on the position of the VOI in the dorsolateral prefrontal region and the size of the VOI, the source of the ^{1}H MR signal is dominated from white matter tissue rather than grey matter tissue (Figure IV.1). Differences in glutamate (or even the other metabolites) between patients and controls may exist only in grey matter. Consequently, these differences would not be observed because of the smaller sampling of grey matter.

During the acquisition of the ^{1}H MRS data, frontal lobe tasks were not instructed. Therefore, in general the observed metabolite levels reflect steady-state levels at rest. There is the possibility that by activating the frontal lobe of these patients with a specific frontal lobe task during the collection of the MRS data, differences may then occur in the ^{1}H metabolites (including neurotransmitters such as glutamate and GABA). This could be analogous to previous EEG and regional cerebral blood flow studies on schizophrenia where differences were more significant during a frontal lobe task than during resting conditions (Morrison-Stewart et al. 1992). To summarize, differences in the

glutamate levels between the DN patients and controls are not observed (at least differences that are approximately 20% or greater compared to controls with this sample size). Therefore, glutamate is not implicated at the early stage of illness.

VI.2.2 Effect of Medication.

An increase in glutamate was observed in the NDM patients compared to controls. In addition, glutamine levels of the post medicated measurements were lower compared to the pre-medication measurements of the schizophrenic patients. Since the increase in glutamate was not observed in either the DN or the CM patients, this would suggest that the initial period of medication (i.e., within the time scale of 14 ± 10 weeks) has altered the glutamate level. Deutsch et al. (1989) suggested that observing an increase in glutamate results in a reduction in the release of glutama' . Additional support for this interpretation of reduced release of glutamate is provided by the decrease in glutamine observed in the post-medicated patients. A decrease in glutamate release can result in a decrease in glutamine due to a decrease in glutamate availability as substrate for the glutamine synthetase activity in glia.

It is of interest that an increase in glutamate was observed in the prefrontal region due to the administration of medication while in *in vitro* studies of rodents under chronic administration of neuroleptics there were no differences observed in this brain region (Perry et al. 1979; Kim et al.1983; Petty et al. 1984; Sherman and Mott 1984). We did hypothesize that the

medication would not alter the glutamate level in the prefrontal region. However, Berger et al. (1991) have demonstrated unexpected differences between rodents and primates in the dopamine system that may account for the inconsistency. Consequently, the altered levels of glutamate and glutamine due to medication may suggest that neuroleptics, which block dopamine receptors, influence the neuronal function of the nigrostriatal dopaminergic pathway which influences the neuronal function of the corticostriatal glutamatergic pathway (Figure II.3).

VI.2.3 Evidence of Neurodegeneration?

The measurement of NAA has been demonstrated to be sensitive in noting neuronal cell loss in several different disease states (Kauppinen et al. 1993). PCr+Cr and Cho_t provide information on the grey/white matter volume ratio within the VOI (Chapter III). From the ^1H MRS study, NAA, PCr+Cr and Cho_t levels of the schizophrenic patients at all stages of illness were comparable to that of the controls. The quantification of NAA, PCr+Cr and Cho_t have been shown to be reliable (with coefficient of variation of $\approx$ 10%). This suggests there is no major neuronal cell loss and hence no evidence of neurodegeneration in these schizophrenic patients. In addition, there is no evidence to suspect any differences in the grey/ white matter volume ratios between the patients and controls.

Observing no evidence of neurodegeneration, especially in the CM patients, is not consistent with our initial hypothesis and with previous

volumetric studies using MRI where tissue deficits have been observed (Breier et al. 1992; Zipursky et al. 1992; Buchanan et al. 1993). The only differences observed in these CM schizophrenic patients, were increased glutamine and taurine levels compared to controls. In addition, a significant positive correlation between glutamine and the LOI was observed in the combined patient group. The correlation was ≈ 0.5 which suggests that glutamine accounts for at least 25% of the dependency on the LOI. Both, glutamine and taurine predominantly reside in glia which would suggest there is an increase in the glia volume in the dorsolateral prefrontal region of schizophrenic patients at the chronic stage of illness. Previous anatomical studies have observed altered density of pyramidal cells, interneurons and glia in the prefrontal region of schizophrenic patients. However, it is unclear if these anatomical differences would account for the increase in glutamine. Presently, our laboratory is in the process of evaluating volumetric information from these patients with MRI which should provide additional information on the anatomy and possible correlations with the MRS metabolites.

VI.2.4 Evidence of Neurodevelopment?

The PDE's were only significantly different in the first episode DN patients compared to the controls. This increase in the PDE's and also the decrease in the PME's of first episode DN patients does replicate the previously reported findings of Pettegrew et al. (1991) which demonstrates how reproducible these altered membrane phospholipid metabolites are in DN

schizophrenic patients. Additionally, levels of the PDE's of the combined patients correlated negatively with the LOI.

PDE's are predominantly breakdown products of membrane phospholipids and the physiological implication of increased PDE levels is unknown. It appears that initially there is an increase in the destruction of membrane phospholipids and as the illness progresses the amount of breakdown products of membrane phospholipids are restored to normal levels. This would be consistent with the hypothesis stated earlier. It is also possible that this process causing the increase in breakdown products occurs much earlier in the illness and we are only observing the tail end of this process. During normal development in late adolescence and in young adulthood, a synaptic pruning process of excess axonal terminals occurs (Hüttenlocher 1979; Purves and Lichtman 1980; Hüttenlocher et al. 1982; Rakic and Riley 1983; Cowan et al. 1984). Coinciding with this normal neurodevelopmental process, a pattern of decreased PME's and increased PDE's are observed between the ages of 10 and 20 years (Pettegrew et al. 1993). Our ^{31}P MRS findings and that of Pettegrew et al. (1991) show similar but enhanced patterns of decreased PME's and increased PDE's in first episode DN schizophrenic patients. Pettegrew et al. suggested that this enhanced pattern observed in schizophrenic patients is due to over exaggerated synaptic pruning of prefrontal axonal terminals. Feinberg (1982) was the first to develop this schizophrenia hypothesis involving an over exaggerated synaptic pruning process. This

potentially may be the process that occurs initially in the illness of schizophrenia. It can be argued that this increase in PDE, which may be associated with a synaptic pruning process, would not be consistent with the ^{1}H MRS findings. There were no evidence of any major neuronal cell loss or differences in the grey/white matter volume ratios observed in the DN patients from the ^{1}H MRS study. However, the alterations in the membrane phospholipid metabolism may be associated with another synaptic function rather than a loss of synapses. In summary, these alterations in the membrane phospholipid metabolism may be the result of an abnormal neurodevelopmental process which occurs early in the illness of schizophrenia.

VI.3 Future Work.

A major achievement of this thesis, was to establish a foundation for schizophrenia research using both *in vivo* ^{1}H and ^{31}P MRS. In doing so, I developed protocols to acquire and process *in vivo* ^{1}H and ^{31}P MRS data. Our objectives of using MRS were to investigate possible *in vivo* metabolite abnormalities from the left dorsal prefrontal cortex of schizophrenic patients compared to controls. Following our initial results, there are three main areas that can be pursued to further advance the research in schizophrenia: *i)* establishing a fully automated procedure to process and quantify the *in vivo* data, *ii)* investigating the potential of functional MRS, and *iii)* investigating other regions in the brain such as the striatum and the limbic system with MRS.

VI.3.1 Automation of the Quantification.

In processing both the ^{1}H and ^{31}P spectra, the one step which was operator dependent, was the phasing of the spectral peaks (i.e., 0^{th} order and 1^{st} order). There are techniques that have been developed to automatically phase the spectra (Sotak et al. 1984), however, these methods are not effective when overlapping resonances are present in the spectra. An alternative would be to model the metabolites from the time domain signal rather than its Fourier transformed signal (de Beer and van Ormondt 1992). The main advantage of fitting the *in vivo* data in the time domain is that the phase of each resonance is included as a fitted parameter. Therefore, the phasing is operator independent. The resonances in the time domain are not modelled with Lorentzian or Gaussian lineshapes as in the frequency domain but with sinusoids that have either exponential or Gaussian damping functions. Furthermore, quantification methods using the time domain signal have demonstrated to be feasible with both *in vivo* ^{1}H and ^{31}P MRS data (Barkhuijsen et al. 1985; van der Veen et al. 1988; de Beer et al. 1992; van Dijk et al. 1992).

VI.3.2 Functional MRS.

In vivo ^{1}H MRS enables us to quantify the levels of neurotransmitters and other metabolites. It is unclear if these metabolites are state dependent within the timescale these in vivo measurements are collected. In this study, during acquisition, the subjects were not asked to perform a specific task. Therefore, the degree of activity in the prefrontal region was not controlled in

these subjects. Recently, numerous functional MRS studies have observed changes in metabolite levels during brain activation involving specific tasks (Shulman et al. 1993). During photic stimulation, decreased glucose and increased lactate levels have been observed in the visual cortex with localized in vivo ^{1}H MRS (Prichard et al 1991; Jenkins et al. 1992; Merboldt et al. 1992; Sappey-Marinier et al. 1992; Chen et al. 1993). Increased lactate levels have been observed in the auditory cortex during stimulation (Singh et al. 1992). In the motor cortex during finger tapping tasks, decreased NAA and increased lactate levels have been reported (Xue et al. 1993) while in our laboratory, decreased glucose levels have been observed (Stanley et al. 1994a). In the frontal lobe, several functional MRI studies have shown activity of normal subjects during word generation tasks (Cohen et al. 1993; Cuenod et al. 1993; MacCarthy et al. 1993; Rueckert et al. 1993). Recently in our laboratory, localized *in vivo* ^{1}H MRS has been used to investigate possible changes in metabolite levels in the dorsolateral prefrontal cortex during word generation tasks compared to resting conditions of normal subjects. Preliminary results have shown a significant increase in PCr+Cr and a trend of decreased glutamine levels on six subjects (Stanley et al. 1994b). These results are preliminary but encouraging which suggests that certain ^{1}H metabolites within the timescale of these measurements are state dependent. Therefore, obtaining information on these metabolites where certain neuronal activities are controlled, introduces another dimension to schizophrenia research. This has

the potential to provide what neurotransmitter(s) or metabolic system(s) is (are) involved where functional deficits have been observed in the frontal lobe of schizophrenic patients (reviewed in Chapter II).

VI.3.3 Abnormalities in Other Brain Regions.

The last main area for future work, involves obtaining spectroscopy data from other regions of the brain. Schizophrenia is an illness where abnormalities have been observed in several brain regions, including the frontal lobes, temporal lobes and the basal ganglia. In this study, the *in vivo* data provided information only in the dorsolateral prefrontal region. There are glutamatergic pathways from the prefrontal cortex that descend to the striatum and the limbic system. Obtaining, information in these other regions would provide a greater overall picture of the behaviour of the neuronal circuitry in terms of the observed metabolites in schizophrenia. Furthermore, we have no spectroscopy data from the right side of the dorsolateral prefrontal region. Questions can be raised such as are these differences observed in the membrane phospholipid metabolism with ^{31}P MRS unilateral effect? CSI is a localization technique that can obtain information from multiple regions with a single measurement. This technique can be applied to either ^{1}H or ^{31}P MRS and that is the case in our laboratory where these techniques are under investigation.

APPENDIX A

A.1 The Equation of Motion for the Magnetization.

Once the magnetization has been perturbed, the time evolution of $M_{x'}$, $M_{y'}$ and M_z have the following behaviour:

$$\frac{dM_{x'}(t)}{dt} = -\frac{M_{x'}(t)}{T_2} \qquad [A.1]$$

$$\frac{dM_{y'}(t)}{dt} = -\frac{M_{y'}(t)}{T_2} \qquad [A.2]$$

$$\frac{dM_z(t)}{dt} = \frac{(M_0 - M_z(t))}{T_1} \qquad [A.3]$$

where T_2 is the spin-spin relaxation time and T_1 is the spin-lattice relaxation time and $T_2 \leq T_1$. Solutions are of the form

$$M_{x'}(t) = M_{x'}(0) \cdot \exp(-\frac{t}{T_2}) \qquad [A.4]$$

$$M_{y'}(t) = M_{y'}(0) \cdot \exp(-\frac{t}{T_2}) \qquad [A.5]$$

$$M_z(t) = M_0 \cdot (1 - \exp(-\frac{t}{T_1})) + M_z(0) \cdot \exp(-\frac{t}{T_1}) \qquad [A.6]$$

where $M_{x'}(0)$, $M_{y'}(0)$ and $M_z(0)$ are the initial magnetizations following the RF

pulse. Spin-lattice relaxation refers to the process of energy exchange between the spin ensemble and the lattice. The result of such energy exchange is the return of M_z to its equilibrium position, M_0, with a time constant T_1. Spin-spin relaxation involves the dephasing of the magnetization in the x,y-plane. As a result of such dephasing the component of the magnetization in the x,y-plane decays to zero with a characteristic time T_2.

For a spin system, which has been perturbed, to return or relax back to equilibrium, transitions must be induced between the spin states (i.e., spin up or spin down) of the nuclei. Such transitions occur when, due to molecular motion, randomly fluctuating magnetic and electric fields, produced at the sites of the nuclei, have frequency components that match the resonance conditions of the nuclei involved. The relaxation rates are proportional to the probability of the above transitions. This probability in turn depends on the interactions causing the transitions. The dominant mechanism by which ^1H or ^{31}P nuclei in biological sample relax is the magnetic dipole-dipole relaxation mechanism.

A.2 Scalar Spin-spin Coupling and J-Modulation.

The chemical structure of biological molecules consists of multiple spin groups such as CH, CH_2, CH_3 and PO_3 which give rise to distinct chemical shifts. These resonances can further split into multiple resonances due to through-bond interactions (mediated by electrons) between different spins within the molucule. The strength of the interaction or the magnitude of the splitting between two spins, A and X (i.e. the scalar product of the two spin vectors) is

characterized by a scalar spin-spin coupling constant, J_{AX}. This coupling constant decreases as the number of covalent bonds between two interacting spins increases. The coupling constant is independent of the magnitude of the applied magnetic field, B_0 and consequently, its value has units of Hz and not ppm. Figure A.1 contains an *in vitro* ^{1}H MR spectrum of glutamate acquired in aqueous solution. The spectral region includes the chemical shift of the α-,γ- and β-CH_2 spin groups. Due to scalar spin-spin coupling, these resonances are further split into complex multiplet structures (Figure A.1) which illustrates how complex the resonances of a molecule can be.

If the MR signal is acquired with a sequence that allows for T_2 relaxation to occur (i.e., an echo pulse sequence such as the STEAM sequence with the TE/2 intervals), two processes will occur during the TE/2 interval. The first process involves T_2 relaxation where the amplitude of the resonances attenuate and the second process involves J-modulation where the resonances within multiplet structures modulate their phase by $\cos(\pi \cdot J \cdot TE)$ in the case of a doublet and by $\cos(2\pi \cdot J \cdot TE)$ in the case of a triplet. The precessional frequency of the outer peaks of a multiplet structure will be at a different frequency then that of the central peak(s), therefore, causing a phase difference on the outer peaks relative to the central peak(s). The effects of J-modulation on a spectrum with a doublet and a triplet is illustrated in Figure A.2 as a function of the TE/2 interval. To minimize the J-modulation of a multiplet structure with a coupling constant J, the TE/2 interval from the echo sequence must be minimized

(TE/2<<1/J) or the TE/2 interval could be a multiples of 1/(2J).

Figure A.1 Th' *in vitro* ^{1}H MR spectrum of glutamate. The top includes the chemical structure of glutamate and the bottom consists of part of a ^{1}H MR spectrum of glutamate acquired in aqueous solution with the STEAM TE=20ms sequence. The chemical shifts of the α-, γ- and β-CH_2 spin groups are indicated with ν_α, ν_γ and ν_β. Due to spin-spin c upling, the spectrum consists of a triplet (α-CH_2) with the $J_{\alpha\beta}$ splitting and two complex multiplet structures (γ- and β-CH_2).

Figure A.2 The effects of J-modulation on a spectrum with a doublet (a) and a triplet (b). The left margin indicates the TE/2 interval from an echo pulse sequence such as STEAM.

APPENDIX B

B.1 The QUALITY Deconvolution Technique.

QUALITY is a deconvolution technique that attempts to restore spectral lineshapes which have deviated from the pure Lorentzian lineshape by factors such as magnetic field inhomogeneities (de Graaf et al. 1990). An acquired water suppressed *in vivo* localized MR signal of N spectral peaks will have the form of

$$S(t) = \sum_{j=1}^{N} M_{0j} \cdot \exp\left(i \cdot \omega_j \cdot t - \frac{t}{T_{2j}}\right) \cdot D \qquad [B.7]$$

where M_{0j}, ω_j and T_{2j} are the equilibrium magnetization, offset frequency and T_2 for peak j (j=1...N), respectively. The D term contains the factor that deviates the Lorentzian lineshapes and is constant for each peak j. The unsuppressed water MR signal, $S_{ref}(t)$, which has a zero offset frequency (i.e., collected on resonance), will have the same form as Eq. [B.1] except N=1, j=ref and the $\exp(i \cdot \omega_{ref} \cdot t)$ term equals one. Therefore, dividing S(t) by the normalized $S_{ref}(t)$ produces a corrected MR signal,

$$S_{cor}(t) = \frac{S(t)}{S_{ref}(t)/M_{oref}} = \sum_{j=1}^{N} M_{0j} \cdot \exp\left(i \cdot \omega_j \cdot t - \frac{t}{T_{2j}}\right) \cdot \exp\left(\frac{t}{T_{2ref}}\right) \qquad [B.8]$$

where the D term is eliminated, providing that $S_{ref}(t) \neq 0$. If the linewidth of the unsuppressed water MR signal ($(\pi \cdot T_{2ref})^{-1}$) is known then $S_{cor}(t)$ can be

multiplied by a negative exponential of that linewidth to restore the amplitudes, M_{oj}, offset frequencies, ω_j, and the areas of the N spectral peaks with pure Lorentzian lineshapes.

B.2 Absolute Quantification of ^{1}H Metabolites.

It is common for investigators to express their metabolite levels as a ratios relative to another metabolite which is assumed constant or relative to the total quantified metabolite area. However, determining the absolute concentration of the metabolites from the observed MR signal provides a standardized mean of comparing values between intra- and inter-laboratory studies. This issue is important because it allows laboratories to reproduce findings of other laboratories, even though, MRS protocols are different in terms of TE's, TM's, TR's, VOI's and type of pulse sequences. There are many different techniques used to obtain absolute concentrations which either use external or internal standards with known concentrations to establish the relationship between signal amplitude in volts and concentration in mmol/kg (Thulborn and Ackerman 1983; Wray and Tofts 1986; Frahm et al. 1989b; Hennig et al. 1992; Christiansen et al. 1993; Michaelis et al. 1993). In this thesis, absolute quantification of the metabolites was determined for the ^{1}H MRS data but not for the ^{31}P MRS data. The main reason for not quantifying absolute values for the ^{31}P MRS data lies on the uncertainty of the excitation tissue volume since the data was acquired with a surface coil.

The technique used in this thesis to obtain the absolute ^{1}H metabolite

levels, utilized the unsuppressed water signal as an internal standard (Christiansen et al.1993). For a particular excitation volume V_{met} that contains a metabolite concentration of [met], the ^1H MR signal (or spectral peak area, A_{met}) of that metabolite with $\#P_{met}$ protons will have the form of

$$A'_{met} = V_{met} \cdot P_{met} \cdot [met] \qquad [B.9]$$

where the quantified spectral peak area, A_{met}, has been corrected for T_1 and T_2 relaxation by

$$A'_{met} = \frac{A_{met}}{\left(\exp\left(-\frac{TE}{T_{2met}}\right)\right) \cdot \left(1 - \exp\left(-\frac{TR}{T_{1met}}\right)\right)} \qquad [B.10]$$

Similarly, the spectral peak area of an unsuppressed water signal, A_{H2O}, from a volume V_{H2O} and tissue water concentration of $[H_2O_{tissue}]$, will have the form of

$$A'_{H2O} = V_{H2O} \cdot P_{H2O} \cdot [H_2O_{tissue}] \qquad [B.11]$$

where A_{H2O} has been corrected for relaxation by

$$A'_{H2O} = \frac{A_{H2O}}{\left(\exp\left(-\frac{TE}{T_{2H2O}}\right)\right) \cdot \left(1 - \exp\left(-\frac{TR}{T_{1H2O}}\right)\right)} \qquad [B.12]$$

If the unsuppressed and suppressed water ^1H STEAM spectra are collected with the identical size of VOI and location, then, the excitation volume of the metabolite and the tissue water are identical. Therefore, with $V_{met}=V_{H2O}$, Eqs. [B.3] and [B.5] can be re-expressed as

$$[\text{met}](\text{mmol/kg wet weight}) = \frac{[H_2O_{tissue}]}{1.047} \cdot \frac{A'_{met}}{A'_{H2O}} \cdot \frac{P_{H2O}}{P_{met}} \qquad [B.13]$$

where the added term, 1.047kg/ L, is the density of grey and white matter (Torack et al. 1976; Brooks et al. 1980; Rieth et al. 1980) which gives the metabolite concentration units of mmol/kg wet weight. Due to the cancellation of the excitation volumes, this technique of estimating the absolute values becomes independent of the applied B_1 magnetic field.

The concentration of tissue water, $[H_2O_{tissue}]$, in the human brain has been estimated and values are 81% and 71% of the concentration of pure water, $[H_2O_{pure}]$, for grey matter and white matter, respectively (Norton et al. 1966). For a VOI that contains grey matter and white matter, the tissue water concentration thus becomes

$$[H_2O_{tissue}] = ((0.81 \cdot f_{grey}) + (0.71 \cdot f_{white})) \cdot 55.6x10^3 mM \qquad [B.14]$$

where f_{grey} and f_{white} are the fraction of grey matter and white matter.

In this thesis, no attempt was made to correct for the attenuation of the MR signal due to T_1 and T_2 relaxation. Estimating the T_2 values of metabolites that have multiplet structures such as glutamate, glutamine and GABA, are problematic due to the J-modulation. Therefore, the quoted absolute metabolite levels,

$$\text{AML (arbitrary units)} = [H_2O_{tissue}] \cdot \frac{A_{met}}{A_{H2O}} \cdot \frac{P_{H2O}}{P_{met}}, \qquad [B.15]$$

have arbitrary units and not units of mmol/Kg wet weight.

There are a couple of caveats with this technique that must be noted. The *in vivo* concentration of ^1H metabolites in CSF is negligible except for glucose (McGale et al. 1977). Therefore, the excitation volume of the unsuppressed water signal which includes the added volume of water from CSF should be adjusted with a $(1-f_{CSF})$ term in Eq. [B.5], where f_{CSF} is the fraction of CSF in the excitation volume (assuming the relaxation parameters of the water signal from CSF is similar to that of the water signal from grey matter). Second, absolute metabolite levels have the potential to be overestimated due to underestimating the total tissue water content from the MR signal (Ernst et al. 1993). Tissue water that are relatively less mobile due to the water-macromolecule interaction, have shorter T_2's and consequently, will tend not to be observed with a TE of 20ms STEAM sequence. Menon and Allen (1991) have observed a short T_2 tissue water component of 13ms which contributed 7% to the total water signal in white matter.

APPENDIX C

Membrane Phospholipid Metabolism and Schizophrenia: an *in vivo* ^{31}P MRS Study

C.1 Introduction.

While most investigators accept that schizophrenia is a brain disease, the pathophysiology of this disease has remained elusive. Of late, interest has focused on the glutamatergic hypothesis (Wachtel and Turski 1990) implicating the prefrontal glutamatergic system (Selemon et al. 1993; Sherman et al. 1991). It has been shown that in late adolescence and in young adulthood, a synaptic pruning process of excess axonal terminals occurs (Hüttenlocher 1979; Purves and Lichtman 1980; Hüttenlocher et al. 1982; Rakic and Riley 1983; Cowan et al. 1984). Possibly an over exaggerated synaptic pruning of prefrontal glutamatergic axonal terminals may occur in schizophrenia patients (Feinberg 1982) which would affect the prefrontal glutamatergic system.

Support for this neurodevelopmental model has been provided by previous ^{31}P MRS studies. A pattern of decreased PME's and increased PDE's was observed during normal human brain development (between the ages of 10 and 20 years) and also during normal aging (ages 50 years and up) (Pettegrew et al. 1993). However, Pettegrew et al. (1991) have reported that first episode DN schizophrenic patients have similar but enhanced pattern of markedly lower levels of PME's and higher levels of PDE's compared to normal

controls. This observation suggested decreased membrane phospholipid synthesis and increased membrane phospholipid breakdown are present early in the illness of schizophrenia before the administration of any medication. Quantifying the PME and PDE levels in schizophrenic patients who are beyond the early onset stage, could provide additional information supporting the neurodevelopmental model. The purpose of the present study was to quantify the PME and PDE levels in ^{31}P MR spectra of the left dorsal prefrontal cortex of medicated, male schizophrenic patients compared to a control group. The controls were matched with the patients by age, sex, education and parental education level. We hypothesize that the increase in breakdown of membrane phospholipid will only be present early in the illness, suggesting that an abnormal neurodevelopment in the prefrontal cortex can underlie the pathophysiology of schizophrenia.

C.2 Method.

C.2.1 Subjects.

Nineteen schizophrenic patients (ages from 16 to 54) were studied. The procedure to screen the subjects was identical to that described in Chapter IV section 2.2. Fourteen were classified as paranoid, three as undifferentiated, and two as residual. All the patients were receiving antipsychotic medication. Sixteen reported that they were also taking an anticholinergic medication for side effects. The LOI ranged from 1 to 24 years (mean±S.D.; 11±8 years). All

but one subject reported that they wrote and threw a ball with their right hand. Education and parental education levels were rated with a four-point scale. All patients had undergone at least one MRI scan previously as part of other studies. A summary of the patient characteristics is shown in Table C.1.

Eighteen normal male volunteers (ages from 18 to 53) were recruited by advertisement or were contacted after participation in other studies. None were receiving medication of any type. All but two reported that they wrote and threw a ball with their right hand. Five had undergone at least one MRI scan previously as part of other studies. Subject characteristics of this group are also shown in Table C.1.

C.2.2 ^{31}P MR Spectroscopy.

In vivo ^{31}P MR spectra were acquired with a 5 cm diameter transmit/receive surface coil on a whole body MR spectrometer operating at 2 Tesla. The surface coil was positioned over the left dorsal prefrontal cortex and correct positioning was confirmed with the surface coil ^{1}H MR sagittal images. Time was taken to maximize the static magnetic field homogeneity over this region (full width half maximum of the H_20 resonance $\approx$ 12 Hz). The ^{31} P MR signal was acquired by applying the FROGS pulse sequence (Sauter et al. 1987). The saturation slice was oriented parallel with the coil and located between the surface of the coil and the cortex area which ensured minimal contamination to the ^{31}P MR signal from the scalp and skull. The TR was 2,000 ms and 600 acquisitions were averaged. The excitation volume of brain tissue

Table C.1. Subject Characteristics.[a]

	Gender	Age (yrs)	Length of Illness (yrs)	Handed-ness	Education Level[b]	Parental Education Level[b]	SANS score	SAPS score
Control Groups								
Controls (NDM)	10 males	23±4	---	8 right	2.6±0.8	2.5±0.5	---	---
Controls (CM)	8 males	40±8	---	8 right	2.6±1.2	1.8±0.7	---	---
Total	18 males	31±10	---	16 right	2.6±1.0	2.2±0.7	----	----
Schizophrenic Patient Groups								
NDM	7 males	22±5	3±2	7 right	2.3±0.8	2.3±0.8	32±12	8±10
CM	12 males	39±6	16±5	11 right	2.6±0.8	2.1±0.9	24±12	9±10
Total	19 males	32±10	11±8	18 right	2.5±0.9	2.2±0.9	27±13	8±10

[a]Values are mean±1 standard deviation.

[b]Levels were rated with a four-point scale as described in Chapter IV section 2.2.

was roughly 15-20cm^3. All the FID's were exponentially filtered (line broadening of 5 Hz), zero-filled to double the number of data points and Fourier transformed with a pre-acquisition delay time of 1000μs. Allowing for this long pre-acquisition delay time minimized the contribution of any short T_2-species (i.e., broad spectral lineshapes from bone and membrane phospholipids) to the ^{31}P MR spectra. The spectra were then phased (0th and 1st order) and baseline corrected for to the pre-acquisition delay time (Allman et al. 1988).

To obtain the relative level of the observed ^{31}P-containing-metabolites, the PME, Pi, PDE, PCr and the ATP peaks were modeled with Lorentzian lineshapes. A nonlinear least-squares fitting algorithm was used (Marquardt 1963). As the β-ATP is a triplet, it was fitted with three Lorentzian lineshapes and the doublets of γ-ATP and α-ATP were fitted with two Lorentzian lineshapes. All metabolic levels are expressed as a % of the total observed ^{31}P MR signal.

C.2.3 Statistical Analysis.

Comparisons between patient and control groups were done using an ANOVA. Both groups were further subdivided to compare the PME and PDE levels of the NDM schizophrenic patients (7 males, mean length of illness; 3±2 years) and the chronic patients (12 males, mean length of illness; 16±5 years) with their age matched controls, Table C.1. All values are reported as mean ± standard deviation. Probability values of less than 0.05 (two-tailed) were considered statistically significant.

C.3 Results.

The observed levels of PME and PDE in patient and control groups are shown in Table C.2. Schizophrenic patients (total) had markedly lower % of PME compared to the control group ($p<0.001$). Even by subdividing the patient group into two, their PME levels were still lower (Table C.2). Using a cut off PME level of 12.0%, 18 out of the 19 patients and 17 out of the 18 normals could be correctly classified into their respective groups. In the patient group (total) an increase in PDE levels just failed to reach significance ($p= 0.053$) compared to the controls. However, a significant increase in the PDE level was observed in the NDM patient subgroup ($p<0.001$) while no significant difference was observed in the chronic patient subgroup compared to their appropriately age matched control group. In addition, the FWHM of PME were significantly narrower in the patient group compared to the controls (35±4Hz vs. 44±4Hz, $p<0.001$), while no significant difference in the PDE linewidths were observed between the two groups.

C.4 Discussion.

As in the previous *in vivo* ^{31}P MRS studies (Pettegrew et al. 1991; Williamson et al, 1991) of the prefrontal region, PME levels in schizophrenic patients were lower than in normal comparison subjects. The PME level is independent to the length of illness and medication (i.e., first episode DN, NDM and CM patients). In this study the difference was particularly robust;

Table C.2. The PME and PDE Levels of Schizophrenic Patients and Controls.

	% of the Total Observed ^{31}P MR Signal[a]			
	PME		PDE	
Control Groups				
Controls (NDM)	13.9±0.7		37.8±1.0	
Controls (CM)	13.0±0.8		38.3±2.2	
Total	13.5±0.9		38.0±1.6	
Schizophrenic Patient Groups				
NDM	10.6±1.0	p<0.001[b]	41.6±1.0	p<0.001[b]
CM	10.7±0.8	p<0.001[c]	38.0±1.6	
Total	10.7±0.9	p<0.001[d]	39.3±2.3	

[a]Values are mean ± 1 standard deviation.

[b]NDM patients vs. controls (NDM)

[c]CM patients vs. controls (CM)

[b]Total patients vs. controls (total)

misclassifying only one patient and one control. PCho, PE and PS are the main metabolites that contribute to the observed PME signal and they are predominantly active in the synthesis of the membrane phospholipids. Therefore, the observed decrease in the PME level in the schizophrenic patients suggests a reduced availability of PME for the synthesis of membrane phospholipids.

Levels of PDE were only significantly increased in the NDM schizophrenic patient subgroup compared to the younger controls. At the chronic stage of the schizophrenic illness, their PDE levels were similar to those of the older control group, as hypothesized. The observed PDE signal primarily consists of GPCho and GPE which are breakdown products of membrane phospholipids. It is possible that at the early stage of the illness of schizophrenia, there is a greater than normal accumulation of breakdown products of membrane phospholipids as reported in the Pettegrew et al. (1991) study of first episode DN patients. However, as this illness progresses the breakdown activity returns to normal levels.

C.5 Summary.

In summary, we believe that this study shows differences in the membrane phospholipid metabolism between schizophrenic patients and normals. Pettegrew et al. (1991) have shown that the decrease in PME and increase in PDE pattern exists in first episode DN schizophrenic patients. Here,

we have shown that NDM schizophrenic patients have a similar pattern. However, at the chronic stage of the illness only the PME differed from the controls. This occurance of aberrant membrane phospholipid metabolism would be consistent with abnormal neurodevelopment during late adolescence and young adulthood of patients with schizophrenia.

BIBLIOGRAPHY

Ackerman, J.J.H.; Grove, T.H.; Wong, G.G.; Gadian, D.G.; and Radda, G.K. Mapping of metabolites in whole animals by P-31 NMR using surface coils. *Nature*, 283:167-170, 1980.

Allman, T.; Holland, G.A.; Lenkinski, R.E.; and Charles, H.C. A simple method for processing NMR spectra in which acquisition is delayed: applications to *in vivo* localized 31P NMR spectra acquired using the DRESS technique. *Magnetic Resonance in Medicine*, 7:88-94, 1988.

Andreasen, N. Scale for the Assessment of Negative Symptoms (SANS). Iowa City, The University of Iowa, 1984a.

Andreasen, N. Scale for the Assessment of Positive Symptoms (SAPS). Iowa City, The University of Iowa, 1984b.

Andreasen, N.C.; Ehrhardt, J.C.; Swayze, V.W.; Alliger, R.J.; Yuh, W.T.C.; Cohen, G.; and Ziebell, S. Magnetic resonance imaging of the brain in schizophrenia. *Archives of General Psychiatry*, 47:35-44, 1990.

Andreasen, N.C.; Rezai, K.; Alliger, R.; Swayze, V.W.; Flaum, M.; Kirchner, P.; Cohen, G.; and O'Leary, D.S. Hypofrontality in neuroleptic-naive patients and in patients with chronic schizophrenia. *Archives of General Psychiatry*, 49:943-953, 1992.

Andreoli, W.M., and Maffei, T. Blood levels of S-adenosylmethionine in schizophrenia. *Lancet*, 2:922, 1979.

Angrist, B.M.; Shopsin, B.; and Gershon, S. Comparative psychotomimetic effects of stereoisomers of amphetamine. *Nature*, 234: 152-154, 1971.

Barkhuijsen, H.; de Beer, R.; Bovée, W.M.M.J.; and van Ormondt, D. Retrieval of frequencies, amplitudes, damping factors, and phases from time-domain signals using a linear least-squares procedure. *Journal of Magnetic Resonance*, 61: 465-481, 1985.

Barta, P.E.; Pearlson, G.D.; Powers, R.E.; Richards, S.S.; and Tune, L.E. Reduced volume of superiors temporal gyrus in schizophrenia: relationship to auditory hallucinations. *American Journal of Psychiatry*, 147: 1457-1462, 1990.

Bauer, C.; Freeman, R.; Frenkiel, T.; Kreeler, J.; and Shaka, A.J. Gaussian Pulses. *Journal of Magnetic Resonance*, 58: 442-457, 1984.

Behar, K.L., and Ogino, T. Assignment of resonances in the ^1H spectrum of rat brain by two-dimensional shift correlated and J-resolved NMR spectroscopy, *Magnetic Resonance in Medicine*, 17: 285-303, 1991.

Behar, K.L., and Ogino, T. Characterization of macromolecule resonances in the ^1H NMR spectrum of rat brain. *Magnetic Resonance in Medicine*, 30: 38-44, 1993.

Benes, F.M.; McSparren, J.; Bird, E.D.; SanGiovanni, J.P.; and Vincent, S.L. Deficits in small interneurons in prefrontal and cingulate cortices of schizophrenic and schizoaffective patients. *Archives of General Psychiatry*, 48:996-1001, 1991.

Bennett, E.R.; Yedgar, S.; Lerer, B.; and Ebstein, R.P. Phospholipase A_2 activity in epstein-barr virus-transformed lymphoblast cells from schizophrenia patients.

Biological Psychiatry, 29: 1058-1062, 1991.

Berger, B.; Gaspar, P.; and Verney, C. Dopaminergic innervation of the cerebral cortex: unexpected differences between rodents and primates. *Trends in Neurosciences*, 14: 21-27, 1991.

Berman, K.F.; Doran, A.R.; Pickar, O.; and Weinberger, D.R. Is the mechanism of prefrontal hypofunction in depression the same as in schizophrenia? Regional cerebral blood flow during cognitive activation. *British Journal of Psychiatry*, 162: 183-192, 1993.

Berman, K.; Illowsky, B.; and Weinberger, D. Physiological dysfunction of the dorsolateral prefrontal cortex in schizophrenia IV: further evidence for regional and behavioural specificity. *Archives of General Psychiatry*, 45: 616-622, 1988.

Berman, K.; Zec, R.; and Weinberger, D. Physiological dysfunction of dorsolateral prefrontal cortex in schizophrenia II: role of neuroleptic treatment, attention and mental effort. *Archives of General Psychiatry*, 43: 126-135, 1986.

Birken, D.L., and Oldendorf, W.H. N-acetyl-L-aspartic acid: A literature review of a compound prominent in ^{1}H-NMR spectroscopic studies of brain. *Neuroscience and Biobehavioral Reviews*, 13: 23-31, 1989.

Blakely, R.D., and Coyle, J.T. The neurobiology of N-acetylaspartylglutamate. *International Review of Neurobiology*, 30:39-100, 1988.

Bogerts, B.; Ashtari, M.; Degreef, G.; Alvir, J.M.J.; Bilder, R.M.; and Lieberman, J.A. Reduced temporal limbic structure volumes on magnetic resonance images in first episode schizophrenia. *Psychiatry Research*, 35: 1-13, 1990.

Boska, M.D.; Hubesch, B.; Meyerhoff, D.J.; Twieg, D.B.; Karczmar, G.S.; Matson, G.B.; and Weiner, M.W. Comparison of ^{31}P MRS and ^{1}H MRI at 1.5 and 2.0T. *Magnetic Resonance in Medicine*, 13: 228-238, 1990.

Bottomley, P.A. Spatial localization in NMR spectroscopy in vivo. *Annals of the New York Acadamy of Science*, 508: p333, 1987.

Bottomley, P.A. Human *in vivo* NMR spectroscopy in diagnostic medicine: clinical tool or research probe? *Radiology*, 170: 1-15, 1989.

Bottomley, P.A. The trouble with spectroscopy papers. *Radiology*, 181:344-350, 1991.

Breier, A.; Buchanan, R.W.; Elkashef, A.; Munson, R.C.; Kirkpatrick, B.; and Gellad, F. Brain morphology and schizophrenia. A magnetic resonance imaging study of limbic, prefrontal cortex, and caudate structures. *Archives of General Psychiatry*, 49: 921-926, 1992.

Brooks, R.A.; DiChiro, G.; and Keller, M.R. Explanation of cerebral white-gray contrast in computed tomography. *Journal of Computer Assisted Tomography*, 4: 489, 1980.

Brown, T.R.; Kincaid, B.M.; and Ugurbil, K. NMR chemical shift imaging in three dimensions. *Proceedings of the National Academy of Sciences USA*, 79:3523-3526, 1982.

Buchanan, R.W.; Breier, A.; Kirkpatrick, B.; Elkashef, A.; Munson, R.C.; Gellad, F.; and Carpenter, W.T. Jr. Structural abnormalities in deficit and nondeficit schizophrenia. *American Journal of Psychiatry*, 150: 59-66, 1993.

Buchsbaum, M.S. The frontal lobes, basal ganglia, and temporal lobes as sites for schizophrenia. *Schizophrenia Bulletin,* 16: 379-389, 1990.

Buchsbaum, M.S.; Haier, R.J.; Potkin, S.G.; Nuechterlein, K.; Bracha, H.S.; Katz, M.; Lohr, J.; Wu, J.; Lottenberg, S.; Jerabek, P.A.; Trenary, M.; Tafalia, R.; Reynolds, C.; and Bunney, W.E. Jr. Frontostriatal disorder of cerebral metabolism in never-medicated schizophrenics. *Archives of General Psychiatry,* 49: 935-942, 1992.

Buchsbaum, M.S.; Neuchterlein, K.H., Haier, R.J.; Wu, J.; Sicotte, N.; Hazlett, E.; Asarnow, R.; Potkin, S.; and Guich, S. Glucose metabolic rate in normals and schizophrenics during the continuous performance test assessed by positron emission tomography. *British Journal of Psychiatry,* 156: 216-227, 1990.

Calabr[illegible], G.; Deicken, R.F.; Fein, G.; Merrin, E.L.; Schoenfeld, F.; and Weiner, M.W. ^{31}Phosphorus magnetic resonance spectroscopy of the temporal lobes in schizophrenia. *Biological Psychiatry,* 32: 26-32, 1992.

Carlsson, A. The current status of the dopamine hypothesis of schizophrenia. *Neuropsychopharmacology,* 1:179-186, 1988.

Carlsson, A., and Lindquist, M. Effect of chlorpromazine or haloperidol on formation of 3-methoxytyramine and normetanephrine mouse brain. *Acta Pharmacologia and Toxicologia,* 20:140-144, 1963.

Chen, W.; Novotny, E.J.; Zhu, X.-H.; Rothman, D.L.; and Shulman, R.G. Localized ^{1}H NMR measurement of glucose consumption in the human brain during visual stimulation. *Proceedings of the 12th Annual Meeting of the Society of Magnetic Resonance in Medicine,* p. 1528, 1993.

Christiansen, P.; Henriksen, O.; Stubgaard, M.; Gideon, P.; and Larsson, H.B.W. *In vivo* quantification of brain metabolites by ^{1}H-MRS using water as an internal standard. *Magnetic Resonance Imaging,* 11:107-118, 1993.

Cohen, J.D.; Forman, S.D.; casey, B.J.; and Noll, D.C. Spiral-scan imaging of dorsolateral prefrontal cortex during a working memory task. *Proceedings of the 12th Annual Meeting of the Society of Magnetic Resonance in Medicine,* p. 1405, 1993.

Cohen, R.; Semple, W.; Gross, M.; Nordahl, T.E.; DeLisi, L.E.; Holcomb, H.H.; Morihisa, J.M.; and Pikar, D. Dysfunction in a prefrontal substate of sustained attention in schizophrenia. *Life Sciences,* 40: 2031-2039, 1987.

Collinge, J., and Curtis, D. Decreased hippocampal expression of a glutamate receptor gene in schizophrenia. *British Journal of Psychiatry,* 159: 857-859, 1991.

Collingridge, G. The role of NMDA receptors in learning and memory. *Nature,* 300: 604-605, 1987.

Cooper, J.R.; Bloom, F.E.; and Roth, R.H. *The biochemical basis of neuropharmacology,* 4th ed. New York, NY: Oxford University Press, 1982.

Cotman, C.W., and Monaghan, D.T. Excitatory amino acid neurotransmission: NMDA receptors and Hebb-type synaptic plasticity. *Annual Review in Neurosciences,* 11: 61-80, 1988.

Cowan, W.M. Regressive events in neurogenesis. *Science,* 225: 1258-1265, 1984.

Crow, T.J. The dopamine hypothesis survives, but there must be a way ahead. *British Journal of Psychiatry*, 151:460-465, 1987.

Crow, T.J. and Johnstone, E.C. Schizophrenia: nature of the disease process and its biological correlates. In: Plum, F., ed. *Handbook of Physiology- The Nervous System.* Baltimore: American Physiological Society, 843-869, 1987.

Cuenod, C.A.; Bookheimer, S.; Pannier, L.; Posse, S.; Bonnerot, V.; Turner, R.; Jezzard, P.; Frank, J.A.; Zeffiro, T.; and Lebihan, D. Functional imaging during word generation using a conventional MRI scanner. *Proceedins of the 12th Annual Meeting of the Society of Magnetic Resonance in Medicne*, p. 1414, 1993.

Curtis, D.R., and Johnston, G.A.R. Amino acid transmitters in the mammalian central nervous system. *Ergebnisse der Physiologie, Biologischemie und Experimentellen Pharmakologie*, 69: 94-188, 1974.

Dager, S.R., and Steen, R.G. Applications of magnetic resonance spectroscopy to the investigation of neuropsychiatric disorders. *Neuropsychopharmacology*, 6: 249-266, 1992.

Dauphinais, D.; DeLisi, L.E.; Crow, T.J.; Alexandropoulos, K.; Colter, N.; Tuma, I.; and Gershon, E.S. Reduction in temporal lobe size in siblings with schizophrenia: a magnetic reonance imaging study. *Psychiatry Research*, 35: 137-147, 1990.

Dawson, R.M.C. Enzymatic pathways of phospholipid metabolism in the nervous system. In: Eichberg J, ed. *Phospholipids in Nervous Tissues.* New York, NY: John Wiley & Sons Ltd., 45-78, 1985.

Deakin, J.W.F.; Slater, P.; Simpson, M.D.C.; Gilchrist, A.C.; Skan, W.J.; Royston, M.C.; Reynolds, G.P.; and Cross, A.J. Frontal cortical and left temporal glutamatergic dysfunction in schizophrenia. *Journal of Neurochemistry,* 52:1781-1786, 1989.

de Beer, R.; van den Boogaart, A.; van Ormondt, D.; and Pijnappel, W.W.F. Application of time-domain fitting in the quantification of *in vivo* ^{1}H spectroscopic imaging data sets. *NMR in Biomedicine,* 5: 171-178, 1992.

de Beer, R., and van Ormondt, D. Analysis of NMR data using time domain fitting procedures. Diehl, P.; Fluck, E. G.; et al., eds. In: *NMR Basics Principles and Progress.* New York, Springer-Verlag, 26: 201-258, 1992.

de Graaf, A.A., and Bovée, W.M.M.J. Improved quantification of *in vivo* ^{1}H NMR spectra by optimization of signal acquisition and processing and by incorporation of prior knowledge into the spectral fitting. *Magnetic Resonance in Medicine,* 15: 305-319, 1990.

de Graaf, A.A.; van Dijk, J.E.; and Bovée, W.M.M.J. QUALITY: Quantification improvement by converting lineshapes to the Lorentzian type. *Magnetic Resonance in Medicine,* 13: 343-357, 1990.

DeLisi, L.E.; Hoff, A.L.; Schwartz, J.E.; Shields, G.W., Halthore, S.N.; Gupta, S.M.; Henn, F.A.; and Anand, A.K. Brain morphology in first-episode schizophrenic-like psychotic patients: a quantitative magnetic resonance imaging study. *Biological Psychiatry,* 29: 159-175, 1991.

Deutsch, S.I.; Mastropaolo, J.; Schwartz, B.L.; Rosse, R.B.; and Morihisa, J.M. A glutamatergic hypothesis of schizophrenia: Rationale for pharmacotherapy with glycine. *Clinical Neuropharmacology,* 12: 1-13, 1989.

Erecińska, M., and Silver, I.A. Metabolism and role of glutamate in mammalian brain. *Progress in Neurobiology*, 35: 245-296, 1990.

Ernst, Th., and Hennig, J. Coupling effects in volume selective ^{1}H spectroscopy of major brain metabolites. *Magnetic Resonance in Medicine*, 21: 82-96, 1991.

Ernst,Th.; Hennig, J.; Ott, D.; and Friedburg, H. The importance of the voxel size in clinical ^{1}H spectroscopy of the human brain. *NMR in Biomedicine*, 2:216-224, 1989.

Ernst, T.; Kreis, R.; and Ross, B.D. Absolute quantitation of water and metabolites in the human brain. I. Compartments and water. *Journal of Magnetic Resonance, Series B,* 102: 1-8, 1993.

Fagg, G.E. L-glutamate, excitatory amino acid receptors and brain function. *Trends in Neurosciences,* 8:207-210, 1985.

Fagg, G.E., and Foster, A.C. Amino acid neurotransmitters and their pathways in the mammalian central nervous system. *Neuroscience,* 9: 701-719, 1983.

Farooqui, A.A.; and Horrocks, L.A. Metabolic and functional aspects of neural membrane phospholipids. In: Horrocks, L.A.; et al., eds. *Phospholipids in the Nervous System: Physiological Roles.* New York, NY: Raven Press Ltd.; 2: 341-348, 1985.

Feinberg, I. Schizophrenia: Caused by a fault in programmed synaptic elimination during adolescence? *Journal of Psychiatric Research*, 17: 319-334, 1982.

Ferrige, A.G., and Lindon, J.C. Resolution enhancement in FT NMR through

the use of a double exponential function. *Journal of Magnetic Resonance*, 31: 337-340, 1978.

Fisher, S.K.; Heacock, A.M.; and Agranoff, B.W. Inositol lipids and signal transduction in the nervous system: an update. *Journal of Neurochemistry*, 58: 18-38, 1992.

Flatman, P.W. Mechanisms of magnesium transport. *Annual Review in Physiology*, 53: 259-271, 1991.

Frahm, J. In vivo spectroscopy offers unique biomedical insights. *MR*, 2:36-45, 1992

Frahm, J.; Bruhn, H.; Gyngell, M.L.; Merboldt, K.D.; Hänicke, W.; and Sauter, R. Localized high-resolution proton NMR spectroscopy using stimulated echoes: Initial applications to human brain *in vivo*. *Magnetic Resonance in Medicine*, 9: 79-93, 1989a.

Frahm, J.; Bruhn, H.; Gyngell, M.L.; Merboldt, K.D.; Hänicke, W.; and Sauter, R. Localized proton NMR spectroscopy in different regions of the human brain in vivo. Relaxation times and concentrations of cerebral metabolites, *Magnetic Resonance in Medicine*, 11: 47-63, 1989b.

Frahm, J.; Michaelis, T.; Merboldt, K.D.; Bruhn, H.; Gyngell, M.L.; and Hänicke, W. Improvements in localized proton NMR spectroscopy of human brain and water suppression, short echo times, and 1ml resolution. *Journal of Magnetic Resonance*, 90: 464-473, 1990.

Frahm, J.; Michaelis, T.; Merboldt, K.D.; Hänicke, W.; Gyngell, M.L.; and Bruhn, H. On the N-acetyl methyl resonance in localized ^{1}H NMR spectra of human

brain *in vivo*. *NMR in Biomedicine*, 4: 201-204, 1991.

Gadian, D.G., and Radda, G.K. NMR studies of tissue metabolism. *Annual Review in Biochemistry*, 50: 69, 1981.

Gattaz, W.F.; Gasser, T.; and Beckmann, H. Multidimensional analysis of the concentrations of 17 substances in the CSF of schizophrenics and controls. *Biological Psychiatry*, 20:360-366, 1985.

Gattaz, W.F.; Hübner, C.V.K.; Nevalaineri, T.J.; Thursen, T.; and Kinnunen, P.K.J. Increased serum phospholipase A2 activity in schizophrenia: A replication study. *Biological Psychiatry*, 28:495-501, 1990.

Gattaz, W.F.; Köllisch, M.; Thuren, T.; Virtanen, J.A.; and Kinnunen, P.K.J. Increased plasma phospholipase-A2 activity in schizophrenic patients: reduction after neuroleptic therapy. *Biological Psychiatry*, 22: 421-426, 1987.

Grace, A.A. Phasic versus tonic dopamine release and the modulation of dopamine system responsivity: a hypothesis for the etiology of schizophrenia. *Neuroscience*, 41:1-24, 1991.

Gruetter, R.; Rothman, D.L.; Novotny, E.J.; Shulman, G.I.; Prichard, J.W.; and Shulman, R.G. Detection and assignment of the glucose signal in ^{1}H NMR difference spectra of the human Brain. *Magnetic Resonance in Medicine*, 27: 183-188, 1992.

Gupta, R.K.; Gupta, P.; and Moore, R.D. MRI studies of intracellular metal ions in intact cells and tissues. *Annual Review in Biophysics and Bioengineering*, 13: 221-246, 1984.

Haase, A., and Frahm, J. Multiple chemical-shift-selective NMR imaging using stimulated echoes. *Journal of Magnetic Resonance*, 64: 94-102, 1985.

Hagberg, G., and Seelig, J. Localized proton spectroscopy of the human brain: Comparison of different methods for absolute quantification. *Proceedings of the 12th Annual Meeting of the Society of Magnetic Resonance in Medicine*, p. 979, 1993.

Hahn, E.L. Spin echoes. *Physical Review*, 80: 580-594, 1950.

Hahn, E.L. Free nuclear induction. *Physics Today*, 6: 4-9, 1953.

Hänicke, W.; Michaelis, T.; Merboldt, K.D.; and Frahm, J. On the use of a fully automated data analysis method for *in vivo* MRS. Metabolite concentrations and relaxation times from proton spectra of human brain. *Proceedings of the 12th Annual Meeting of the Society of Magnetic Resonance in Medicine*, p. 977, 1993.

Hanstock, C.C.; Rothman, D.L.; Prichard, J.W.; Jue, T.; and Shulman, R.G. Spatially localized ^{1}H NMR spectra of metabolites in the human brain. *Proceedings of the National Academy of Sciences USA*, 85: 1821-1825, 1988.

Harrison, P.J.; McLaughlin, D.; and Kerwin, R.W. Decreased hippocampal expression of a glutamate receptor gene in schizophrenia. *Lancet*, 337:450-452, 1991.

Haselgrove, J.C.; Subramanian, V.H.; Christen, R.; and Leigh, J.S. Analysis of in vivo NMR spectra. *Review of Magnetic Resonance in Medicine*, 2: 167-222, 1987.

Healey, D. D_1 and D_2 and D_3. *British Journal of Psychiatry*, 159: 319-324, 1991.

Hennig, J.; Pfister, H.; Ernst, T.; and Ott, D. Direct absolute quantification of metabolites in the human brain with *in vivo* localized proton spectroscopy, *NMR in Biomedicine*, 5: 193-199, 1992.

Hitzemann, R.; Hirschowitz, J.; and Garver, D. Membrane abnormalities in the psychoses and affective disorders. *Journal of Psychiatric Research*, 18:319-326, 1984.

Hitzemann, R.J.; Mark, C.; Hirschowitz, J.; and Garver, D.L. Characteristics of phospholipid methylation in human erythrocyte ghosts: Relationship(s) to the psychoses and affective disorders. *Biological Psychiatry*, 20:297-407, 1985.

Hoffman, R.E.; Buchsbaum, M.S.; Escobar, M.D.; Makuch, R.W.; Nuechterlein, K.H.; and Guich, S.M. EEG coherence of prefrontal areas in normal and schizophrenic males during perceptual activation. *Journal of Neuropsychiatry and Clinical Neuroscience*, 3: 169-175, 1991.

Holopainen, I.; Kontro, P.; and Oja, S.S. Release of preloaded taurine and hypotaurine from astrocytes in primary culture: stimulation by calcium-free media. *Neurochemistry Research*, 10: 123-131, 1985.

Holowenko, D.; Peeling, J.; and Sutherland, G. ^{1}H NMR properties of N-acetylaspartylglutamate in extracts of nervous tissue of the rat. *NMR in Biomedicine*, 5:43-47, 1992.

Hudson, C.J.; Trevor Young, L.; Li, P.P.; and Warsh, J.J. CNS signal transduction in the pathophysiology and pharmacotherapy of affective disorders

and schizophrenia. *Synapse*, 13:278-293, 1993.

Hugg, J.W.; Matson, G.B.; Twieg, D.B.; Maudsley, A.A.; Sappey-Marinier, D.; and Weiner, M.W. Phosphorous-31 MR spectroscopic imaging (MRSI) of normal and pathological brains. *Magnetic Resonance Imaging*, 10: 227-243, 1992.

Hüttenlocher, P.R. Synaptic density in human frontal cortex: Developmental changes and effects of aging. *Brain Research*, 163:195-205, 1979.

Hüttenlocher, P.R.; deCourten, C.; Garey, L.J.; and Van Der Loos, H. Synaptogenesis in human visual cortex: Evidence for synapse elimination during normal development. *Neuroscience Letters*, 33: 247-252, 1982.

Javitt, D.C. Negative symptomatology and the PCP (Phencyclidine) model of schizophrenia. *Hillside Journal of Clinical Psychiatry*, 9:12-35, 1987.

Javitt, D.C., and Zukin, S.R. The role of excitatory amino acids in neuropsychiatric illness. *Journal of Neuropsychiatry*, 2: 44-52, 1990.

Javitt, D.C., and Zukin S.R. Recent advances in the phencyclidine model of schizophrenia. *American Journal of Psychiatry*, 148: 1301-1308, 1991.

Jernigan, T.L.; Zisook, S.; Heaton, R.K.; Moranville, J.T.; Hesselink, J.R.; and Braff, D.L. Magnetic resonance imaging abnormalities in lenticular nuclei and cerebral cortex in schizophrenia. *Archives of General Psychiatry*, 48: 881-890, 1991.

Jenkins, B.G.; Belliveau, J.W.; and Rosen B.R. Confirmation of lactate production during photic stimulation. Improved protocols using inter- and intra-

subject averaging. *Proceedings of the 11th Annual Meeting of the Society of Magnetic Resonance in Medicine,* p. 2145, 1992.

Johnson, J.W., and Ascher, P. Voltage-dependent block by intracellular Mg^{2+} of N-methyl-D-aspartate-active channels. *Biophysical Journal,* 57: 1085-1090, 1990.

Johnson, K.M. Phencyclidine: behavioural and biochemical evidence supporting a role for dopamine. *Federation Proceedings (Bathesda, Md),* 42: 2579-2583, 1983.

Joliot, M.; Mazoyer, B.M.; and Huesman, R.H. In vivo NMR spectral parameter estimation. A comparison between time and frequency domain methods. *Magnetic Resonance in Medicine,* 18:358-370, 1991.

Jones, P., and Murray, R.M. The genetics of schizophrenia is the genetics of neurodevelopment. *British Journal of Psychiatry,* 158: 615-623, 1991.

Kato, T.; Shioiri, T.; Takahashi, S.; and Inubushi, T. Measurement of brain phosphoinositide metabolism in bipolar patients using in vivo ^{31}P-MRS. *Journal of Affective Disorders,* 22:185-190, 1991.

Kauppinen, R.A.; Kokko, H.; and Williams, S.R. Detection of mobile proteins by proton nuclear magnetic resonance spectroscopy in the guinea pig brain ex vivo and their partial purification. *Journal of Neurochemistry,* 58: 967-974, 1992.

Kauppinen, R.A.; Williams, S.R.; Busza, A.L.; and van Bruggen, N. Applications of magnetic resonance spectroscopy and diffusion-weighted imaging to the study of brain biochemistry and pathology. *Trends in Neurosciences,* 16: 88-95, 1993.

Kelsoe, J.R.; Cadet, J.L.; Pickar, D.; and Weinberger, D.R. Quantitative neuroanatomy in schizophrenia: a controlled magnetic resonance imaging study. *Archives of General Psychiatry*, 45:533-541, 1988.

Kelsoe, J.R. Jr; Tolbert, L.C.; Crews, E.L.; and Smythies, J.R. Kinetic evidence for decreased methionine adenosyltransferase activity in erythrocytes from schizophrenics. *Journal of Neuroscience Research*, 8: 99-103, 1982.

Kerkerian, L.; Dusticier, N.; and Nieoullon, A. Modulatory effect of dopamine on high-affinity glutamate uptake in the rat striatum. *Journal of Neurochemistry*, 48:1301-1306, 1987.

Kerwin, R.; Patel, S.; and Meldrum, B. Quantitative autoradiographic analysis of glutamate binding sites in the hippocampal formation in normal and schizophrenic brain post mortem. *Neuroscience* 39: 25-32, 1990.

Kerwin, R.W.; Patel, S.; Meldrum, B.S.; Czudek, C.; and Reynilds, G.P. Asymmetrical loss of glutamate receptor subtype in left hippocampus in schizophrenia. *Lancet* 1: 583-584, 1988.

Kerwin, R.W.; Rupniak, N.M.J.; Jenner, P.; and Marsden, C.D. A comparison of the effects of acute and one year's continuous neuroleptic treatment on the release of [^{3}H] glutamate and [^{3}H] acetylcholine from rat striatal slices. *Neuroscience*, 11: 205-210, 1984.

Keshavan, M.S.; Mallinger, A.G.; Pettegrew, J.W.; and Dippold, C. Erythrocyte membrane phospholipids in psychotic patients. *Journal of Psychiatry Research*, 49: 89-95, 1993a.

Keshavan, M.S.; Sanders, R.D.; Pettegrew, J.W.; Dombrowsky, S.M.; and

Panchalingam, K.S. Frontal lobe metabolism and cerebral morphology in schizophrenia: ^{31}P MRS and MRI studies. *Schizophrenia Research*, 10: 241-246, 1993b.

Keshavan, M.S.; Shitij, K.; and Pettegrew, J.W. Magnetic resonance spectroscopy in psychiatry: potential, pitfalls, and promise. *American Journal of Psychiatry*, 148: 976-985, 1991.

Kim, J.S.; Claus, D.; and Kornhuber, H.H. Cerebral glutamate, neuroleptic drugs and schizophrenia: Increase of cerebrospinal fluid glutamate levels and decrease of striate body glutamate levels following sulpiride treatment in rats. *European Neurology*, 22: 367-370, 1983.

Kim, J.S.; Kornhuber, H.H.; Schid-Burgk, W.; and Holzmüller, B. Low cerebrospinal fluid glutamate in schizophrenic patients and a new hypothesis on schizophrenia. *Neuroscience Letters*, 20: 379-382, 1980.

Kornhuber, J., and Kornhuber, M.E. Presynaptic dopaminergic modulation of cortical input to the striatum. *Life Sciences*, 39: 669-674, 1986.

Kornhuber, J.; Mack-Burkhardt, F.; Riederer, P.; Hebenstreit, G.F.; Reynolds, G.P.; Andrews, H.B.; and Beckermann, H. [^{3}H]MK-801 binding sites in postmortem brain regions of schizophrenic patients. *Journal of Neural Transmission*, 77: 231-236, 1989.

Korpi, E.T.; Kauffman, C.A.; Marnela, K.M.; and Weinberger, D.R. Cerebrospinal fluid amino acid concentrations in chronic schizophrenia. *Psychiatry Research*, 20: 337-345, 1987.

Kreis, R.; Ernst, T.; and Ross, B.D. Absolute quantitation of water and

metabolites in the human brain. II. Metabolite concentrations. *Journal of Magnetic Resonance, Series B*, 102: 9-19, 1993.

Kurumaji, A.; Ishimaru, M.; and Toru, M. Quisqualate receptors in post-mortem brain of chronic schizophrenics. *Proceedings of Kyoto: New Trends in Schizophrenia and Mood Disorders*, p. 29, 1990.

Kwee, I.L., and Nakada, T. Phospholipid profile of the human brain: ^{31}P NMR spectroscopic study. *Magnetic Resonance in Medicine*, 6: 296-299, 1988.

Lautin, A.; Mandio Cordasco, D.; Segarnick, D.J.; Wod, L.; Mason, M.F.; and Rotrosen, J. Red cell phospholipids in schizophrenia. *Life Sciences*, 31:3051-3056, 1982.

Lodge, D., and Johnson, K.M. Noncompetitive excitatory amino acid receptor antagonists. *Trends in Pharmacological Sciences*, 11: 81-86, 1990.

Lowry, O.H.; Berger, S.J.; Chi, M.M.Y.; Carter, J.G.; Blackshaw, A.; and Outlaw, W. Diversity of metabolic patterns in human brain tumors. I. High energy phosphate compounds and basic composition, *Journal of Neurochemistry*, 29: 959, 1977.

Macciardi, F.; Petronis, A.; van Tol, H.H.M.; Marino, C.; Cavallini, M.C.; Smeraldi, E.; and Kennedy, J.L. Analysis of the D_4 dopamine receptor gene variant in an Italian schizophrenia kindred. *Archives of General Psychiatry*, 51: 288-293, 1994.

Marquardt, D.W. An algorithm for least-squares estimation of non-linear parameters. *Journal. Society of Industrial and Applied Mathematics.* 11: 431-441, 1963.

Martin, D.L., and Rimvall, K. Regulation of γ-aminobutyric acid synthesis in the brain. *Journal of Neurochemistry*, 60: 395-407, 1993.

Matalon, R.; Michals, K.; Sebesta, D.; Deanching, M.; Gashkoff, P.; and Casanova, J. Aspartoacylase deficiency and N-acetylaspartic aciduria in patients with Canavan disease. *American Journal of Medical Genetics*, 29: 463-471, 1988.

Mazzeo, A.R., and Levy, G.C. An evaluation of new processing protocols for in vivo NMR spectroscopy. *Magnetic Resonance in Medicine*, 17: 483-495, 1991.

McCarthy, G.; Blamire, A.M.; Rothman, D.L.; Gruetter, R.; Shulman, R.G. Echo-planar magnetic resonance imaging studies of frontal cortex activation during word generation in humans. *Proceedings of the National Academy of Sciences USA*, 90: 4952, 1993.

McGale, E.H.F.; Pye, I.F.; Stonier, C.; Hutchinson, E.C.; and Aber, G.M. Studies of the interrelationship between cerebrospinal fluid and plasma amino acid concentrations in normal individuals. *Journal of Neurochemistry*, 29: 291-297, 1977.

McGuire, T.M. Measuring the economic costs of schizophrenia. *Schizophrenia Bulletin*, 17:376-388, 1991.

Meltzer, H.Y., and Stahl, S.M. Dopamine hypothesis of schizophrenia: A review. *Schizophrenia Bulletin*, 2: 19-76, 1976.

Menon, R.S., and Allen, P.S. Application of continuous relaxation time distributions to the fitting of data from model systems and excised tissue. *Magnetic Resonance in Medicine*, 20: 214-227, 1991.

Merboldt, K.D.; Bruhn, H.; Hänicke, W.; Michaelis, T.; and Frahm, J. Decrease of glucose in the human visual cortex during photic stimulation. *Magnetic Resonance in Medicine*, 25: 187-194, 1992.

Merboldt, K.D.; Chien, D.; Hänicke, W.; Gyngell, M.L.; Bruhn, H.; and Frahm, J. Localized ^{31}P NMR spectroscopy of the adult human brain *in vivo* using stimulated-echo (STEAM) sequences. *Journal of Magnetic Resonance*, 89: 343-361, 1990.

Meyerand, M.E.; Tan, G.;Strandt, J.A.; and Li, S.-J. The effect of stimulation on the proton metabolite spectrum of the motor cortex. *Proceedings of the 12th Annual Meeting of the Society of Magnetic Resonance in Medicine*, p. 374, 1993.

Michaelis, T.; Helms, G.; Merboldt, K.D.; Hänicke, W.; Bruhn, H.; and Frahm, J. First observation of scyllo-inositol in proton NMR spectra of human brain *in vitro* and *in vivo*. *Proceedings of the 11th Annual Meeting of the Society of Magnetic Resonance in Medicine*, p. 541, 1992.

Michaelis, T.; Merboldt, K.D.; Bruhn, H.; Hänicke, H.; and Frahm, J. Absolute concentrations of metabolites in the adult human brain *in vivo*: Quantification of localized proton MR spectra. *Radiology*, 187: 219-227, 1993.

Michaelis, T.; Merboldt, K.D.; Hänicke, W.; Gyngell, M.L.; Bruhn, H.; and Frahm, J. On the identification of cerebral metabolites in localized ^{1}H NMR spectra of human brain *in vivo*. *NMR in Biomedicine*, 4: 90-98, 1991.

Moises, H.W.; Gelernter, J.; Giuffra, L.A.; Zarcone, V.; Wetterberg, L.; Civelli, O.; Kidd, K.K.; Cavalli-Storza, L.L.; Grandy, D.K.; Kennedy, J.L.; Vinogradov, S.; Mauer, J.; Litt, M.; and Sjogren, B. No linkage between D_2 dopamine receptor

gene region and schizophrenia. *Archives of General Psychiatry*, 48: 643-647, 1991.

Moon, R.B., and Richards, J.H. Determination of intracellular pH by ^{31}P magnetic resonance. *Journal of Biological Chemistry*, 248: 7276-7278, 1973.

Moonen, C.T.W.; von Kienlin, M.; and van Zijl, P.C.M. Comparison of single-shot localization methods (STEAM and PRESS) for in vivo proton NMR spectroscopy. *NMR in Biomedicine*, 2:201-208, 1989.

Moore, C.M.; Redmond, O.M.; Buckley, P.; Larkin, C.; Stack, J.P.; Waddington, J.; and Ennis, J.T. In vivo proton NMR spectroscopy (STEAM) in patients with schizophrenia. *Proceedings of the 11th Annual Meeting of the Society of Magnetic Resonance in Medicine*, p. 1933, 1992.

Morrison-Stewart, S.L.; Williamson, P.C.; Corning, W.C.; Kutcher, S.P.; and Merskey, H. Coherence on electroencephalography and aberrant functional organization of the brain in schizophrenic patients during activation tasks. *British Journal of Psychiatry*, 159: 636-644, 1991.

Murphy, E.J.; Rajagopalan, B.; Brindle, K.M.; and Radda, G.K. Phospholipibilayer contribution to ^{31}P NMR spectra in vivo. *Magnetic Resonance in Medicine*, 12: 282-289, 1989.

Nadler, J.V., and Cooper, J.R. N-acetyl-L-aspartic acid content of human neural tumours and bovine peripheral nervous tissues. *Journal of Neurochemistry*, 19: 313-319, 1972.

Narayana, P.A.; Fotedar, L.K.; Jackson, E.F.; Bohan, T.P.; Butler, I.J.; and Wolinsky, J.S. Regional *in vivo* proton magnetic resonance spectroscopy of

brain. *Journal of Magnetic Resonance*, 83: 44-52, 1989.

Narayana, P.A. ; Johnston, D.; and Flamig, D.P. *In vivo* proton magnetic resonance spectroscopy studies of human brain. *Magnetic Resonance Imaging*, 9: 303-308, 1991.

Nasrallah, H.A. Neurodevelopmental pathogenesis of schizophrenia. *Psychiatric Clinics of North America*, 16:269-280, 1993.

Nasrallah, H.A.; Skinner, T.E.; Schmalbrock, P.; Obringer, A.; Robitaille, P.-M.L. ^{1}H nuclear magnetic resonance spectroscopy of the hippocampus in schizophrenia. Presented at the Annual Meeting of the American Psychiatric Association, Washington DC, May 1992.

Nelson, S.J., and Brown, T.R. The accuracy of quantification from 1D NMR spectra using the PIQABLE algorithm. *Journal of Magnetic Resonance*, 84: 95-109, 1989.

Nicholls, D.G. Release of glutamate, aspartate and γ-aminobutyric acid from isolated nerve terminals. *Journal of Neurochemistry*, 52: 331-341, 1989.

Nicholls, D., and Attwell, D. The release and uptake of excitatory amino acids. *Trends in Pharmacological Sciences*, 11: 462-468, 1990.

Nieoullon, A.; Kerkerian, L.; and Dusticier, N. Presynaptic dopaminergic control of high affinity glutamate uptake in the striatum. *Neuroscience Letters*, 43:191-196, 1983.

Nishikawa, T.; Takashima, M.; and Toru, M. Increased ^{3}H-kainic acid binding in the prefrontal cortex in schizophrenia. *Neuroscience Letters*, 40:245-250, 1983.

Norton, W.T. ; Poduslo, S.E.; and Suzuki, K. Subacute sclerosing leukoencephalitis. II. Chemical studies including abnormal myelin and an abnormal ganglioside pattern, *Journal of Neuropathology and Experimental Neurology*, 25: 582-597, 1966.

O'Callaghan, E.; Redmond, O.; Ennis, R.; Stack, J.; Kinsella, A.; Ennis, J.T.; Conall, L.; and Waddington, J.L. Initial investigation of the left temporoparietal region in schizophrenia by 31P magnetic resonance spectroscopy. *Biological Psychiatry*, 29: 1149-1152, 1991.

Ordidge, R.J. Localized chemical shift measurements in phosphorus and protons. *Proceedings of the 4th Annual Meeting of the Society of Magnetic Resonance in Medicine*, 131-132, 1985.

Ordidge, R.J.; Connelly, A.; and Lohman, J.A.B. Image selected in vivo spectroscopy (ISIS). A new technique for spatially selective NMR spectroscopy. *Journal of Magnetic Resonance*, 66:283-294, 1986.

Ottersen, O.P.; Madsen, S.; Storm-Mathisen, J.; Somogyi, P.; Scopsi, L.; and Larsson, L-I. Immunocytochemical evidence suggests that taurine is colocalized with GABA in the Purkinje cell terminals, but that the stellate cell terminals predominantly contain GABA: a light- and electronmicroscopic study of the rat cerebellum. *Experimental Brain Research*, 72: 407-416, 1988.

Owen, M.J. and Mullan, M.J. Molecular genetic studies of manic-depression and schizophrenia. *Trends in Neurosciences*, 13: 29-31, 1990.

Pangerl, A.M.; Steudle, A.; Jaroni, H.W.; Rufer, R.; and Gattaz, W.F. Increased platelet membrane lysophosphatidylcholine in schizophrenia. *Biological Psychiatry*, 30: 837-840, 1991.

Perry, T.L. Normal cerebrospinal fluid and brain glutamate levels in schizophrenics do not support the hypothesis of glutamatergic neuronal dysfunction. *Neuroscience Letters*, 28:81-85, 1982.

Perry, T.L.; Hansen, S.; Berry, K.; Mok, C.; and Lesk, D. Free amino acids and related compounds in biopsies of human brain. *Journal of Neurochemistry*, 18: 521-528, 1971.

Perry, T.L.; Hansen, S.; and Gandham, S.S. Postmortem changes of amino compounds in human and rat brain. *Journal of Neurochemistry*, 36: 406-412, 1981.

Perry, T.L.; Hansen, S.; Kennedy, J.; Wada, J.A.; and Thompson, G.B. Amino acids in human epileptogenic foci. *Archives of Neurology*, 32: 752-754, 1975.

Perry, T.L.; Hansen, S.; and Kish, S.J. Effects of chronic administration of antipsychotic drugs on GABA and other amino acids in the mesolimbic area of rat brain. *Life Sciences*, 24: 283-288, 1979.

Petroff, O.A.C.; Prichard, J.W.; Behar, K.L.; Alger, J.R.; den Hollander, J.A.; and Shulman, R.G. Cerebral intracellular pH by ^{31}P nuclear magnetic resonance spectroscopy. *Neurology*, 35:781-788, 1985.

Petroff, O.A.C.; Spencer, D.D.; Alger, J.R.; and Prichard, J.W. High-field proton magnetic resonance spectroscopy of human cerebrum obtained during surgery for epilepsy. *Neurology*, 39: 1197-1202, 1989.

Pettegrew, J.W.; Keshavan, M.S.; and Minshew, N.J. ^{31}P Nuclear magnetic resonance spectroscopy: neurodevelopment and schizophrenia. *Schizophrenia Bulletin*, 19: 35-53, 1993.

Pettegrew, J.W.; Keshavan, M.S.; Panchalingam, K.; Strychor, S.; Kaplan, D.B.; Tretta, M.G.; and Allen, M. Alterations in brain high-energy phosphate and membrane phospholipid metabolism in first-episode, drug-naive schizophrenics: A pilot study of the dorsolateral prefrontal cortex by *in vivo* phosphorus 31 nuclear magnetic resonance spectroscopy. *Archives of General Psychiatry*, 48: 563-568, 1991.

Pettegrew, J.W.; Kopp, S.J.; Dadok, J.; Minshew, N.J.; Feliksik, J.M.; Glonek, T.; and Cohen, M.M. Chemical characterization of a prominent phosphomonoester resonance from mammlian brain: ^{31}P and ^{1}H NMR analysis at 4.7 and 14.1 tesla. *Journal of Magnetic Resonance*, 67: 443-450, 1986.

Pettegrew, J.W; Kopp, S.J.; Minshew, N.J.; Glonek, T.; Feliksik, J.M.; Tow, J.P.; and Cohen, M.M. ^{31}P nuclear magnetic resonance studies of phosphoglyceride metabolism in developing and degenerating brain: Preliminary observations. *Journal of Neuropathology and Experimental Neurology*, 46: 419-430, 1987.

Prichard, J.; Rothman, D.; Novotny, E.; Petroff, O.; Kuwabara, T.; Avison, M.; Howseman, A.; Hanstock, C.; and Shulman, R. Lactate rise detected by 1H NMR in human visual cortex during physiologic stimulation. *Proceedings of the National Academy of Sciences USA*, 88: 5829-5831, 1991.

Provencher, S.W. Estimation of metabolite concentrations from localized *in vivo* proton NMR spectra. *Magnetic Resonance in Medicine*, 30:672-679, 1993.

Purves, D., and Lichtman, J.W. Elimination of synapses in the developing nervous system. *Science*, 210: 153-157, 1980.

Rabi, I.I.; Zachanrias, J.R.; Millman, S.; and Kusch, P. A new method of measuring nuclear magnetic moment. *Physical Review*, 53: 318, 1938.

Radda, G.K. The use of NMR spectroscopy for the understanding of disease. *Science*, 233: 640-645, 1986.

Rakic, P., and Riley, K.P. Over-production and elimination of retinal axons in the fetal rhesus monkey. *Science*, 219: 1441-1444, 1983.

Reynolds, G.P. Beyond the dopamine hypothesis; the neurochemical pathology of schizophrenia. *British Journal of Psychiatry*, 155: 305-316, 1989.

Riederer, P.; Lange, K.W.; Kornhuber, J.; and Jellinger, K. Glutamate receptor antagonism: neurotoxicity, anti-akinetic effects, and psychosis. *Journal of Neural Transmission*, 34:203-210, 1991.

Rieth, K.G.; Fujiwara, K.; DiChiro, G.; Klatzo, I.; Brooks, R.A.; Johnston, G.S.; O'Connor, C.M.; and Mitchell, L.G. Serial measurements of CT attenuation and specific gravity in Experimental Cerebral Edema. *Radiology*, 135: 343, 1980.

Robb, R.A. A software system for interactive and quantitative analysis of biomedical images, In: Hohne, K.H.; Fuchs, H.; and Pizer, S.M., eds. *3D Imaging in Medicine*. NATO ASI Series, Vol. F 60, 1990. pp. 333-361.

Ross, B.D.; Radda, G.K.; Gadian, D.G.; Rocker, G.; Esiri, M.; and Falconer-Smith, J. Examination of a case of suspected McArdle's syndrome by ^{31}P nuclear magnetic resonance. *New England Journal of Medicine*, 304: 1338-1342, 1981.

Rossi, A.; Stratta, P.; D'Albenzio, L.;Tartaro, A.; Shiayza, G.; diMichele, V.; Bolino, F.; and Casacchia, M. Reduced temporal lobe areas in schizophrenia: preliminary evidence from a controlled multiplanar magnetic resonance imaging study. *Biological Psychiatry*, 27: 61-68, 1990.

Rothman, D.L.; Hanstock, C.C.; Petroff, O.A.C.; Novoyny, E.J.; Prichard, J.W.; and Shulman, R.G. Localized ^{1}H NMR spectra of glutamate in the human brain. *Magnetic Resonance in Medicine*, 25: 94-106, 1992.

Rueckert, L.; Appollonio, I.; Grafman, J.; Jezzard, P.; Johnson Jr., R.; Le Bihan, D.; and Turner, R. Functional activation of left frontal cortex during covert word production. *Proceedings of the 12th Annual Meeting of the Society of Magnetic Resonance in Medicine*, p. 60, 1993.

Ryer, H., and Rotrosen, J. Phospholipids and schizophrenia. In: Bazan, N.G.; Horrocks, L.A.; and Toffiano, G. eds. *Phospholipids in the Nervous System: Biochemical and Molecular Pathology*. Padova: Liviana Press, 1989. 17: pp.177-182.

Sappey-Marinier, D.; Calabrese, G.; Fein, G.; Hugg, J.W.; Biggins, C.; and Weiner, M.W. Effect of photic stimulation on human visual cortex lactate and phosphates using 1H and 31P magnetic resonance spectroscopy. *Journal of Cerebral Blood Flow Metabolism,* 12, 584-592, 1992.

Sauter, R.; Mueller, S.; and Weber, H. Localization *in vivo* 31P NMR spectroscopy by combining surface coils and slice-selective saturation. *Journal of Magnetic Resonance*, 75: 167-173, 1987.

Scatton, B.; Worms, P.; Lloyd, K.G.; and Bartholini, G. Cortical modulation of striatal function. *Brain Research*, 232: 331-343, 1982.

Schmidt, W.J. Intrastriatal injection of DL-2-amino-5-phosphonovaleric acid (AP-5) induces sniffing stereotypy that is antagonized by holoperidol and clozapine. *Psychopharmacology,* 90:123-130, 1986.

Seeman, P. Dopamine receptors and the dopamine hypothesis of schizophrenia. *Synapse*, 1: 133-152, 1987.

Selemon, L.D.; Rajkowska, G.; and Goldman-Rakic, P.S. "A morphometric analysis of prefrontal areas 9 and 46 in the schizophrenic and normal human brain." Presented at the Annual Meeting of the American Psychiatric Association, Washington, DC, May 1992.

Sengupta, N.; Datta, S.C.; and Sengupta, D. Platelet and erythrocyte membrane lipid and phospholipid patterns in different types of mental patients. *Biochemistry in Medicine*, 25: 267-275, 1981.

Shenton, M.E.; Kikinis, R.; Jolesz, F.A.; Pollak, S.D.; LeMay, M.; Wible, C.G.; Hokama, H.; Martin, J.; Metcalf, D.; Coleman, M.; and McCarley, R.W. Abnormalities of the left tempoal lobe and thought disorder in schizophrenia. *New England Journal of Medicine*, 327: 604-612, 1992.

Sherman, A.D.; Davidson, A.T.; Baruah, S.; Hegwood, T.S.; and Waziri, R. Evidence of glutamatergic deficiency in schizophrenia. *Neuroscience Letters*, 121:77-80, 1991.

Sherman, A.D., and Mott, J. Direct effect of neuroleptics on glutamate release. *Neuropharmacology*, 23: 1253-1259, 1984.

Sherman, W.R.; Stewart, M.A.; Kurien, M.M.; and Goodwin, S.L. The measurement of *myo*-inositol, *myo*-inosose-2 and *scyllo*-inositol in mammalian tissues. *Biochimica et Biophysica Acta*, 158:197-205, 1968.

Shulman, R.G.; Blamire, A.M.; Rothman, D.L.; and McCarthy, G. Nuclear magnetic resonance imaging and spectroscopy of human brain function.

Proceedins of the National Academy of Sciences USA, 90: 3127-3133, 1993.

Singh, M.; Kim, H.; Huang, H.; and Kim, T. Effect of stimulus rate on lactate in the human auditory cortex. *Proceedings of the 11th Annual Meeting of the Society of Magnetic Resonance in Medicine*, p. 2146, 1992.

Snyder, S.H. Phencyclidine. *Nature* 285: 355-356, 1980.

Soderberg, M.; Edlund, C.; Kristensson, K.; and Dallner, G. Lipid compositions of different regions of the human brain during aging. *Journal of Neurochemistry*, 54:415-423, 1990.

Sotak, C.H.; Dumoulin, C.L.; and Newsham, M.D. Automatic phase correction of Fourier transform NMR spectra based on the dispersion versus absorption (DISPA) lineshape analysis. *Journal of Magnetic Resonance*, 57: 453-462, 1984.

Spitzer, R., and Williams, J. Structured Clinical Interview for DSM-III-R. New York Psychiatric Institute, New York, 1985.

Stanfield, P.R. Intracellular Mg^{2+} may act a co-factor in ion channel function. *Trends in Neurosciences*,11: 475-477, 1988.

Stanley, J.A.; Bartha, R.; Drost, D.J.; Williamson, P.C. Comparison of metabolite levels due to long and short motor cortex activation using ^1H MR spectroscopy. *Proceedings of the 13th Annual Meeting of the Society of Magnetic Resonance in Medicine*, 1994a (submitted).

Stanley, J.A.; Williamson, P.C.; Bartha, R.; Drost, D.J. Evidence of metabolite activity during frontal lobe task with in vivo ^1H MR spectroscopy. *Proceedings*

of the 13th Annual Meeting of the Society of Magnetic Resonance in Medicine, 1994b (submitted).

Stephenson, D.S. Linear prediction and maximum entropy methods in NMR spectroscopy. *Progress in Nuclear Magnetic Resonance Spectroscopy*, 20:515-626, 1988.

Stevens, J.D. The distribution of phospholipid fractions in the red cell membrane of schizophrenics. *Schizophrenia Bulletin*, 6:60-61, 1972.

Stevens, J.R. An anatomy of schizophrenia? *Archives of General Psychiatry*, 29: 177-189, 1973.

Suddath, R.L.; Casanova, M.F.; Goldberg, T.E.; Daniel, D.G.; Kelsoe, J.; and Weinberger, D.R. Temporal lobe pathology in schizophrenia: a quantitative magnetic resonance imaging study. *American Journal of Psychiatry*, 146: 464-472, 1989.

Suddath, R.L.; Christisan, G.W.; Torrey, E.F.; Casanova, M.F.; and Weinberger, D.R. Anatomic abnormalities in the brains of monozygotic twins discordant for schizophrenia. *New England Journal of Medicine*, 332: 62-67, 1990.

Suga, I.; Kobayashi, T.; Ogata, H. et al. Increased ^{3}H-MK801 binding sites in post-mortem brains of chronic schizophrenic patients. *Proceedings of Kyoto: New Trends in Schizophrenia and Mood Disorders Research*, p 28, 1990.

Swayze, V.W.; Andreasen, N.C.; Alliger, A.J.; et al. Subcortical and temporal structures in affected disorder and schizophrenia: a magnetic resonance imaging study. *Biological Psychiatry*, 31: 221-240, 1992.

Szerb, J.C. Rate-limiting steps in the synthesis of GABA and glutamate. In: Avolu, M., Reader, T.A., Dyke, R.W., et al. eds. *Neurotransmitters and Cortical Function.* New York, NY: Plenum, 1988. pp. 153-166.

Tallan, H.H. Studies on the distribution of N-acetyl-L-aspartic acid in brain. *Journal of Biological Chemistry,* 224:41-45, 1957.

Thulborn, K.R., and Ackerman, J.J.H. Absolute molar concentrations by NMR in inhomogeneous B_1. A scheme for analysis of *in vivo* metabolites. *Journal of Magnetic Resonance,* 55:357-371, 1983.

Tofts, P.S., and Wray, S. A critical assessment of methods of measuring metabolite concentrations by NMR spectroscopy. *NMR in Biomedicine,* 1: 1-10, 1988.

Tolbert, L.C.; Monti, J.A.; O'Shields, H.; Walter-Ryan, W.; Meadows, D.; and Smythies, J.R. Defects in transmethylation and membrane lipids in schizophrenia. *Psycopharmacology Bulletin,* 19:594-599, 1983.

Torack, R.M.; Alcala, H.; Gado, M.; and Burton, R. *Journal of Neuropathology and Experimental Neurology,* 35: 385, 1976.

Ulas, J., and Cotman, C.W. Excitatory amino acid receptors in schizophrenia. *Schizophrenia Bulletin,* 19: 105-117, 1993.

Urenjak, J.; Williams, S.R.; Godown, D.G.; and Noble, M. Proton nuclear magnetic resonance spectroscopy unambiguously identifies different neural cell types. *The Journal of Neuroscience,* 13: 981-989, 1993.

van der Veen, J.W.C.; de Beer, R.; Luyten, P.R.; and van Ormondt, D.

Accurate quantification of *in vivo* ^{31}P NMR signals using the variable projection method and prior knowledge. *Magnetic Resonance in Medicine*, 6: 92-98, 1988.

van Dijk, J.E.; Mehlkopf, A.F.; van Ormondt, D.; and Bovée, W.M.M.J. Determination of concentration by time domain fitting of proton NMR echo signals using prior knowledge. *Magnetic Resonance in Medicine*, 27:76-96, 1992.

van Gelder, N.M. A central mechanism of action of taurine: Osmoregulation, bivalent cations and excitation threshold. *Neurochemistry Research*, 8: 687-699, 1983.

Volkow, N.; Wolfe, S.; van Gelder, P.; Brodie, J.D.; Overall, J.E.; Cancero, R.; and Gomez-Mont, F. Phenomenological correlates of metabolism activity in 18 patients with chronic schizophrenia. *American Journal of Psychiatry*, 144: 151-158, 1987.

Wachtel, H., and Turski, L. Glutamate: a new target in schizophrenia? *Trends in Pharmacological Sciences*, 11:219-220, 1990

Weinberger, D. Implications of normal brain development for the pathogenesis of schizophrenia. *Archives General Psychiatry*, 44: 660-669, 1987.

Weinberger, D.; Berman, K.; and Zec, R. Physiological dysfunction of dorsolateral and prefrontal cortex in schizophrenia I: regional cerebral blood flow evidence. *Archives of General Psychiatry*, 43: 114-124, 1986.

Weinberger, D.; Berman, K.; and Illowsky, B. Physiological dysfunction of the dorsolateral prefrontal cortex in schizophrenia III. A new cohort and evidence

for a monoaminergic mechanism. *Archives of General Psychiatry*, 45: 609-615, 1988.

Weissman, A.D.; Casanova, M.F.; Kleinman, J.E.; London, E.; and Desouza, E.B. Selective loss of cerebral cortical sigma, but not PCP binding sites in schizophrenia. *Biological Psychiatry*, 29: 41-54, 1991.

White, A.M.; Varney, M.A.; Watson, S.P.; Rigby, S.; Liu, C.S.; Ward, J.G.; Reese, C.B.; Graham, H.C.; and Williams, R.J. Influence of Mg^{2+} and pH on NMR spectra and radiological binding of inositol 1,4,5-triphosphate. *Biochemistry Journal*, 278: 759-764, 1991.

Williamson, P.C.; Drost, D.; Stanley, J.; Carr, T.; Morrison, S.; and Merskey, H. Localized phosphorus 31 magnetic resonance spectroscopy in chronic schizophrenic patients and normal controls. *Archives of General Psychiatry*, 48: 578, 1991. Letter.

Williamson, P.C.; Pelz, D.; Merskey, H.; Morrison, S.; Karlik, S.; Drost, D.; Carr, T.; and Conlon, P. Frontal, temporal and striatal proton relaxation times in schizophrenic patients and normal comparison subjects. *American Journal of Psychiatry*, 149: 549-551, 1992.

Williamson, P.C.; Stanley, J.A.; Drost, D.J.; Carr, T.; Thompson, T.; Rylett, J.; and Malla, A. Specificity of phosphorous 31 magnetic resonance spectroscopy findings in schizophrenia. *Schizophrenia Annual Meeting, Vancouver, Canada,* August 1994.

Wilman, A.H., and Allen, P.S. An analytical and experimental evaluation of STEAM versus PRESS for the observation of the lactate doublet. *Journal of Magnetic Resonance, Series B*, 101:102-105, 1993.

Wray, S.; and Tofts, P.S. Direct *in vivo* measurement of absolute metabolite concentrations using ^{31}P nuclear magnetic resonance spectroscopy. *Biochimica et Biophysica Acta*, 886: 399-405, 1986.

Xue, M.; Ng, T.C.; Comair, Y.G.; and Modie, M. Decreased NAA and increased lactate in the activated motor cortex detected with localized spectroscopy guided with functional MRI. *Proceedings of the 12th Annual Meeting of the Society of Magnetic Resonance in Medicine*, p. 59, 1993.

Young, A.H.; Blackwood, D.H.R.; Roxborough, H.; McQueen, J.K.; Martin, M.J.; and Kean, D. A magnetic resonance imaging study of schizophrenia: brain structure and clinical symptoms. *British Journal of Psychiatry*, 158: 158-164, 1991.

Yurgelun-Todd, D.A.; Renshaw, P.F.; Waternaux, C.M.; Gruber, S.A.; and Cohen, B.M. ^{1}H spectroscopy of the temporal lobes in schizophrenic and bipolar patients. *Proceedings of the 12th Annual Meeting of the Society of Magnetic Resonance in Medicine*, p. 1539, 1993.

Zipursky, R.B.; Lim, K.O.; Sullivan, E.V.; Brown, B.W.; and Pfefferbaum, A. Widespread cerebral gray matter volume deficits in schizophrenia. *Archives of General Psychiatry*, 49: 195-205, 1992.